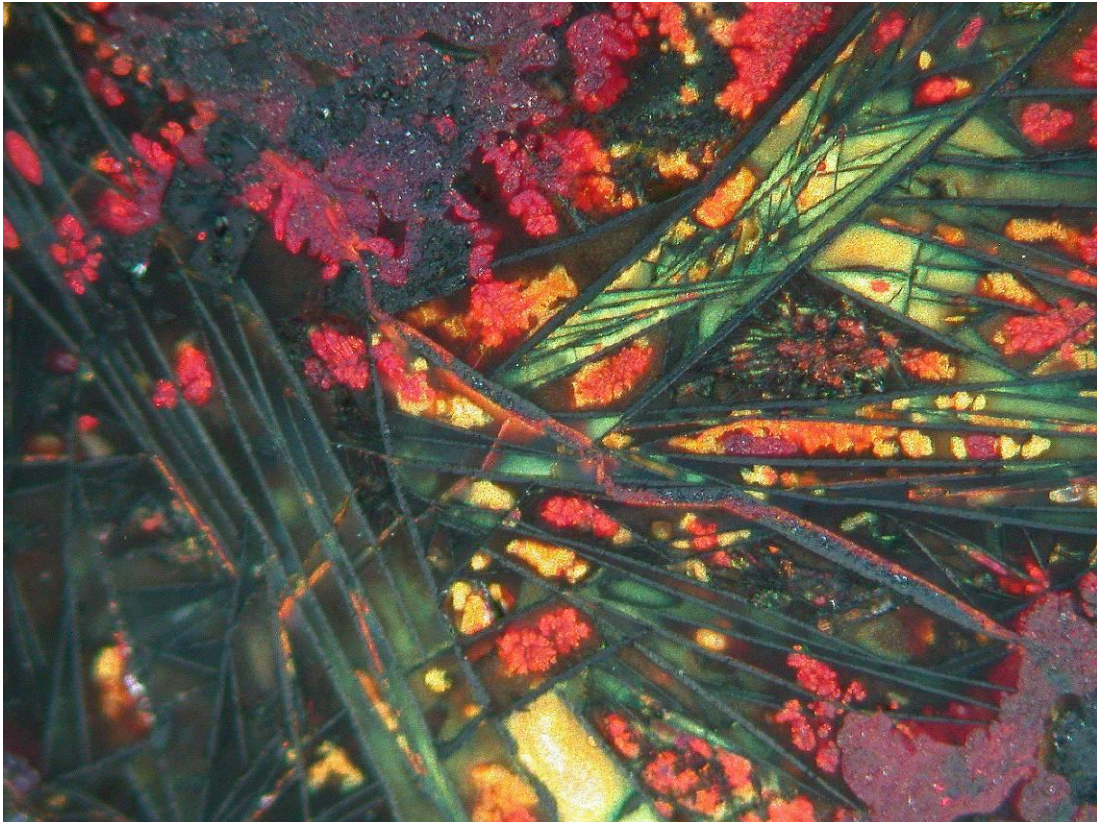


EVIDENCE FOR EARLY COPPER SMELTING IN BELOVODE, A VINČA CULTURE SITE IN EASTERN SERBIA

MILJANA RADIVOJEVIĆ



Dissertation submitted in partial fulfillment of the requirements for the degree of
MSc in Technology and Analysis of Archaeological Materials
of the University of London in 2007

UCL INSTITUTE OF ARCHAEOLOGY

Note: This Dissertation is an unrevised examination copy for consultation only and it
should not be quoted or cited without the permission of the Director of the Institute

Abstract

In this thesis the author will discuss evidence for the earliest copper smelting in Europe, documented during excavations of Belovode, a Vinča culture site in Eastern Serbia. The remains of slags, malachite beads, ceramics with bone-ash lagging and ores associated with ancient mines found in the vicinity of the site, surface finding of a copper ingot, offer insight into the organization and technology of the exploitation of copper ores for jewellery and metal production, respectively, at the end of the 6th millennium BC; representing one of the earliest known cases for metal smelting in the Neolithic world.

The microscopic and compositional analyses have revealed smelting activities carried out in Belovode throughout the occupational period. Furthermore, lead isotope and trace element analyses confirmed exploitation of several copper deposits in the vicinity, one of which is Rudna Glava, already confirmed as the Vinča culture mine.

Overall, this study demonstrated the consistent copper production over 500 years of occupational period of Belovode, which involved specialized crafts at a time copper represented a crucial commodity. It has provided an insight into what was surely an advanced technology at the end of 6th millennium, clearly pointing at the necessity of revising modern understanding of the development of metallurgy in the Old World.

Key words

Vinča culture, Chalcolithic, copper smelting, slag, copper ores, SEM-EDS, XRF, metallography, provenance

Table of Contents

List of Illustrations	iv
List of Tables	ix
Acknowledgements.....	1
Introduction.....	2
<i>Metallurgical activities in the Vinča culture</i>	8
<i>History of Research and Previous Studies of Belovode</i>	18
Definition of Problem	31
Methods and methodology.....	33
Results of Research: Analysis of Slag Samples.....	36
<i>Bulk chemical analysis of slag matrix</i>	36
<i>Oxides</i>	41
<i>Silicates</i>	46
<i>Metal prills</i>	49
Results of Research: Analysis of Ore Samples.....	52
<i>Geological ores</i>	52
<i>Archaeological ores</i>	53
Results of Research: Analysis of Artefacts.....	68
<i>Malachite beads</i>	68
<i>Copper metal lump</i>	71
<i>Copper ingot</i>	74
Results of Research: Analysis of Ceramics	79
<i>Belovode 26</i>	79
<i>Belovode 29 and Belovode 30</i>	84
Provenance studies: Lead isotope and trace element analysis	91
<i>The provenance of material from Belovode: lead isotope analysis</i>	98
<i>The provenance of copper ingot from Belovode: trace element analysis</i>	106
<i>Discussion on provenance of samples from Belovode</i>	109
Discussion and conclusion.....	113
<i>Summary and wider discussion</i>	113
<i>Directions for further research</i>	117
<i>Conclusion</i>	118
Bibliography	119

List of Illustrations

Figure 1		3
	The largest copper sources in Europe and Southwest Asia	
Figure 2		4
	The Vinča culture mines and sites located near copper ore deposits	
Figure 3		6
	C14 data for Rudna Glava, Belovode, Pločnik, Divostin and Gomolava	
Figure 4		9
	Shaft-hole in Rudna Glava, Eastern Serbia	
Figure 5		9
	The excavation plan of Rudna Glava	
Figure 6		10
	Hoard from Rudna Glava	
Figure 7		11
	Stone mallets from Mali Šturac	
Figure 8		11
	Shaft holes at Mali Šturac	
Figure 9		12
	Stone mallet from Jarmovac	
Figure 10		12
	Map of Starčevo and Vinča culture sites with malachite and azurite ores, beads and pendants	
Figure 11		13
	The find frequency of copper ore lumps in Vinča	
Figure 12		14
	Map of Vinča culture sites with documented finds of copper artefacts and slags	
Figure 13		15
	Grave of an adult from Gomolava	
Figure 14		16
	Selected copper artefacts from Pločnik's assemblages	
Figure 15		17
	Slag from Selevac	
Figure 16		17
	A piece of slag from Gornja Tuzla	
Figure 17		18
	C14 data for Belovode, Vinča culture horizon	
Figure 18		19
	Relative chronology and phase stratification of Belovode	
Figure 19		20
	Location of Belovode in the Mlava Valley	
Figure 20		22
	Open-air Trenches at Ždrelo	

Figure 21		22
	Shaft-hole at Ždrelo	
Figure 22		23
	Malachite lumps from Belovode	
Figure 23		24
	Malachite from Trench VII, Belovode	
Figure 24		25
	Field context of the shallow-pit furnace	
Figure 25		26
	Amphorae and malachite lumps from Belovode	
Figure 26		26
	Malachite beads and pendant from Belovode	
Figure 27		27
	Stone mallet from Trench VII in Belovode	
Figure 28		28
	Ceramic “chimneys” from Belovode	
Figure 29		29
	Reconstruction of the possible usage of “chimneys” found at Belovode	
Figure 30		29
	Copper chisel found in the vicinity of Belovode	
Figure 31		30
	Copper ingot found in the vicinity of Belovode	
Figure 32		30
	Surface finding: ceramic mould from Belovode	
Figure 33		37
	Figure showing the average composition of bulk chemical analyses of slag matrix	
Figure 34		39
	Figures showing correlation of readings in MnO, ZnO and CoO	
Figure 35		40
	Ternary phase diagram for SiO ₂ -FeO-Al ₂ O ₃	
Figure 36		40
	Ternary phase diagram for SiO ₂ - MgO+CaO+MnO+FeO+ZnO-Al ₂ O ₃ +P ₂ O ₅	
Figure 37		41
	Photomicrograph of cuprite in Slag 20	
Figure 38		41
	Photomicrograph of dendritic cuprite in Slag 21	
Figure 39		42
	Backscattered electron image of cuprite	
Figure 40		43
	Photomicrograph of grey cubic spinels in Slag 22b	
Figure 41		44
	Figure showing the average ratio of metal oxides forming spinels in all slag samples	
Figure 42		44
	Photomicrograph of delafossite in Slag 23	
Figure 43		45
	Backscattered electron image of delafossite in Slag 21	

Figure 44		46
	Photomicrograph of delafossite in Slag 21	
Figure 45		46
	Photomicrograph of silicates in Slag 22b	
Figure 46		47
	Photomicrograph of dark grey transparent leucite crystals in Slag 22a	
Figure 47		49
	Figure showing average composition of optically grey glass matrix in all samples	
Figure 48		50
	Photomicrograph of copper metal in Slag 21	
Figure 49		51
	Photomicrograph of charcoal in Slag 22a	
Figure 50		52
	One of the shaft-hole entrances in Ždrelo	
Figure 51		54
	Photomicrograph of phases in Ore 9	
Figure 52		55
	Photomicrograph of phases in Ore 12	
Figure 53		56
	Back scattered electron image of phases in Ore 12	
Figure 54		57
	Photomicrograph of Ore 19	
Figure 55		57
	Photomicrograph of azurite and malachite in Ore 19	
Figure 56		58
	Back scattered electron image of the ooids in the dark grey matrix in Ore 19	
Figure 57		59
	Photomicrograph of phases in Ore 13	
Figure 58		60
	Photomicrograph of the green phase in Ore 13	
Figure 59		60
	Photomicrograph of the tenorite/cuprite phase in Ore 13	
Figure 60		61
	Photomicrograph of bright (copper) prills in Ore 13	
Figure 61		61
	Back scattered electron image of dark grey phase containing silver sulphide prills, Ore 13	
Figure 62		62
	Photomicrograph of the copper sulphide grain developing in the dark grey matrix, Ore 13	
Figure 63		63
	Back scattered electron image of cuprite in form of convoluted agglomerations, Ore 13	
Figure 64		64
	Photomicrograph of main phases in Ore 17	

Figure 65		64
	Photomicrograph of pyrite in Ore 17	
Figure 66		65
	Photomicrograph of covellite crystals, Ore 17	
Figure 67		65
	Back scattered electron image of the lead oxide particle	
Figure 68		68
	Photomicrograph of Belovode 33 under Environmental Scanning Electron Detector	
Figure 69		70
	Photomicrograph of the green phase in bead Belovode 33	
Figure 70		70
	Photomicrograph of the green and dark red phase in Belovode 33	
Figure 71		71
	Photomicrograph of the optically bright yellow phase, Belovode 14	
Figure 72		72
	Photomicrograph of the corroded copper phase in Belovode 14	
Figure 73		73
	Photomicrograph of the light green corrosion product on Belovode 14	
Figure 74		74
	Image of the ingot showing sampled section	
Figure 75		75
	Photomicrograph of the unetched Belovode 34	
Figure 76		76
	Photomicrograph of Belovode 34	
Figure 77		76
	Photomicrograph of Belovode 34	
Figure 78		77
	Figure showing the Hv values taken along the sequence of Belovode 34	
Figure 79		78
	Photomicrograph of the metal body and corrosion in Belovode 34	
Figure 80		80
	ED-XRF compositional data for the inside and outside walls of Belovode 26	
Figure 81		80
	Photomicrograph of the fabric in Belovode 26	
Figure 82		81
	Photomicrograph of the ore-rich layer adhered on outer walls of Belovode 26	
Figure 83		81
	Photomicrograph of the ore-rich layer adhered on outer walls of Belovode 26	
Figure 84		82
	Backscattered electron image of the corroded copper metal	
Figure 85		83
	Backscattered electron image of the piece of charcoal, Belovode 26	
Figure 86		84
	ED-XRF compositional data for the inside and outside walls of Belovode 29 and Belovode 30	

Figure 87		84
	Photomicrograph of the fabric in Belovode 29 and Belovode 30	
Figure 88		85
	Back scattered electron image of the fabric in Belovode 30wh	
Figure 89		85
	Back scattered electron image of bone used as tempering material in the fabric of Belovode 30	
Figure 90		87
	Photomicrograph of the calcium phosphate lagging on the outside walls of Belovode 29	
Figure 91		87
	Photomicrograph of the calcium phosphate lagging on the inside walls of Belovode 30wh	
Figure 92		88
	Back scattered electron image of the calcium phosphate lagging	
Figure 93		88
	Back scattered electron image of the calcium phosphate lagging	
Figure 94		89
	Photomicrograph of the charcoal filled with calcium phosphate	
Figure 95		89
	Back scattered electron image of the crushed ore layer on the inside walls of Belovode 29	
Figure 96		93
	Lead isotope abundance ratios in samples from Belovode and Ždrelo	
Figure 97		95
	Locations of ore and slag samples from Eastern Serbia	
Figure 98		98
	Mineralized regions of Bulgaria and Eastern Serbia	
Figure 99		99
	Lead isotope abundance ratios in Belovode Group A and Group B	
Figure 100		101
	Lead isotope abundance ratios of Belovode Group C	
Figure 101		102
	Lead isotope abundance ratios of Belovode Group C	
Figure 102		103
	Lead isotope abundance ratios of Belovode Group C	
Figure 103		106
	Lead isotope abundance ratios in samples from Belovode and Ždrelo	
Figure 104		107
	Figure showing trace element data falling into pattern of Majdanpek ore deposits	
Figure 105		108
	Concentrations of Co and Ni in native copper from the Balkans and Anatolia	

List of Tables

Table 1	Relative chronology of the Late Neolithic- Middle Eneolithic (Chalcolithic) cultures in Southeast Europe	Appendix Tables
Table 2	Chemical composition of slag (sample No. 3866), outlined generally in major (HM) and minute (Sp) concentrations (<i>after</i> Neuniger, Pittioni and Siegl 1964: 99, Tab. 1)	7
Table 3	Documented remnants of metallurgical activities in the Vinča culture sites	Appendix Tables
Table 4	Analyses of ore vein in the Vukan mountain (<i>after</i> Jovanović 1991: 190)	21
Table 5	Materials indicating metallurgical activities documented at Belovode excavations, Trenches I- XI	Appendix Tables
Table 6	Characteristics of the analytical methods conducted on studied samples	35
Table 7	EPMA- compositional data for Belovode slag samples, normalized to 100% (areas low in cuprite and copper metal)	37
Table 8	EPMA- compositional data for Belovode slag samples, normalized to 100%	28
Table 9	SEM-EDS compositional data for cuprite normalized to 100%	42
Table 10	SEM-EDS compositional data for spinels, normalized to 100%	43
Table 11	SEM-EDS compositional data for delafossite, normalized to 100%	45
Table 12	SEM-EDS compositional data for leucite formed in glass matrix, normalized to 100%	47
Table 13	SEM-EDS compositional data for the optically dark grey glass matrix in the sample Slag 21, normalized to 100%	48
Table 14	SEM-EDS compositional data for the optically grey glass matrix in slag samples, normalized to 100%	48
Table 15	EPMA compositional data for metal prills in Belovode slag samples, normalized to 100%	50
Table 16	ED-XRF compositional data for ores from Ždrelo, normalized to 100%	53
Table 17	SEM-EDS compositional data for minimum, maximum and average values for the optically green phase in Ore 9	55
Table 18	SEM-EDS compositional data for minimum, maximum and average values for the optically light grey phase in Ore 9	55
Table 19	SEM-EDS compositional data for minimum, maximum and average values for the optically green phase in Ore 12	56
Table 20	SEM-EDS compositional data for minimum, maximum and average values for the optically reddish- brown phase in Ore 12	56
Table 21	SEM-EDS compositional data for minimum, maximum and average values for the optically dark grey phase in Ore 12	56
Table 22	SEM-EDS compositional data for minimum, maximum and average values for the optically dark blue phase in Ore 19	57

Table 23		58
	SEM-EDS compositional data for minimum, maximum and average values for the optically grey phase in Ore 19	
Table 24		58
	SEM-EDS compositional data for minimum, maximum and average values for the optically dark grey phase in Ore 19	
Table 25		61
	SEM-EDS compositional data for minimum, maximum and average values for the optically dark phase in grey matrix of Ore 13	
Table 26		62
	SEM-EDS compositional data for silver sulphide prills in Ore 13	
Table 27		62
	SEM-EDS compositional data for copper sulphide prill in Ore 13	
Table 28		62
	SEM-EDS compositional data for the green matrix in Ore 13	
Table 29		63
	SEM-EDS compositional data for cuprite in green matrix in Ore 13	
Table 30		65
	SEM-EDS compositional data for minimum, maximum and average values for chalcocite in Ore 17	
Table 31		66
	SEM-EDS compositional data for minimum, maximum and average values for the optically dark grey phase in Ore 17	
Table 32		66
	SEM-EDS compositional data for minimum, maximum and average values for silver sulphide particles in Ore 17	
Table 33		66
	SEM-EDS compositional data for minimum, maximum and average values for lead oxide particles in Ore 17	
Table 34		66
	SEM-EDS compositional data for minimum, maximum and average values for pyrite (optically yellow) in Ore 17	
Table 35		66
	SEM-EDS compositional data for minimum, maximum and average values for pyrite (optically light grey) in Ore 17	
Table 36		67
	SEM-EDS compositional data for minimum, maximum and average values for the optically dark phase surrounding pyrite (optically yellow) in Ore 17	
Table 37		67
	SEM-EDS compositional data for minimum, maximum and average values for the optically dark phase surrounding pyrite (optically light grey) in Ore 17	
Table 38		69
	SEM-EDS compositional data for inner surface of the malachite bead Belovode 32(drill hole)	
Table 39		69
	SEM-EDS compositional data for outer surface of the malachite bead Belovode 32	
Table 40		70
	SEM-EDS compositional data for minimum, maximum and average values for optically green phase in Belovode33	
Table 41		71
	SEM-EDS compositional data for minimum, maximum and average values for the optically dark red phase in Belovode 33	
Table 42		72
	SEM-EDS compositional data of the optically bright yellow phase in Belovode 14	
Table 43		73
	SEM-EDS compositional data for minimum, maximum and average values for the first layer of corrosion (Belovode 14)	
Table 44		73
	SEM-EDS compositional data for minimum, maximum and average values for the second layer of corrosion (Belovode 14)	

Table 45		75
	SEM-EDS compositional data for minimum, maximum and average values for α grains in Belovode 34	
Table 46		76
	SEM-EDS compositional data for minimum, maximum and average values for cuprite in Belovode 34	
Table 47		78
	SEM-EDS compositional data for minimum, maximum and average values for the first layer of corrosion in Belovode 34	
Table 48		78
	SEM-EDS compositional data for average values for the second layer of corrosion in Belovode 34	
Table 49		Appendix Tables
	ED-XRF compositional data for inside and outside surface of Belovode 26	
Table 50		81
	SEM-EDS compositional analysis of minimum, maximum and average values of body of Belovode 26	
Table 51		82
	SEM-EDS compositional analysis of copper phase in the adhered ore-rich layer in Belovode 26	
Table 52		82
	SEM-EDS compositional analysis of minimum, maximum and average values of the oolitic structures in the adhered ore-rich layer in Belovode 26	
Table 53		83
	SEM-EDS compositional analysis of average values of the optically grey phase in the oolitic structures in Belovode 26	
Table 54		83
	SEM-EDS compositional analysis of charcoal in the adhered ore-rich layer in Belovode 26	
Table 55		Appendix Tables
	ED-XRF compositional data for inside and outside surface of Belovode 29	
Table 56		Appendix Tables
	ED-XRF compositional data for inside and outside surface of Belovode 30	
Table 57		86
	SEM-EDS compositional analysis of minimum, maximum and average values of body of Belovode 29	
Table 58		86
	SEM-EDS compositional analysis of minimum, maximum and average values of body of Belovode 30ch	
Table 59		86
	SEM-EDS compositional analysis of minimum, maximum and average values of body of Belovode 30wh	
Table 60		89
	SEM-EDS compositional analysis of minimum, maximum and average values of the crushed ore layer, Belovode 29	
Table 61		92
	Lead isotope abundance ratios in material from Belovode and Ždrelo	
Table 62		96
	Lead isotope abundance ratios in ores and slags from Serbia	
Table 63		97
	Lead isotope abundance ratios of copper ores from Bulgaria	
Table 64		105
	Lead isotope abundance ratios in Late Neolithic/Early Chalcolithic artefacts	
Table 65		107
	ICP-MS trace element data for copper ingot Belovode 34	
Table 66		111
	Analyses of copper ore from Rudna Glava and the products of smelt	
Table 67		111
	Chemical composition of ore samples from Rudna Glava	

Acknowledgements

First and foremost, I would like to thank Professor Thilo Rehren for the immense patience and unending support throughout the year, particularly during the thesis work; thank you for the most valuable guidance I have ever had! I also express thanks to Dr Marcos Martinon-Torres, without whom the whole program would have not been as organized and well prepared as it was! I thank him for all the help and persistence he had in teaching us how to conduct the proper scientific research; many thanks for helpful discussions and supervision!

I would also like to thank to Simon Groom and Kevin Reeves for their invaluable technical guidance in the basement labs.

The credits for my studies at the UCL Institute of Archaeology in terms of funding go to Marie Curie Early Stage Training Actions, the Government of Serbia, the Tokyo Foundation for Young Leaders and particularly to Professor Dejan Popović, the former rector of the University of Belgrade, who recommended me and supported in applying for these grants. Special thanks go to Mr. Ryoichi Sasakawa, who provided funds for lead isotope analysis performed in the Curt-Engelhorn-Zentrum für Archäometrie gGmbH An-Institut der Universität Tübingen, Mannheim, Germany. Thanks must go to the staff in this laboratory, and especially to Mr. Michael Brauns, and his expertise in handling delicate archaeological materials.

The greatest thanks must go to those who supported me from the very beginning: Julka Kuzmanović-Cvetković, Dušan Šljivar and Borislav Jovanović; their incredible generosity was largely appreciated, thank you! I would also like to thank Dušan Borić, for allowing me to use yet unpublished C14 data, as well as providing me with great support during the studies. Thanks go to Ben Roberts and Chris Thornton, for their considerable help and guidance in my research.

I also want to thank my classmates, MSc Techs '07, for their patience and understanding. My immense gratitude goes to a special angel in my life, Aura Maria Rico Sardi, whose rock-solid tolerance and great energy kept me on the ground throughout the year.

Last but not least, I want to thank my parents for encouragement and support throughout my studies; as well as the Rajkovača family, who offered me a taste of home in their house in Cambridge throughout the year.

Introduction

The independent development of metallurgy in Southeast Europe has been long recognized as an invention earlier than and thereby independent of Near Eastern influence (Renfrew 1969; cf. 1973). A new eagerness for “Ex Balcanae lux” (as coined by Todorova 1978) fostered a pursuit in this region for the origins of all aspects of material culture in the Chalcolithic, as well as back to the Neolithic period itself. Thus, a long-standing debate between advocates of independent invention and supporters of migration/diffusion models was established (see Bognar-Kutzian 1976). However, distinctive features of early metallurgical cultures in Southeast Europe have been outlined by work of Jovanović (1971, 1982), Todorova (1978, 1981) and Chernykh (1978a). They have also recognized differences in accepting innovation in the Chalcolithic Balkan societies, which was mainly mirrored in the production of distinctive types of tools in two contemporary cultures, Vinča and Karanovo cultural complex. As a consequence, a great deal is today known both about typological morphology (Gaul 1942; Garašanin 1950; Schubert 1965; Vulpe 1974; Kuna 1981; Todorova 1981; Patay 1984; Žeravica 1993) and the elemental composition (Junghans, Sangmeister and Schröder 1968; Черных 1978a) of prehistoric copper artefacts in the Balkans.

Moreover, the discovery of copper mines exploited in the Late Neolithic/Early Chalcolithic period, such as Rudna Glava (Jovanović 1982) and Ai Bunar (Černych 1978b), encouraged pursuit for other sources of exploitation, but yet little has been found to correspond to the vast amount of massive copper artefacts present. This fact, in turn, led to assumptions that massive implements were imported from Anatolia, or made from native copper using stone tool manufacturing techniques like heating and hammering (Hartmann and Sangmeister 1972). The usage of these techniques was not considered to represent the so-called “intelligent metallurgy”, defined by G. Childe (1944) as the practice of smelting metal from ores and casting artefacts from molten metal.

Nevertheless, the introduction of chemical studies (mainly lead-isotope analyses) in the interpretation of early copper processing in Southeast Europe convincingly demonstrated the Balkan origins of copper ore extracted and manufactured for producing metal artefacts (Черных 1978a; Pernicka, Begemann and Schmitt-Strecker 1993; Pernicka *et al.* 1997; Gale *et al.* 2003). This method, though widely accepted and applied, still leaves space for various interpretations and general assumptions on the artefact(s) origin (*cf.* Jovanović 1993). Its most valuable contribution is an indication for certain areas in the Balkans to be rediscovered in the pursuit for prehistoric copper mines; clearly pointing at the necessity for reconsidering previous archaeologists' assumptions on the location of the early mines.

Nowadays, it is believed that the accessibility of copper mines and the richness of resources determined the Balkans as the area of the earliest metallurgy in Europe (Черных 1978a ; Pernicka 1990; Fig. 1).

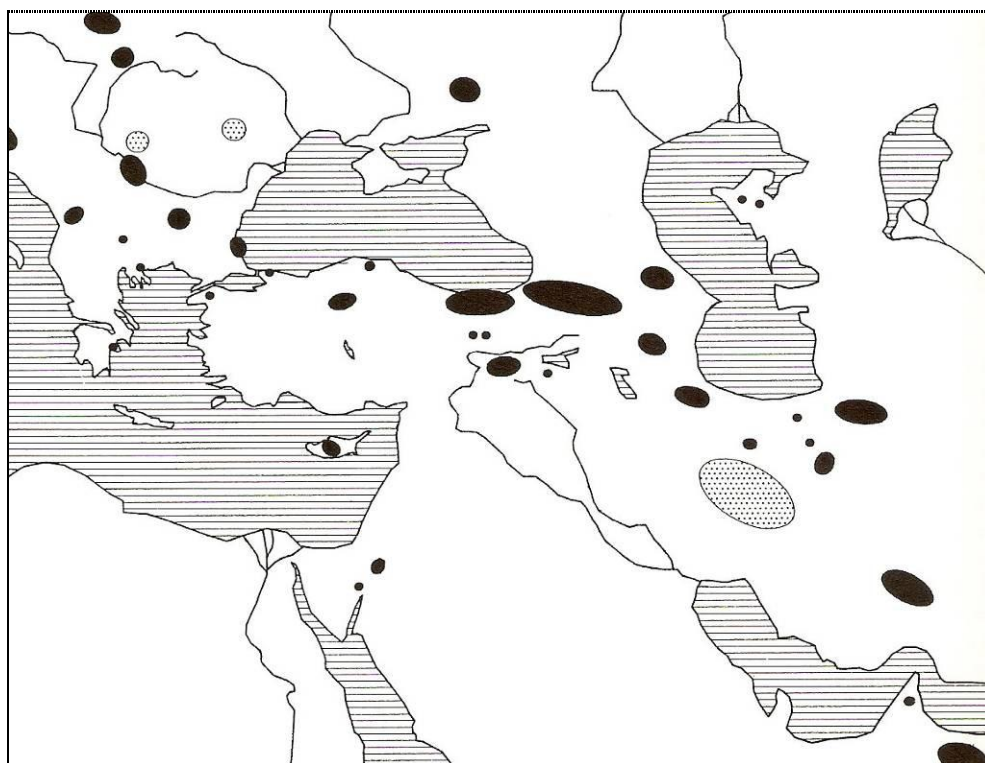


Fig. 1- The largest copper sources in Europe and Southwest Asia
(after Pernicka 1990: 90, Abb. 68)

A belt rich in copper mineralization is known to cut across Bulgaria and eastern Serbia (Gale et al. 2003: 124, *cf.* Dokov et al. 1989). Based on chemical analyses of this mineralization, Chernykh (1978a) recognizes three metallurgical provinces in Southeast Europe, located around three distinctive production centres in the Chalcolithic period: Rudna Glava, Ai Bunar and as yet unknown mining centre in the Carpathian Mountains. This classification produced a far-reaching theory about recognizing metallurgical provinces in the Balkans and the extensive exchange and movement of copper ores/finished products in the region (Черных 1978a: 17 *ff.*). What is more, Krajnović and Janković (1990) defined additional metallogenic zone in the west Balkans, rich in sulphide and oxide copper ores, with indications for early exploitation in the Chalcolithic period (see Fig. 2).

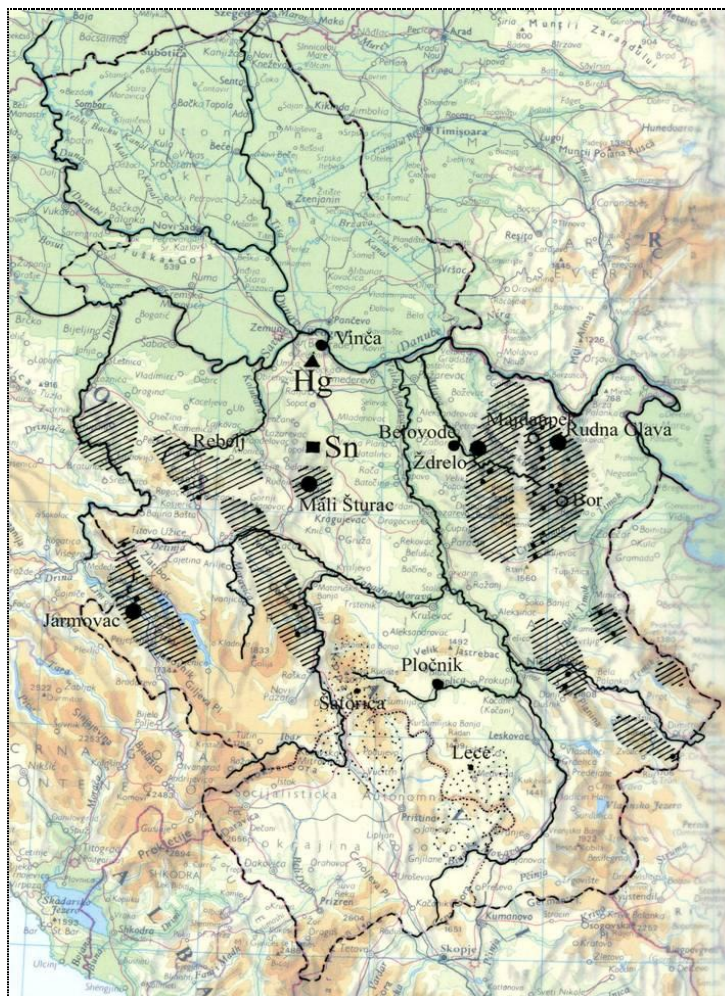


Fig. 2- The Vinča culture mines and sites located near copper ore deposits (hatched and dotted areas) in the Late Neolithic/Early Chalcolithic Serbia. Note also deposits of tin and mercury nearby (map courtesy of Dragana Antonović, Archaeological Institute, Belgrade).

It is here important to emphasize that the period of introducing metals in past societies is recognized as technologically advanced in general, mirrored in the emergence of settlements, intensive trade and usage of graphite painted pottery, as well as the emergence of symbols for communication (?) (cf. Bailey 2000; Nikolova (ed.) 2003). In terms of cultures, we are identifying the Vinča culture (Serbia) as contemporaneous with the Kodžadermen-Gumelnica-Karanovo VI complex in Bulgaria, Dimini V in Greece and late Körös in Romania and Hungary (see Table 1 in Appendix Tables). At this time, the late 6th and early 5th millennium BC, the concepts of copper metal and ore exploitation and production seem to have been introduced from the Balkans and not from Anatolia, which is based on the presence of gold (Makkay 1991) and obsidian from the Carpathians (Kilikoglou *et al.* 1996), one of many distinctive features of the Early Chalcolithic material culture in the Balkans.

These innovations are chronologically set from the third quarter of the 6th millennium BC until the first half of the 5th millennium (Bailey 2000; Nikolova 1999: 18). As outlined by Garašanin (1994-1995: 16-17), the technological advancement, particularly regarding copper processing, must have started well before the end of the 6th millennium, and the C14 dates proposed by Nikolova (1999) correspond with this assumption. More recently, new C14 analyses conducted on material from the Vinča culture sites with metallurgical activities, like Rudna Glava, Belovode, Pločnik, Divostin and Gomolava, indicated very early calibrated dates- in the range of 6100 BC for Rudna Glava to 4600 BC for Gomolava (Borić 2007; Fig. 3).

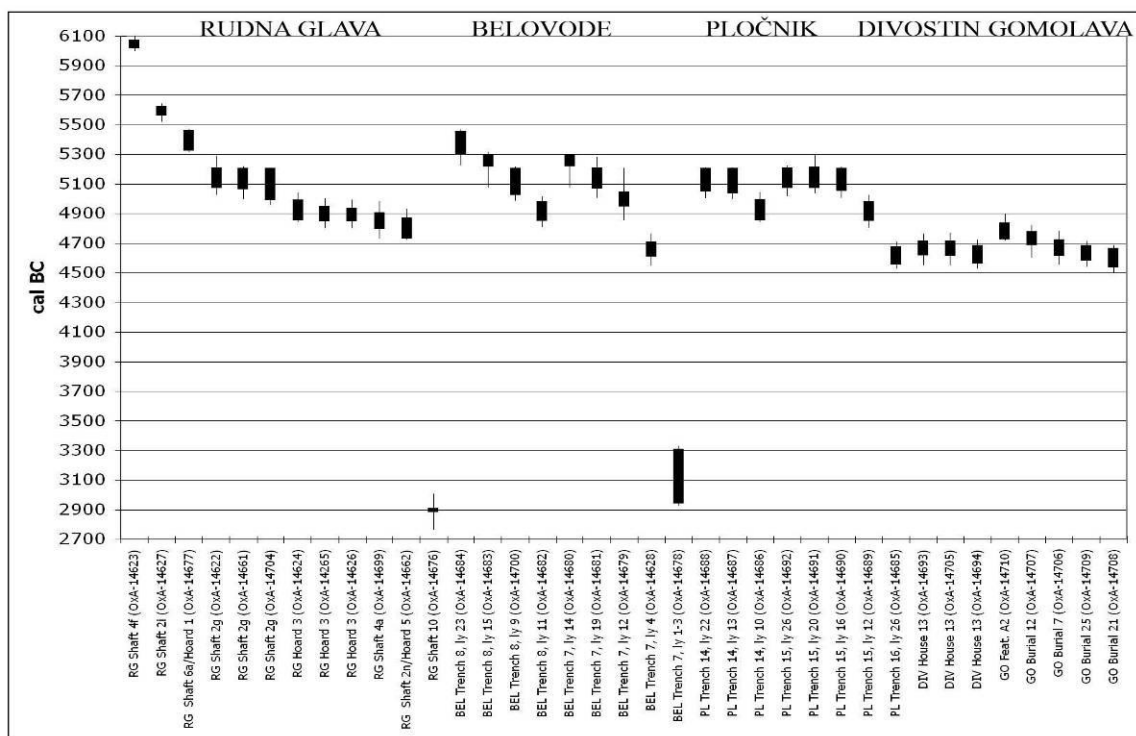


Fig. 3- C14 data for Rudna Glava, Belovode, Pločnik, Divostin and Gomolava. Note the intrusion of Kostolac phase on Belovode (after Borić 2007)

These data confirm previous assumptions on the very early beginnings of copper processing in the region, emphasizing the role of the Vinča culture in the development of metallurgy in the Balkans, and representing the focus of the research described here.

To illustrate the level of technological knowledge related to metallurgical activities, one should also look at Anatolian sites, which show evidence for copper smelting from the end of the 6th millennium BC. The production of pendants, beads and bracelets of hammered native copper or drilled malachite is known from Çayönü Tepesi, dating back to the 9th millennium BC (Muhly 1989; Stech 1990; Maddin, Stech and Muhly 1991; cf. Özdoğan and Özdoğan 1999). However, smelting activities are documented only for few sites, and not all of these have been analysed. A piece of copper slag (?) was discovered on the house floor, layer VI at Çatalhöyük, suggesting copper smelting activities from the end of the 7th millennium BC. Neuniger, Pittioni and Siegl (1964) reported

significant amount of Fe and Cu in the slag, with minute concentrations of As, Ni, Zn, Cr and Co (Table 2).

No.	Object	Cu	Sn	Ag	As	Fe	Mn	Ni	Pb	Sb	Zn	Bi	Cr	Au	Co	V	Al	Ca	Mg	Si
3866	“Erz”	-	-	?	Sp	HM	-	Sp	-	-	Sp	-	Sp	-	Sp	Sp	-	-	Sp	-

Table 2- Chemical composition of slag (sample No. 3866), outlined generally in major (HM) and minute (Sp) concentrations (*after* Neuniger, Pittioni and Siegl 1964: 99, Tab. 1)

The specimen was described as typically brownish in colour, with red inclusions from cuprite, and green copper minerals underneath. Two main phases were detected: delafossite (CuFeO₂) and tenorite, but not metallic copper; which, according to the authors, is a missing feature in determining this sample as a slag (Neuniger, Pittioni and Siegl 1964: 110; Hauptmann 1989; Pernicka 1990; Hauptmann *et al.* 1993; Craddock 1995: 126).

A few lumps of “slag” dating from 5000 BC were found at Değirmentepe (Yalçın 2000; Craddock 2001; cf. Esin 1969), but analyses have not revealed indications for a smelting process. Since its copper content was found to be in the range of 100 to 900 ppm, and iron up to 4%, Yalçın (2000) identified it as ceramic slag. Lumps of slag originating from the same period have been discovered at Tülintepe and Tepeçik in Turkey, as well as at Tal-i-Iblis in Iran (Pigott 1999; Craddock 2001). In addition, a slagged fragment of crucible was recorded in Amuq, Syria, and dated back to the early 6th millennium BC (Yener 2000; cf. Wertime 1973).

Metallurgical activities in the Vinča culture

The abundance of ore deposits available within the Balkans encouraged Early Neolithic inhabitants to start experimenting with copper ores (see Fig. 2). The earliest artefacts, pendants, malachite and azurite beads, were found in the dwelling pits at Lepenski Vir, layers IIIa and IIIb (Srejović 1969; Srejović and Babović 1981; Glumac and Tringham 1990), and in contemporary sites, Divostin I and Zmajevac (Chapman 1981; Glumac 1988; see fig. 11), the earliest of them dating back to 6500 BC (Glumac and Tringham 1990: 559, table 15.5). These isolated finds were not connected with metallurgy in the sense of smelting and extracting, but used for ornamental purposes. However, they were part of the process of introducing ores to material culture, and probably experimenting with their material properties, particularly encouraged by the immediate vicinity of copper bearing regions in eastern Serbia (Tylecote 1983; Antonović 2006).

These archaeological layers belong to the Starčevo culture, and are generally succeeded by Vinča culture inhabitants; more than 400 sites were identified as situated within easy access of copper ore bodies known in former Yugoslavia, Romania and Hungary (Chapman 1981). This culture lasted for nearly one millennium in the area, spreading from the Carpathian Mountains in the north to the Vardar river valley in the south, central Bosnia in the west and Sofia Valley in the east (Garašanin 1979).

Metallurgical activities within the Vinča culture are represented by discoveries of mine shafts, malachite and azurite ores discovered at sites, beads and other ornaments, pieces of slag and copper tools. They all display an exceptional record of metallurgical activities carried out by Vinča culture's craftsmen, and will be described in detail below.

Mining activities in the Vinča culture are known to be carried out in several locations, one of which is Rudna Glava, the oldest copper mine in the Balkans (Jovanović 1971; 1982; see Table 3 in Appendix Tables; Fig. 4).

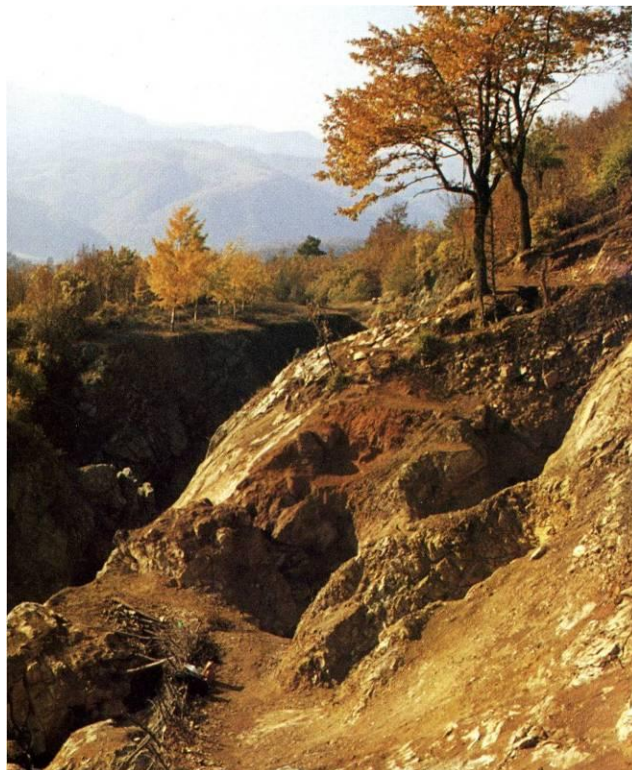


Fig. 4- Shaft-hole in Rudna Glava, Eastern Serbia
(courtesy of Dragana Antonović, Archaeological Institute, Belgrade)

The site consisted of eight groups of mine shafts with access platforms, all following veins rich in magnetite, chalcopyrite and carbonate copper ores (Fig. 5).

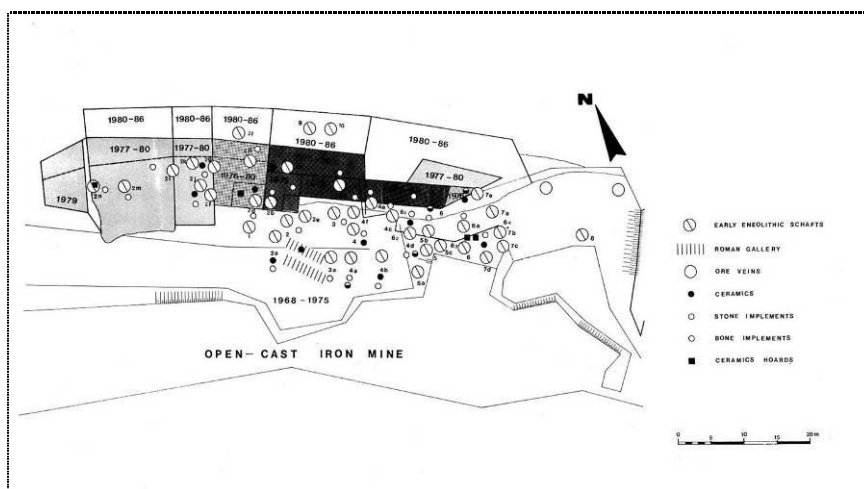


Fig. 5- The excavation plan of Rudna Glava
(courtesy of Dragana Antonović, Archaeological Institute, Belgrade)

Near the entrances of shaft- holes, hoards containing large jugs or amphorae (Fig. 6a) and stone mallets (Fig. 6b) were found, which along with mining instruments, such as deer antlers (Fig. 6c) discovered inside the mines, represent working tools of the first miners in the Balkans. The ceramic material has distinctive features of the Vinča culture, phase Vinča Tordos II, undoubtedly confirming its cultural provenience.

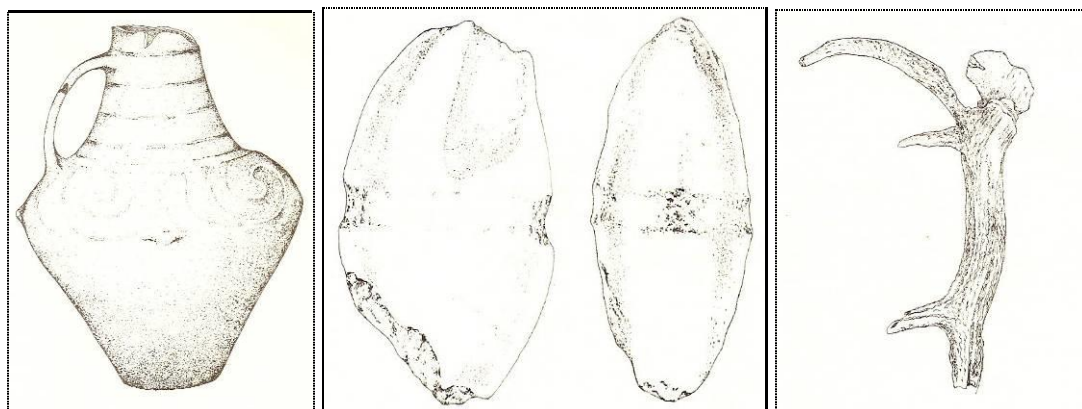


Fig. 6- a) Amphorae from hoard 1 from Rudna Glava. Height 35cm (after Jovanović 1982: 45); b) stone mallet from Shaft 4a, Rudna Glava. Dimensions 14x18x7 cm (after Jovanović 1982: 29); c) deer antler from Shaft 4a, Rudna Glava. Length 46 cm, width 4-6 cm (after Jovanović 1982: 31)

Moreover, findings of stone mallets with the groove in the middle (Fig. 7), similar to those from Rudna Glava, were discovered at Mali Šturac, an ancient mine located on Mt. Rudnik (Jovanović 1983; Fig. 8), as well as in Jarmovac, mine situated near Priboj on Lim (cf. Davies 1937; Jovanović 1982; Fig. 9). Identical artefacts have been found in the Vinča culture settlements Mačina and Merovac, both situated in the vicinity of the ore-rich mountain Kopaonik, Southern Serbia (Kuzmanović- Cvetković 1998; Radivojević 1998).

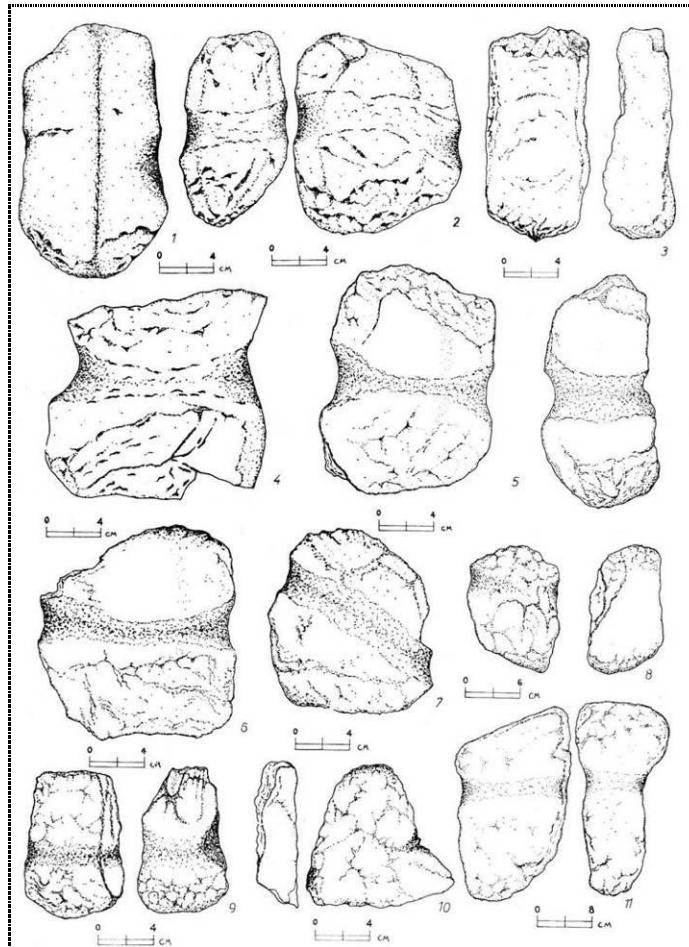


Fig. 7- Stone mallets from Mali Šturac, analogous with findings from Rudna Glava (courtesy of Dragana Antonović, Archaeological Institute, Belgrade)

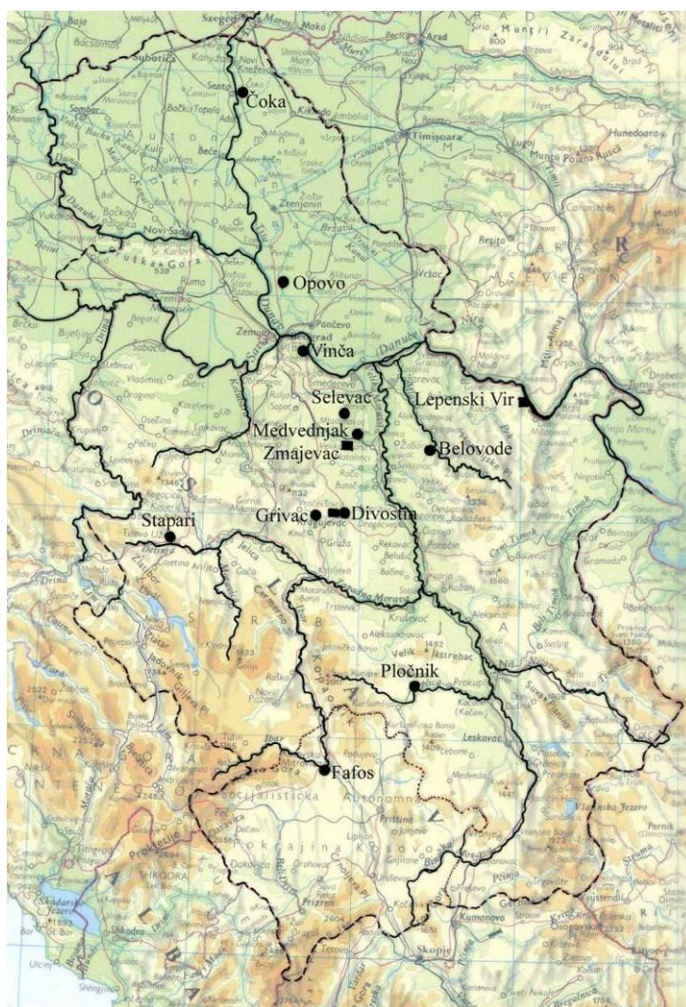


Fig. 8- Shaft holes at Mali Šturac. Note stone mallet found *in situ* (courtesy of Dragana Antonović, Archaeological Institute, Belgrade)



Fig. 9- Stone mallet from Jarmovac, similar to those found in Rudna Glava and Mali Šturac (after Davies 1937)

The largest amount of malachite and azurite ores were found in Belovode, situated in Eastern Serbia. Malachite ores were also found at the eponymous site Vinča, in pits and dwellings in the earliest levels (Antonović 2006; Vasić 1932; Fig. 10).



**Fig. 10- ■ map of Starčevo culture sites with malachite and azurite ores, beads and pendants;
● map of Vinča culture sites with findings malachite and azurite ores
(map courtesy of Dragana Antonović, Archaeological Institute, Belgrade)**

Some of them were discovered in large lumps mixed with charcoal, showing marks of firing. The find frequency within cultural phases is higher in the later periods of Vinča culture (Fig. 11), which prompted M. Vasić almost a century ago to assume metallurgical activities (Antonović 2002).

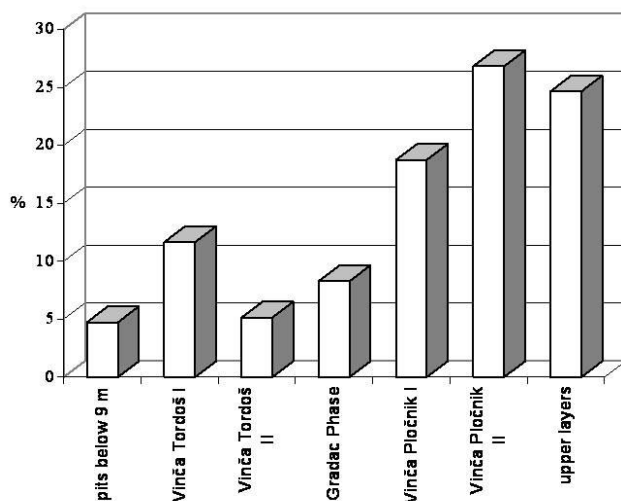


Fig. 11- The find frequency of copper ore lumps in Vinča (after Antonović 2006: 87, fig. 2)

Small malachite and azurite ore lumps were also discovered in Divostin II and Selevac, both located in central Serbia. At Divostin II, 110 samples of malachite and azurite lumps were detected in one area of the site (Glumac 1988). In Selevac, 211 lumps of these minerals (Glumac and Tringham 1990) were found concentrated only in four houses at the site. Moreover, in Medvednjak, the nearby site, malachite beads were discovered in one of the houses (Glumac 1983; Galović 1975), in addition to a few lumps of copper oxides from the late Vinča sites Opovo and Čoka (Tringham, Brukner and Voytek 1985). Fafos I, situated in Southern Serbia, revealed lumps of malachite ore with cuprite, some of which were burnt (Jovanović 1961; 1984). In the early Vinča horizons in Pločnik, as well as in Velika Gradina near Stapari, lumps of malachite were discovered throughout the levels of habitation (Antonović 2006; Jurišić 1960). Further in the west, at Obre I, a piece of malachite ore was detected in one of the houses (cf. Gimbutas 1974).

In the context of copper ores exploitation and selection, a complete workshop for manufacturing malachite beads was discovered in Divostin II (Glumac 1988). Small copper beads were also found at Selevac (Glumac and Tringham 1990), Grivac (Gavela 1956-1957) and Belovode (Šljivar 2006). A copper bracelet with fragmented copper wire was detected in a house in Velika Gradina, dating from the early phases of the Vinča culture (Jurišić 1960; see Fig. 12).

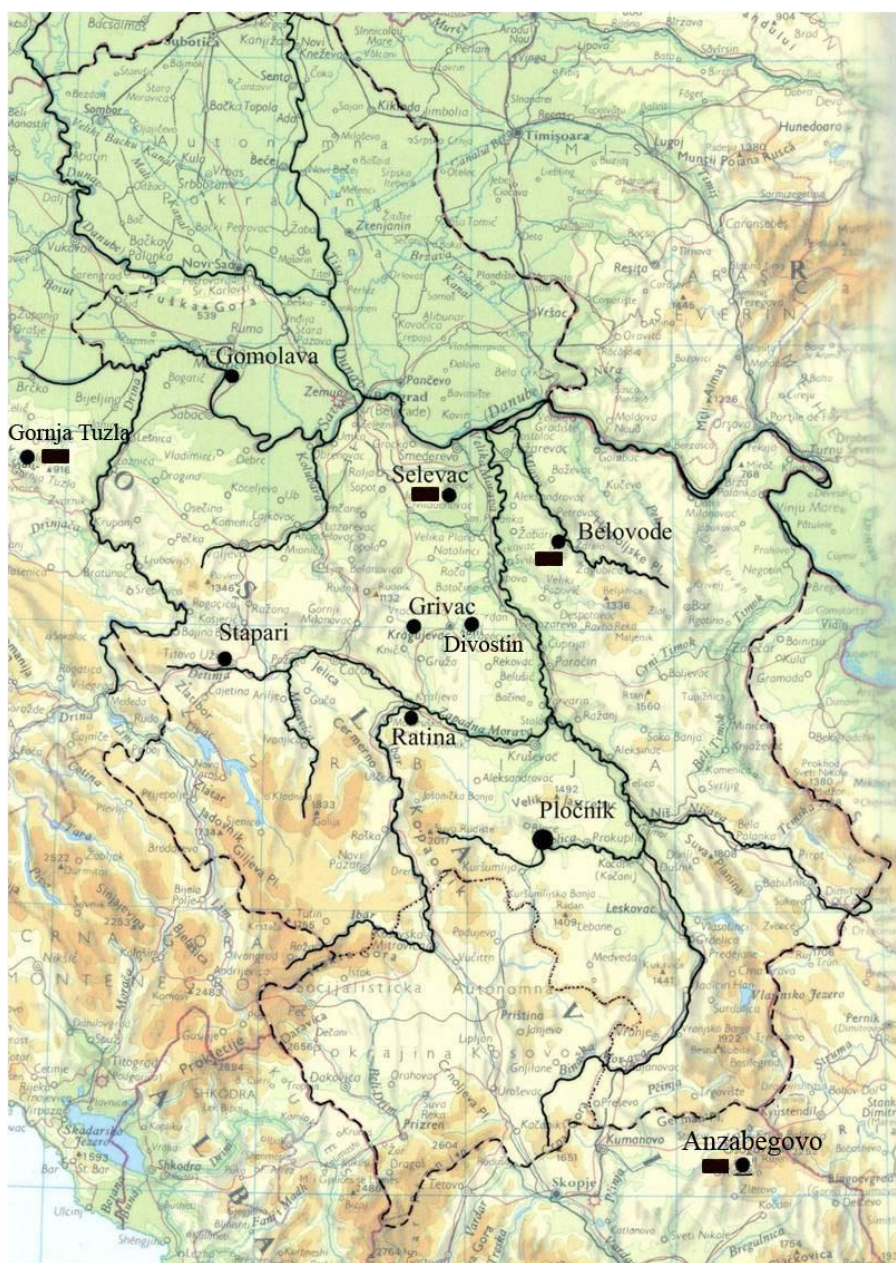


Fig. 12- • map of Vinča culture sites with documented finds of copper artefacts (both jewellery and tools); ■ map of Vinča culture sites with documented slag samples (map courtesy of Dragana Antonović, Archaeological Institute, Belgrade)

In Gornja Tuzla, copper jewellery was found throughout the levels; malachite beads, a ring, a fragment of thin copper wire and a fragmented copper pin originate from the earliest levels. The rest of the assemblage, a copper sheet hammered into a bracelet, a needle, two hooks, fragmented copper wire and a number of malachite beads, belong to later phases of the Vinča culture (Čović 1961).

A massive copper bracelet and fragments of copper jewellery were found in Gomolava, the only known burial site of the Vinča culture (Brukner 1980; Fig. 13).

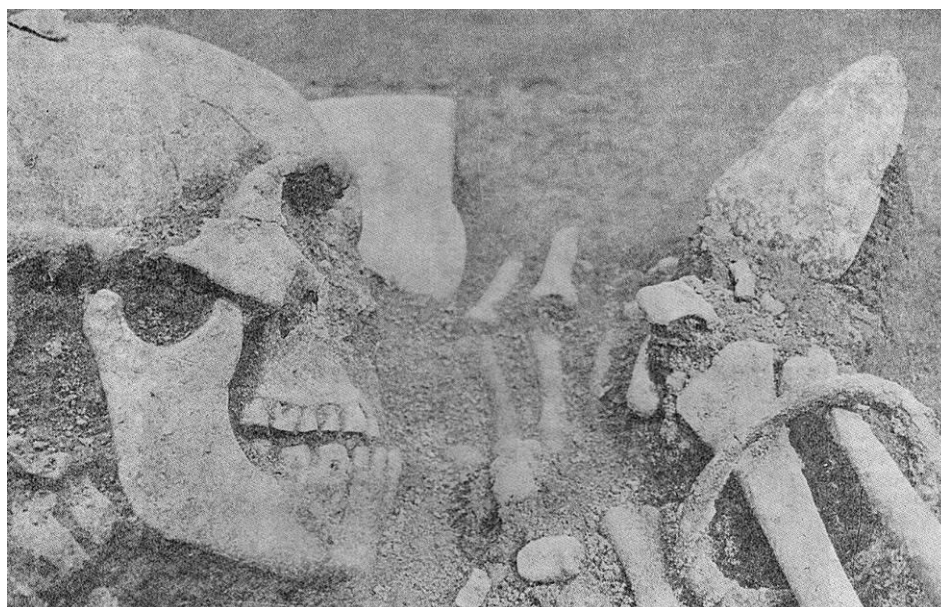


Fig. 13- Grave of an adult from Gomolava. Note the copper bracelet placed around the right wrist (after Brukner 1980: fig. 17)

The analyses of these artefacts revealed a high amount of tin, 6.6 % (Ottaway 1979). Also, the analysis of a loop of copper wire found in the Vinča culture settlement Ratina, Central Serbia revealed significant concentration of tin present (Valović 1985; Ljamic-Valović and Valović 1988; Glumac and Todd 1991). It is assumed that the tin content was probably due to the nearest source of tin ores situated in Mt. Cer, Western Serbia (cf. Janković 1967; Taylor and McGeehan 1987).

Nevertheless, the most exceptional findings confirming metallurgical activities in the Vinča culture are four assemblages of massive copper artefacts originating from the Vinča culture settlement Pločnik (Grbić 1929; Stalio 1960, 1962). The assemblages consist of a distinctive type of copper hammer-axes, named type Pločnik in the typology

of metal artefacts in Southeast Europe (Schubert 1965; Черных 1978a; Kuna 1981; Todorova 1981; Žeravica 1993; Radivojević 2007) followed by chisels, massive armbands, a miniature ceramic pot and white stone tools (Fig. 14).

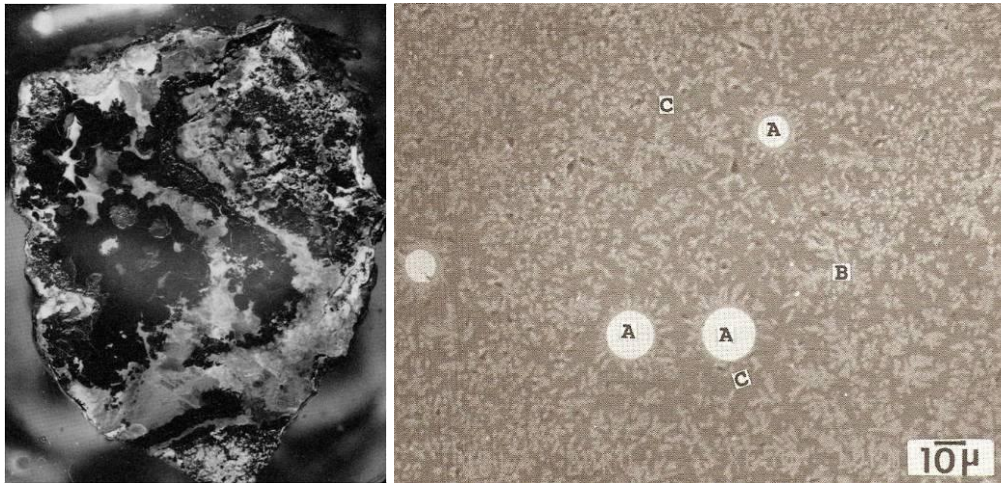


Fig. 14- Selected copper artefacts from Pločnik's assemblages. Scale 3:1 (courtesy of Dragana Antonović, Archaeological Institute, Belgrade)

However, since all Pločnik artefacts had been found accidentally, it was long thought that their cultural provenience is the Late Eneolithic culture Bubanj-Hum, suggested to be present in Pločnik (Garašanin 1973). On the other hand, during the resumed campaign of Pločnik excavations, three massive copper chisels stratified in the end of the early Vinča culture phase confirmed metallurgical activities within the site and hence the provenience of these massive copper artefacts (Šljivar 1996; ШЛЖИВАР И КУЗМАНОВИЋ-ЦВЕТКОВИЋ 1998; Šljivar 1999). It is also important to emphasize that all artefacts were discovered concentrated in the northern zone of the site, which gives possibly valuable information for our knowledge of the organisation of metallurgical activities within Vinča culture settlements.

As opposed to the amount of massive copper implements, jewellery and ores found in the Vinča culture sites, only a few pieces of slag have been detected to date. A piece of slag coming from a context defined as oven in the house floor is recorded at Selevac (Glumac 1983; Tringham and Stevanović 1990; Glumac and Todd 1991; Figs. 15a, 15b),

and analysis confirmed copper prills and cuprite agglomerations embedded in a copper-calcium-iron silicate matrix.



**Fig. 15- a) image of slag sample from Selevac (courtesy of Dragana Antonović, Archaeological Institute, Belgrade);
b) photomicrograph of slag from Selevac. Note copper prills (A), cuprite (B) and glassy matrix (C)
(after Glumac and Todd 1991: 11, fig. 3)**

In addition, slag pieces are recorded in Gornja Tuzla and Stapari, but no analyses have been published (Jurišić 1959; Čović 1961; Glumac and Todd 1991; Fig. 16). In Anzabegovo stratum IV, Gimbutas (1976) reported a piece of slag in a level C14 dated to 5200 BC. Moreover, recent excavations of Belovode yielded a few pieces of slag in one of the Trenches (Šljivar 2006), which will be presented in detail in this thesis.



Fig. 16- A piece of slag from Gornja Tuzla (after Glumac and Todd 1991: 12, fig. 4)

Crucibles have been reported in two sites, Vinča and Belovode, but none have been analysed hitherto. A fragmented bottom of a crude vessel, half-full of pulverised malachite was recorded in Vasić's excavation of Vinča settlement (Antonović 2006),

assumed to represent a proof of metallurgical activities. At Belovode, few fragments of crude vessels with copper- rich material adhered to its walls were discovered (Šljivar 2006), and will be described in more detail below.

History of Research and Previous Studies of Belovode

Belovode- Veliko Laole represents thus far the Vinča culture settlement with the most diverse material indicating metallurgical activities recorded during excavations. The C14 dates set 5400 BC as the beginning of the occupational period, and 4600 BC as the time when it was abandoned (Borić 2007; Fig. 17). The site generally holds only Vinča culture horizons, where a small pit from one of the Trenches (No. VI) was found to belong to the Late Chalcolithic culture Kostolac (Шљивар и Јацановић 1998).

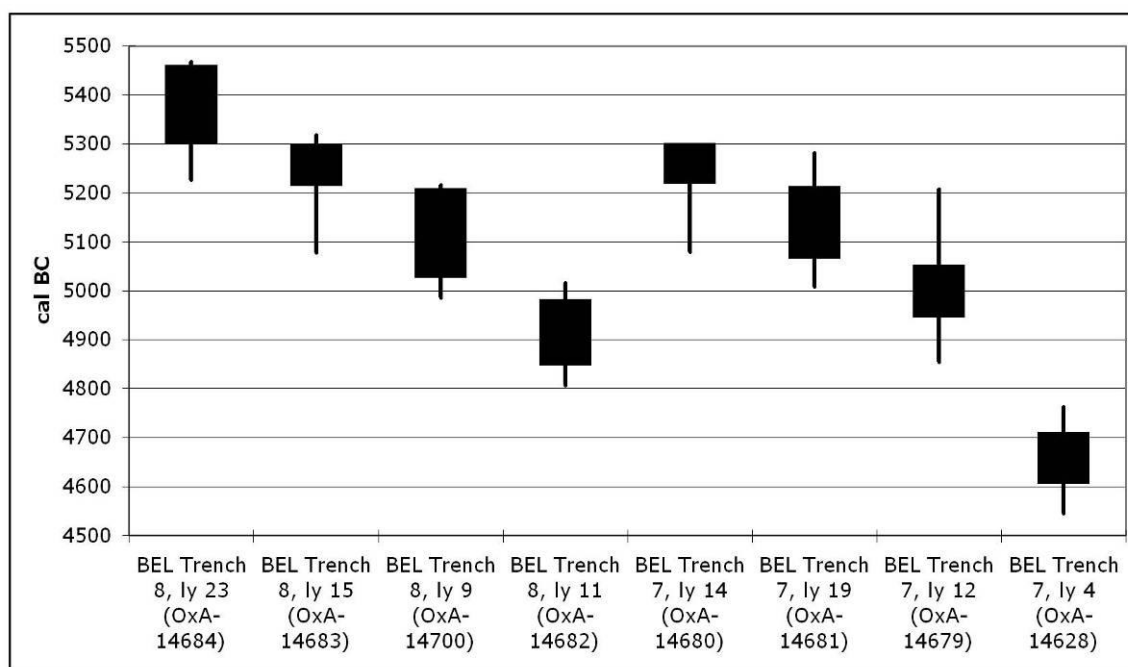


Fig. 17- C14 data for Belovode, Vinča culture horizon (after Borić 2007)

According to the relative chronology, Belovode was inhabited during the early phases of the Vinča culture, namely Vinča-Tordos to Gradac phase (Garašanin 1991; 1994-1995) or Vinča A to Vinča B2 (Milojčić 1949), which is at Belovode present as levels Belovode A to D (Šljivar and Jacanović 1996; Fig. 18).

BELOVODE		SUPSKA		SELEVAC			VINČA	GARAŠANIN	MILOJČIĆ
				Building Horizont ----- 1977-1978		Strati. Architec Phase			
Phase	A	Stratum	9 8				8m	VINČA-TORDOŠ I	VINČA A
Phase	B C	Stratum	7 6	I-IV V-VI	I II	I	6,5 m	VINČA-TORDOŠ II (two phases ?)	VINČA B1 (dept. CCA 7m)
Phase	D	Stratum	5	VII-VIII	III	II	6m	GRADAC PHASE	VINČA B2
		Stratum	4	IX	IV	III	4,1m	VINČA-PLOCNIK I	VINČA B2-C (dept above 5 m)
		Stratum	3 2 1		V	IV	3,48 m	VINČA-PLOCNIK IIa	VINČA C
								VINČA-PLOCNIK IIb	VINČA D

Fig. 18- Relative chronology and phase stratification of Belovode according to division of Garašanin and Milojčić of the Vinča culture, compared with Supska, Selevac and Vinča (after Šljivar, Jacanović and Kuzmanović- Cvetković 2006)

The site itself has been excavated from the beginning of the 1990's, and the research is conducted as part of a joint program of the National Museum of Belgrade and the Museum in Požarevac. It is located in the wider zone of the Morava river basin; about 130 km south of Belgrade (see Figs. 10 and 12). The site itself is set on a windy plateau, near the Mlava River (Fig. 19), and the estimated area inhabited is over 100 hectares.

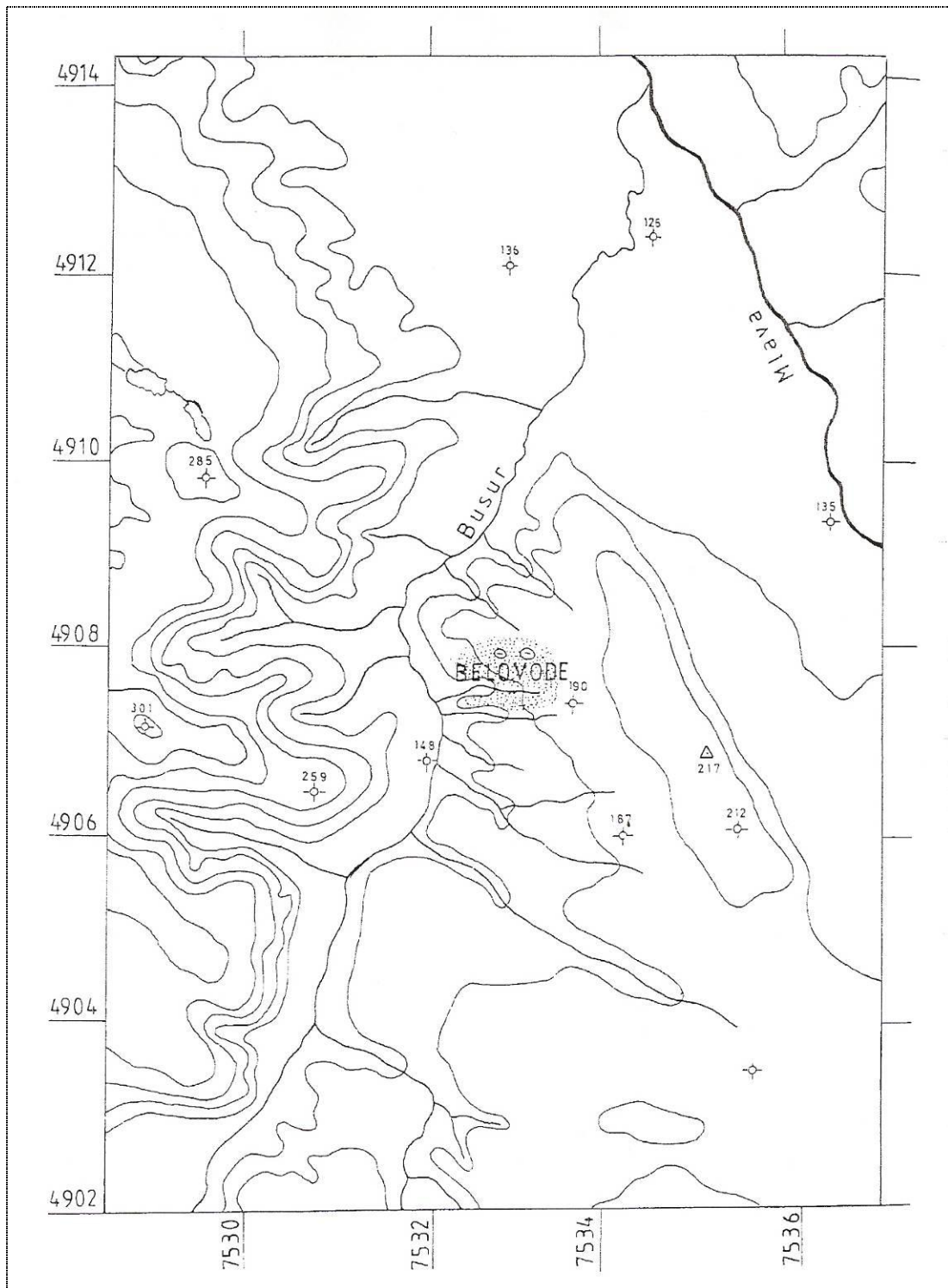


Fig. 19- Location of Belovode in the Mlava Valley (after Šljivar and Jacanović 1996)

Thus far, only 270 square meters have been investigated, within which 3 m of cultural layers were recognized and four building horizons distinguished (Šljivar and Jacanović 1996). The houses itself were documented with small assemblages of building materials near bigger ones, probably representing big and small units within a household with different economic purposes. After levels Belovode B and D, the settlement was set on fire; after the last attempt, it was abandoned eternally (Шљивар и Јацановић 1997; Archive of the National Museum of Belgrade).

The location of the site corresponds with typical Vinča culture settlement settings: a large rolling plateau of ellipsoidal shape with the Belovode spring running through the site (cf. Garašanin 1973). At an altitude of 200 m, agricultural activities were suitable, here probably followed by cattle breeding on dense forests and pastures in the surrounding area (Šljivar, Jacanović and Kuzmanović- Cvetković 2006). The nearby Mlava River goes deep in the volcanic mountain Homolje, which belongs to the zone of primary copper mining and metallurgy (Krajnović and Janković 1995). The whole surrounding area of the Gornjak gorge and mountain Vukan have been described as abundant in ancient mining shafts by Hofman (Jovanović 1991: 190), who recognized old shafts with slag heaps nearby. Analysing one of the ore veins in the Vukan Mountain, Jovanović (1991) documented pyrite, chalcopyrite, magnetite, galenite and sphalerite as the main minerals filling (Table 4).

sample	S	CaO	Mn	Fe	Cu	Zn	Pb	Un-dissolved material
	%	%	%	%	%	%	%	%
Ore	19.93	11.14	0.39	31.97	7.91	0.17	12.58	15.89

Table 4- Analyses of ore vein in the Vukan Mountain (*after* Jovanović 1991: 190)

These facts prompted a site survey which resulted in discovering a small mining shaft in the village Ždrelo, 10 km away from Belovode and close to the spring of the Reškovića River, by which archaeometallurgical activities were registered from the Bronze Age onwards (Шљивар и Јацановић 2003).



Fig. 20- Open-air Trenches at Ždrelo (photo by Dušan Šljivar)



**Fig. 21- a) Entrance of the shaft- hole at Ždrelo. Note copper mineralizations (green and blue veins) (photo by Dušan Šljivar);
b) Shaft-hole at Ždrelo. Note dimensions of the opening- c. 1m (photo by Dušan Šljivar)**

The mine was found in the exceptionally steep slopes cut with symmetrical vertical Trenches starting from the bank of the river Reškovića to the very top of the hill (Fig. 20). It is assumed that mineralizations of malachite and azurite were followed on the surface, resulting in digging the shaft, which had 1 m opening diameter (Figs. 21a and

21b). No artefacts have been found in the shaft hole, and the vein rich in malachite was sampled for further analyses (Šljivar, Jacanović and Kuzmanović- Cvetković 2006).

The whole settlement lies on deposits of mineral coal, which in the western areas of the plateau reaches the surface. This appears to be convenient for metallurgical as well as other economic activities, particularly having in mind that these rich deposits were exploited by the mid-20th century by the inhabitants of modern Belovode village.

Lumps of malachite and azurite represent the most numerous finds encountered in all layers in the settlement. Most of them were found mixed with ash and small pieces of charcoal, hence assumed to display the thermal treatment applied (Šljivar, Jacanović and Kuzmanović- Cvetković 2006; see Table 5 in Appendix Tables, Fig. 22).

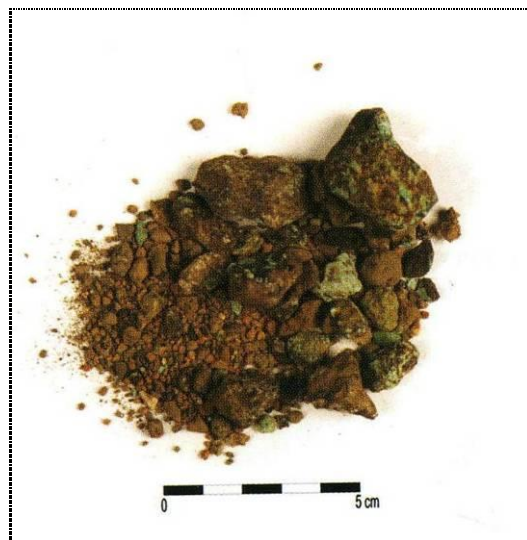


Fig. 22- Malachite lumps from Belovode
(after Šljivar, Jacanović and Kuzmanović- Cvetković 2006: Pl. I/7)

The vast majority of copper ores, mainly malachite, was found in Trench VII, situated in the southern part of the settlement (Шљивар и Јацановић 2003). From a large area in this Trench (approximately 2x2 m) the quantity of collected malachite was about 800 gr, obtained on the spot by flotation and separated from the small lumps of charcoal (Šljivar, Jacanović and Kuzmanović- Cvetković 2006; Fig. 23).



Fig. 23- Malachite from Trench VII, Belovode. Note charcoal separated on the right side (after Šljivar, Jacanović and Kuzmanović- Cvetković 2006: Pl. I/6)

The archaeological record also reveals a stone construction in this Trench, with deposition of stone axes, pestles and millstones on it; which led the excavators to assume the remains of a workshop in this Trench. Moreover, earlier levels belonging to Belovode B-C revealed two heavily burnt surfaces (5-8 cm thick) which contained remnants of charcoal, ash and copper ores adhered to them. In addition, a big lump of slag (?) was found, which section is described as reddish- yellowish with metallic appearance (Шљивар и Јацановић 2003).

All copper ores in the archaeological record from Belovode are described as malachite, though many of them have diverse geological inclusions and hence belong to other types of ores. They are found in all Trenches, varying in size and context of finding (see table 3). The context varies from dwelling structures to depositing pits, and ritual activities discovered in Trench VI. Three kilns, founded with ceramic sherds and stone and lined with greyish-white clay, were discovered sitting on a clean embankment, with large zoomorphic figurines of oxen, cow and calf placed in their centre (Шљивар и Јацановић 1998).

Trenches VIII to XI represent courtyards of houses situated next to each other. No. X and XI yielded two shallow pits (“furnaces”?), rimmed with ceramic sherds and burnt layer of clay (Fig. 24). One of them is associated with malachite lumps in the vicinity, believed to be deposited in amphorae from the same Trench (Šljivar 2006; Figs. 25a and 25b).



**Fig. 24- Field context of the shallow-pit furnace (upper right corner), Trench X
(photo by Dušan Šljivar)**



Fig. 25- a) photo of fragmented amphorae, assumed to had contained malachite lumps (photo by Dušan Šljivar); **b)** photo of malachite lumps found near the shallow pit from Trench XI. Note two piles of fine and coarse lumps, and separated charcoal on the right side of the image (photo by Dušan Šljivar)

The second most numerous finds encountered in all cultural horizons at Belovode are beads made of malachite (Fig. 26a), and a total of 20 beads with diameters varying from 4 mm to 1.5 cm were discovered. The vast majority was found in the southern part of the settlement, related to ores and slag, workshop activities or dwelling structures. As an exception, a deltoid pendant with perforation was found in Trench I (Fig. 26b), coming from Belovode A phase (Šljivar, Jacanović and Kuzmanović- Cvetković 2006).



Fig. 26- a) malachite beads from Belovode (after Šljivar, Jacanović and Kuzmanović- Cvetković 2006: Pl. I/8); **b)** deltoid pendant made of malachite from Belovode, Trench I (after Šljivar, Jacanović and Kuzmanović- Cvetković 2006: Pl. II/1)

Beads and malachite lumps are yet the only samples studied from this site: three amorphous pieces of green, blue and brown colour, a green pendant and a green bead

from Trenches I and II have gone under mineralogical study (Jović 1996). Under X-Ray Diffraction, the green piece showed the structure of malachite, with tenorite and calumetite; the blue piece was azurite, and brown consisted of tenorite, malachite and kolwezite. Both bead and pendant had malachite as the main compound and small amounts of tenorite and kolwezite (Jović 1996).

Two stone mallets with a groove in the middle were discovered on the “working” surface of Trench VII, and in the house from Trench I. Both of them, along with two more surface findings, resemble stone mallets from Rudna Glava (Fig. 27), used for ore crushing (Šljivar, Jacanović and Kuzmanović- Cvetković 2006).



Fig. 27- Stone mallet from Trench VII in Belovode
(after Šljivar, Jacanović and Kuzmanović- Cvetković 2006: Pl. I/4)

Small lumps of slag were found only in Trench III, described as a depositing pit. They originate from four excavation layers, and were found associated with copper ores, malachite beads, as well as thick layers of charcoal. One lump of slag was discovered associated with animal bone, which obtained a green staining as a result of contact with copper ores in post-depositional processes (Šljivar i Jacanović 1996).

Few small-sized pottery vessels of conical shape and coarse fabric found on the site are believed to represent crucibles, but no analyses have been conducted to date. All three “crucibles” originate from Trenches VII and VIII, situated in the southern part of the settlement. Whilst Trench VII revealed indications for workshop activities, the

“crucible” from Trench VIII was found covered with ash, and lumps of malachite (Archive of the National Museum of Belgrade).

Two shallow pits originating from Trenches X and XI are thought to represent early furnaces, mainly based on analogous finding from Durankulak in Bulgaria, where the pit had traces of thermally treated malachite (Dimitrov 2002). The finding of a fragmented human jaw near to these pits could potentially indicate their purpose (Šljivar 2006).

In addition, three pottery objects in the shape of chimneys were found- two from Trench VI and one from Trench IX (Figs. 28a, 28b). They are hollow cylindrical objects with slightly conical shape, which is suggested to serve as part of metallurgical installation, aimed to stimulate air circulation for copper ore smelting (Šljivar, Jacanović and Kuzmanović- Cvetković 2006; Fig. 29).



Figs. 28a, 28b – Ceramic “chimneys” from Belovode, reconstructed. Note marks of secondary burning (photo by Dušan Šljivar)

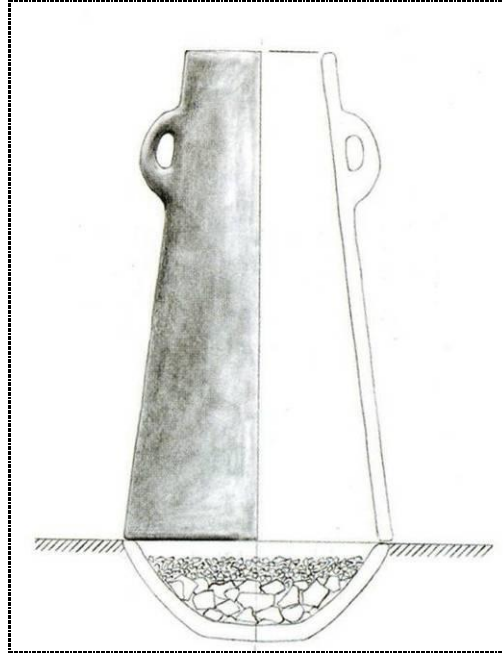


Fig. 29- Reconstruction of the possible usage of “chimneys” found at Belovode
(after Šljivar, Jacanović and Kuzmanović- Cvetković 2006: Pl. II/5)

The surface area yielded two more objects made of copper: a chisel (Fig. 30) and a bun-shaped ingot (Fig. 31). They are all found in the vicinity of the settlement, and could possibly be ascribed to Belovode’s cultural assemblage.



Fig. 30- Copper chisel found in the vicinity of Belovode (surface finding)
(after Šljivar, Jacanović and Kuzmanović- Cvetković 2006: Pl. I/1)

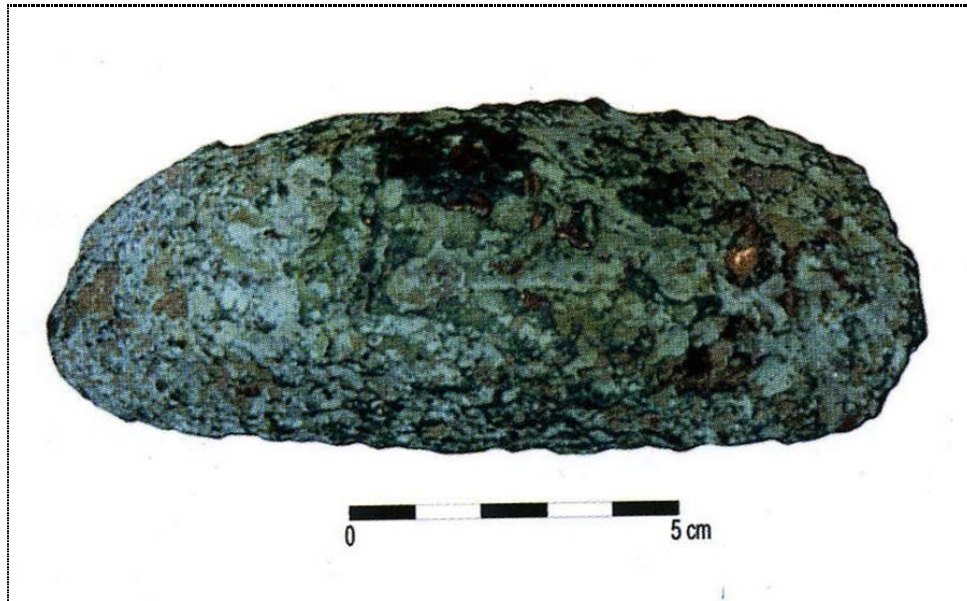


Fig. 31- Copper ingot found in the vicinity of Belovode (surface finding)
(after Šljivar, Jacanović and Kuzmanović- Cvetković 2006: Pl. I/2)

Furthermore, a fragment of a ceramic mould was found on the site surface, probably belonging to its latest level, Belovode D (Fig. 32).



Fig. 32- Surface finding: ceramic mould from Belovode
(after Šljivar, Jacanović and Kuzmanović- Cvetković 2006: Pl. I/3)

Definition of Problem

Although diverse materials indicate metallurgical activities in the Vinča culture, little has been done hitherto to facilitate a clear understanding of metal processing in this culture. Few analyses conducted thus far suggested the presence of smelted copper ore (slag from Selevac) and massive copper implements made of high-purity copper (implements from Pločnik). What is more, several sites yielded evidence for a specific organization of the living space, particularly in terms of setting the metallurgical activities on the periphery of the settlement or in defined zones (Selevac, Divostin II, Belovode, Pločnik). These records, along with technological advancement detected at the very end of the 6th millennium BC, tell us about the economical as well as social influence of the apparently new material- metal introduced in the Late Neolithic cultures in Southeast Europe. The emphasis of this discussion is on pyrotechnological activities with copper ores, or what was long-termed as “intelligent” metallurgy (Childe 1944), as opposed to cold processing of native copper or malachite.

Thus, there is an open question of how the remnants of copper processing relate to each other, and how much they can tell us about the metallurgical activities carried out in the Vinča culture. As Ottaway (2001) recognized, the *chaîne opératoire* of metal production always requests a complex set of actions, such as prospecting of minerals, extraction, beneficiation, transportation to the smelting location, building the furnace, its preheating, choosing the number and position of tuyeres, finding fuel, choosing the ratio of ore to fuel and controlling smelting conditions. In the case of the Vinča culture, evidence for this kind of specialization in metal processing is scarce (if any), but there is a clear indication of metallurgical activities performed at the sites nearby large ore deposits, or set on windy platforms. In addition, various materials that indicate ore processing (cold or hot treatment) discovered in the Vinča culture layers, along with mainly un-stratified massive copper implements, clearly lack the evidence for workshops.

Therefore, the diverse evidence for copper- related activities recorded at Belovode could indicate the presence of a workshop within the settlement, yielding its raw material- ores and debris- slag in one particular area. These materials, together with stone mallets, the

copper ingot and the ceramic mould from the surface, along with a mine in the vicinity, could for the first time offer evidence for smelting activities in the Vinča culture, setting the beginnings of metallurgy in this region much earlier than it was previously thought. The aim of this research is to characterize the structure and composition of materials indicating metallurgical activities in Belovode and explore their relation within the site and with ore deposits in the vicinity. The goal of the results presented here is to demonstrate and test evidence for copper smelting in Belovode, setting them in the wider archaeological context of the Vinča culture, and the Late Neolithic/Early Chalcolithic surrounding in Southeast Europe. The particular emphasis in interpretation will be placed on its cultural and chronological relations with Anatolian sites, aiming to widen our knowledge about the beginnings of copper smelting in the Old World.

Methods and methodology

The material indicating metallurgical activities from Belovode (around 500 samples) is deposited in the National Museum Belgrade, Department of Prehistory, out of which a total of 34 were selected to represent each grouping: slags, archaeological ores (Belovode), geological ores (Ždrelo), artefacts (ingot and malachite beads) and ceramics. The sample selection was performed in the National Museum in Belgrade, where selection itself was done based on macroscopic and cross-section features of the samples. The approach of this research was to relate chemically and mineralogically the objects to each other, in order to identify the past metallurgical processes that had produced them.

Twenty samples were chosen for research: two were ground to pellets, one was observed microscopically and seventeen were mounted in epoxy resin and polished with diamond paste, with final polish being $\frac{1}{4}$ μm . Depending on their size, the samples were either mounted completely or cut to shape, after being described macroscopically (see Catalogue in Appendix). Prepared as described above, samples were suitable for optical microscopy, ED-XRF, SEM-EDS and EPMA analyses (see Table 6). A total of 12 samples (geological ores, archaeological ores, slags, malachite bead and copper ingot) were analysed with ICP-MS for lead isotope and trace element analysis. For slag samples, the first question was how their chemical compositions relate to archaeological ores from the site and geological ores from Ždrelo. This allows identifying slag phases, with particular emphasis on gangue material (indicating smelting rather than melting process). Also, the amounts of silica, potash, lime and iron oxide present in the slag were considered to discuss the fuel charge, as well as possible addition of flux. Secondly, the degree of oxidation of the phases in slags was considered, suggesting redox conditions of the metallurgical process, as well as corrosion from post-depositional processes. In addition, the composition of slag matrix was used to estimate average temperature of the smelting process. Thirdly, the metallic phases entrapped in the slag were examined to assess the nature of the metal produced, their relation to ores and ingot, as well as redox conditions of the smelting activity.

The artefacts (malachite beads, a lump of copper metal and the ingot) were studied to determine the technology of making and working and their relation to the slag and ore samples from the site. Trace element analysis of the copper ingot was performed in order to assess its relation to the excavated assemblage from Belovode.

Ceramic samples were analysed in order to assess indications of metallurgical processes carried out in them and evaluate whether they were particularly refractory.

The chemistry and mineralogy of both archaeological and geological ore samples were studied to relate them to the previously analysed objects. The main objective was to determine whether these samples could account for the metal associated with the slag, or the slag itself. Aspects to be discussed here include the content of copper, iron, manganese, magnesium, the nature of the gangue minerals and their relation to the slag chemistry, as well as the nature of the ore minerals: oxidic or sulphidic. Lead isotope analysis was conducted in order to relate lead abundance ratios of excavated samples from Belovode to the copper deposits in Ždrelo and other copper-rich areas in the region.

In addition, the XRF data for ceramic have to be considered only qualitatively, due to the fact that these samples were studied non-destructively as objects (ceramic sherds). The data provided with the analysis of prepared pellets of geological ores are taken into account on the qualitative basis for further comparison with slag composition. They were also considered as a rough estimate on the quantitative level.

All analyses were carried out at the Wolfson Archaeological Science Laboratory at the UCL Institute of Archaeology, except for provenance studies (ICP-MS) performed at the Curt-Engelhorn-Zentrum für Archäometrie, Reiss-Engelhorn-Museen in Mannheim (Germany).

Method	Aim of Analysis	Analytical Parameters
Microhardness testing (Vickers microhardness indenter, Cooke, Troughton and Simms, UK)	Characterization of sample's (metal) hardness	Vickers method (Hv) is applied, with an attachment for microhardness testing under 50 gr load (Vickers Instruments, UK). The indenter was calibrated with standardized steel block (148 Hv).
Reflected Polarized Light Microscopy (Leica DMLM)	Characterisation of microstructure of all samples.	Plane polarized light and crossed polarized light were applied to examine phases in the sample, their colour, homogeneity, porosity and inclusions (shape, size and uniformity). Cross-polarized light was also applied for internal reflection and identifying the composition of phases present. The microscope was equipped with a Nikon digital camera, with highest magnification of 1000x.
SEM-EDS Scanning Electron Microscope with an Energy Dispersive Spectrometer (Hitachi S-3400N Scanning Electron Microscope)	<ol style="list-style-type: none"> 1. Phase identification of ores, slags, copper ingot, malachite beads and ceramics, using electron images and area/point analyses 2. Quantitative compositional analyses of the phases observed within the sample 	<p>Secondary electron (SE) and backscattered electron (BSE) imaging applied. Environmental Scanning Electron Detector in VP-SEM (vacuum) mode was applied for analyses of malachite beads (Belovode 32, 33).</p> <p>The accelerating voltage was 20 kV, with average dead-time of 35-40 % and working distance of 10 mm. All data are presented as normalized with stoichiometrically added oxygen, if not otherwise stated.</p>
EPMA Electron Probe Micro Analyzer (JEOL JXA-8100)	Quantitative determination of metal and glassy (Si-rich) phases in slags	The machine was set up for Na, Mg, Al, Si, P, S, K, Ca, Ti, Cr, Mn, Fe, Co, Ni, Cu, Zn, As, Ba and Pb
ED- XRF Energy Dispersive X-Ray Fluorescence (Spectro X-Lab 2000)	Qualitative bulk analysis of samples	A three-target method (Turbo Quant-0261a) was used to analyse samples Belovode 1Mn and 2Mal prepared as pellets, and Belovode 26, 29 and 30 (all ceramics) as whole objects (inside and outside).
ICP-MS Inductively Coupled Plasma Mass Spectrometry (HR ICP-MS Axiom VG Elemental)	Lead isotope and trace element analysis	The measures were performed on 1.5 ml of a 200 ppm Pb solution using an Aridus (Cetac) to inject the sample. Each sample was measured once, where a measurement includes 3 runs.

Table 6. Characteristics of the analytical methods conducted on studied samples.

Results of Research: Analysis of Slag Samples

Slag represents material often produced in large quantities, usually discarded at the end of the process, which can withstand weathering with minimal chemical alteration and therefore provide valuable information on reconstructing past smelting technologies (Tylecote 1962; Bachmann 1982). For the earliest stages of metallurgy, however, slag is often preserved only in small quantities. All five samples so far identified from Belovode were analysed with reflected light microscopy, SEM-EDS, EPMA and lead-isotope analysis, in order to define phases, their composition, the distribution of elements, as well as their possible provenance and relation with the rest of the assemblage from Belovode.

Optical microscopy, SEM-EDS and EPMA analyses revealed slag to be extremely heterogeneous, slag containing various minerals and metal prills, with corrosion products developing on the sample's edges and between the phases. The main components identified with these analyses are oxides (cuprite and spinel), silicates and copper metal prills embedded in a partially crystallized glass matrix.

Bulk chemical analysis of slag matrix

The bulk chemical analyses of slag, avoiding copper oxide and copper prills were conducted using EPMA (Table 7). Although these dominated in all slag samples, the aim of the analyses was to determine the composition of the non-metallic (or siliceous) part of the slag, in order to better understand its origin as smelting or melting slag.

	Na2O	MgO	Al2O3	SiO2	P2O5	SO3	K2O	CaO	TiO2	MnO	FeO	CoO	NiO	CuO	ZnO	BaO	Total
	wt %	wt %	wt %	wt %	wt %	wt%	wt%	wt%	wt %	wt %	wt%	wt%	wt%	wt %	wt%	wt%	wt %
Av.20	0.19	1.25	11.60	26.68	10.36	0.04	1.26	5.04	0.33	4.11	9.32	0.52	0.04	27.79	1.20	0.27	90.74
Av.21	0.38	1.64	8.52	33.04	4.60	0.03	2.67	9.62	0.13	8.45	14.51	0.80	0.03	12.59	2.67	0.33	99.43
Av.22a	0.39	1.38	12.01	42.68	4.98	0.04	3.45	8.06	0.31	6.03	7.77	0.63	0.06	10.89	1.04	0.28	95.70
Av.22b	0.63	1.60	12.87	37.24	3.31	0.02	6.44	9.38	0.24	7.11	8.80	0.70	0.06	10.14	1.16	0.29	100.75
Av. 23	0.18	1.39	7.87	31.76	1.06	0.00	1.17	7.97	0.18	13.61	9.50	1.55	0.09	19.50	3.88	0.29	102.20

Table 7. EPMA- compositional data for Belovode slag samples, normalized to 100% (areas low in cuprite and copper metal). All values are the average of four to five analyses of each sample; the full data is reported in the catalogue of slag samples. Column “total” shows average analytical total prior to normalisation. The results for As₂O₃, PbO and Cr₂O₃ are not reported, as they were consistently below the detection limit of the instrument, of an estimated 100 ppm.

All samples have a rather similar composition, with greatest variations in copper, iron, manganese, silicon, calcium and potassium content (Fig. 33), which were mainly caused by various events taking place throughout the period of Belovode’s occupation, hence strengthening the assumption of different ores and fuels used.

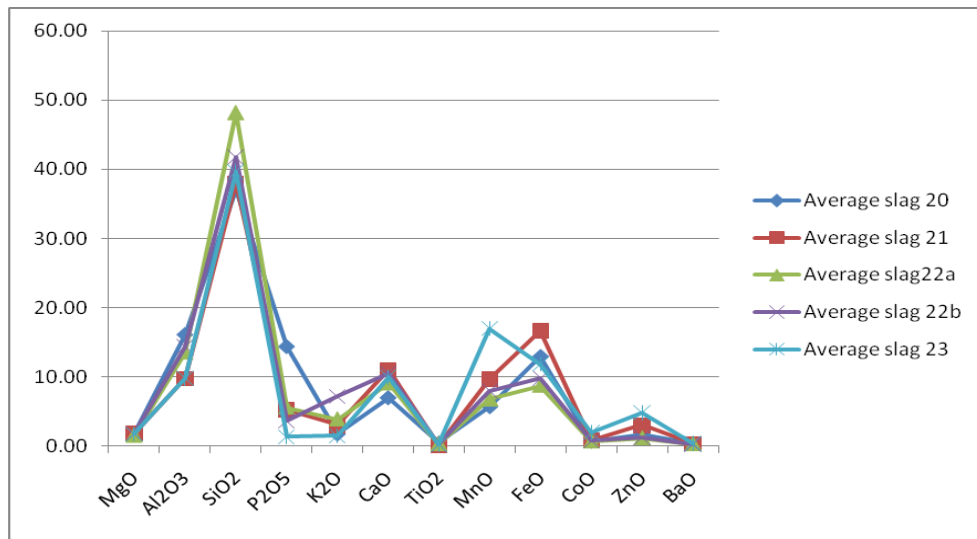


Fig. 33- Figure showing the average composition of bulk chemical analyses of slag matrix. Only metal oxides (except copper oxide) and phosphorus presented, normalized to 100% (see Table 8). Note differences in metal oxides content (FeO, MnO, ZnO) throughout the slag samples.

	MgO	Al ₂ O ₃	SiO ₂	P ₂ O ₅	K ₂ O	CaO	TiO ₂	MnO	FeO	CoO	ZnO	BaO
	wt%	wt%	wt%	wt%	wt%	wt%	wt%	wt%	wt%	wt%	wt%	wt%
<i>Average Slag 20</i>	1.74	16.12	37.09	14.40	1.75	7.01	0.46	5.71	12.96	0.72	1.67	0.38
<i>Average Slag 21</i>	1.89	9.80	37.99	5.29	3.07	11.06	0.15	9.72	16.68	0.91	3.07	0.37
<i>Average Slag 22a</i>	1.56	13.55	48.16	5.62	3.89	9.10	0.35	6.80	8.77	0.71	1.17	0.32
<i>Average Slag 22b</i>	1.79	14.44	41.78	3.71	7.22	10.52	0.27	7.98	9.87	0.79	1.30	0.33
<i>Average Slag 23</i>	1.73	9.81	39.58	1.32	1.46	9.93	0.22	16.96	11.84	1.94	4.84	0.36

Table 8. EPMA- compositional data for Belovode slag samples, normalized to 100%. Only metal oxides except for copper oxide, and phosphorus presented (see Table 7). All values are the average of four to five analyses of each sample; the full data is reported in the catalogue of slag samples.

The concentration of silica varies significantly, suggesting most likely diverse gangue material present in ores. All iron oxide levels are very low compared to later copper slags, ranging from c. 9% to 17 %, with a mean value of 12 % (see Table 8), indicating probably no flux added and the usage of self-fluxing ores. The readings for manganese oxide correlate with zinc oxide readings, in the range of 4:1/ 3:1 parts in all samples, suggesting their common origin from the ore. Also, ore composition could be indicated by the levels of cobalt, with significant values- up to 1.94 wt%. The plotting of readings in manganese, zinc and cobalt oxides (Fig. 34) exhibits good correlation among these components, with strong clusters for Slag 23 and 21 most likely indicating different batches of ore being used; possibly originating from a common ore source. The grouping of the remaining samples is set within one area as well, but less indicative for discrete batches. The iron oxide content plotted here with zinc oxide suggests that the iron in this case could have come from an external source, as crucible body, but less likely from the ore solely.

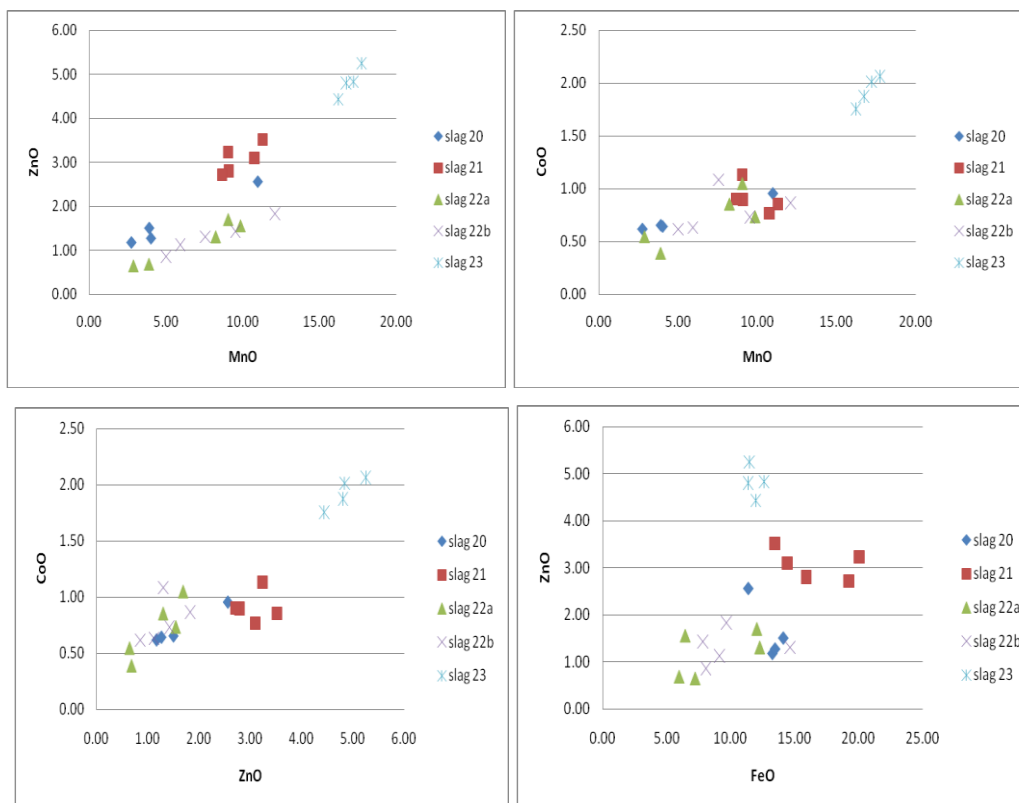


Fig. 34- Figures showing correlation of readings in MnO, ZnO and CoO, as opposed to FeO in bulk chemical analyses of slag matrix (data from Table 8 used).

In order to gain a more complete understanding of how this system would have operated, the slag compositions were plotted in a ternary diagram FeO-Al₂O₃-SiO₂ to facilitate comparison with equilibrium phase diagrams. From this diagram, would seem to be the operational temperature around 1470° (Fig. 35, see Appendix Figures; Slag Atlas 1995: 111). However, the presence of further oxides has to be taken into account; once plotted together in the diagram, the majority of data indicated lower temperature, around 1150°, hence more realistic to be achieved in the early smelting practice (Fig. 36).

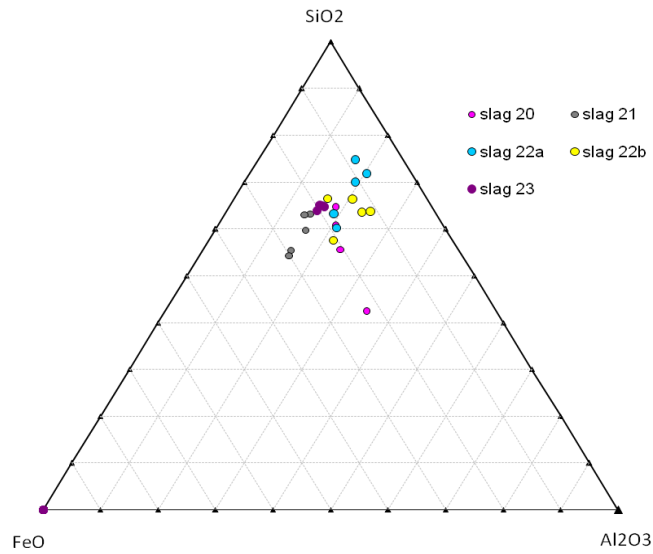


Fig. 35- Ternary phase diagram for SiO₂-FeO-Al₂O₃ indicating slag eutectic temperature around 1470° (see Appendix Figures).

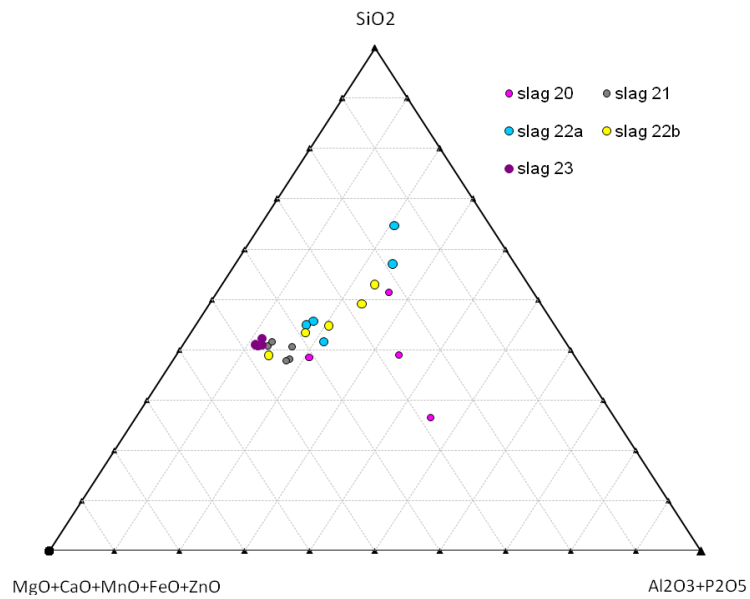


Fig. 36- Ternary phase diagram for SiO₂- MgO+CaO+MnO+FeO+ZnO-Al₂O₃+P₂O₅ indicating slag eutectic temperature around 1150° (see Appendix Figures).

Oxides

Copper oxides are the main phase present in all slag samples, both as cuprite (Fig. 37a and 37b) or corrosion product deriving from post-depositional processes (Fig. 37b).

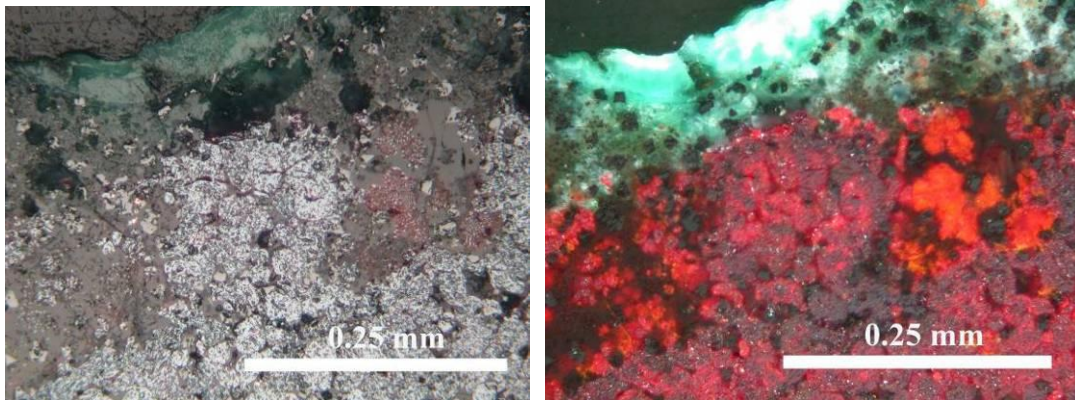


Fig. 37- a) Photomicrograph of cuprite (light grey) under plane polarized light (Slag 20); b) photomicrograph of cuprite (red/orange) and corrosion products (bright green) under cross polarized light (Slag 20). Note optically grey rhomboid inclusions, spinels, scattered in this area.

Distinguished by its typical bright red/orange internal reflection, cuprite is mostly represented with convoluted agglomerations developing in specific zones. It is also present as second and third generations of tiny fir-tree like crystals; the latter with yellow and light green reflections under cross polarized light (Fig. 38a, 38b).

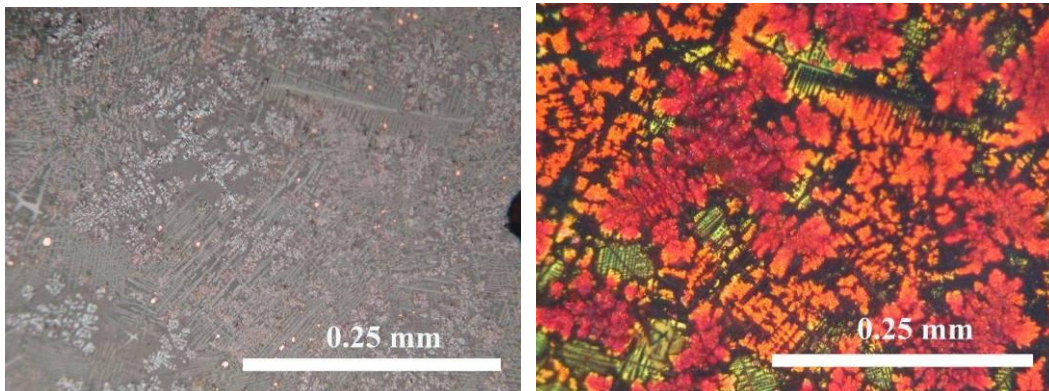


Fig. 38- a) Photomicrograph of dendritic cuprite (light grey) under plane polarized light (Slag 21). Note light grey dendrites of cuprite embedded in the grey glass matrix, with spinel dendrites developing in the same area. Bright spots are copper metal prills; b) photomicrograph of dendritic cuprite under cross polarized light (Slag 21). Note various colours of the second (red) and third (orange and green) generations of cuprite growing in the area.

The large areas of cuprite in slags are generally recognized as “dross”, a type of slag typically associated with melting processes (Bachmann 1982). Nevertheless, the microanalysis underlines the manganese and iron content present in the dross (Table 9; Fig. 39), allowing the assumption that they had derived directly from ores in the smelting process.

	MnO	FeO	CuO
	wt %	wt %	wt %
<i>Average Slag 20</i>	0.4	0.7	98.9
<i>Average Slag 21</i>	0.1	1.4	98.5
<i>Average Slag 22a</i>	0.2	0.5	99.3
<i>Average Slag 22b</i>	0.4	0.8	98.8
<i>Average Slag 23</i>	0.8	0.6	98.6

Table 9. SEM-EDS compositional data for cuprite normalized to 100%. All values are the average of two to ten analyses of each sample; full data is reported in the catalogue of slag samples.

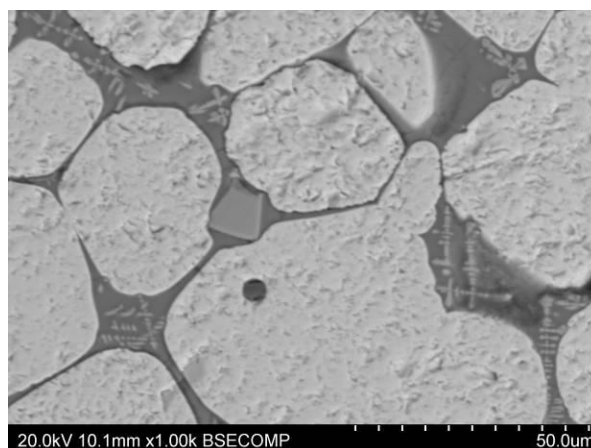


Fig. 39- Backscattered electron image of cuprite (light grey) embedded in grey glass matrix along with rhomboid and dendritic spinels. Compositional analyses (spot and area) revealed iron and manganese content in the cuprite inclusions (see Table 9).

Cuprite requires for its formation partially oxidising conditions, and as such is less commonly present in furnace slag. When forming the main part of slag samples it is rather related to the oxidising nature of smelting or melting processes in the crucible, possibly aided with air from blowpipes; but no evidence for such a device has been found on the site thus far.

After cuprite, spinels are the most common phases in the glass matrix. They were noted first under the optical microscopy as a grey phase of medium-sized cubic crystals or grains (Figs. 40a and 40b), or as dendritic crystals (Figs. 38a and 38b).

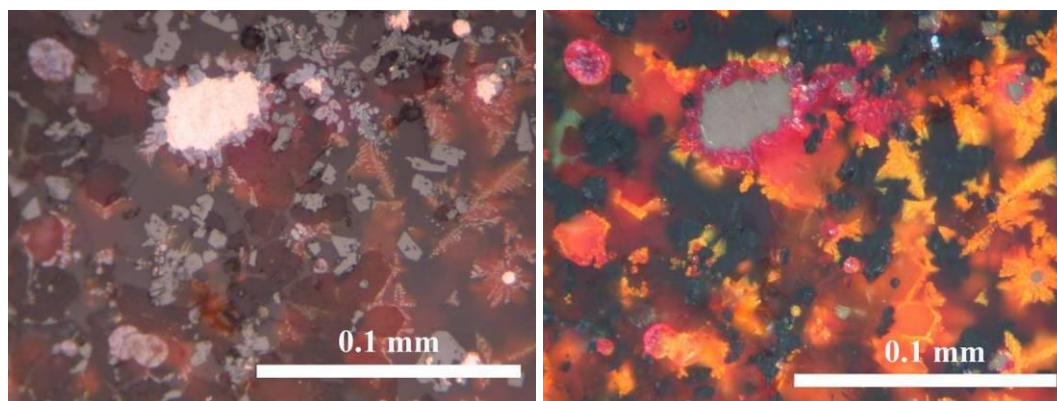


Fig. 40- Photomicrograph of grey cubic spinels under plane polarized light, embedded in glass matrix with corroded copper prills and dendritic cuprite (Slag 22b); b) photomicrograph of grey spinels under cross polarized light (Slag 22b), with copper prills and various formations of cuprite (red/orange/yellow).

These spinels generally have a ratio iron oxide to manganese oxide 3:1 (Table 10, Fig. 41), or 2:1/1:1 in dendritic formations, as well as with significant readings of aluminium, zinc, nickel and cobalt (for detail see Catalogue).

	MgO	Al ₂ O ₃	SiO ₂	P ₂ O ₅	K ₂ O	CaO	TiO ₂	Cr ₂ O ₃	MnO	FeO	CoO	NiO	CuO	ZnO
	wt %	wt %	wt %	wt %	wt %	wt %	wt %	wt %	wt %	wt %	wt %	wt %	wt %	wt %
Av. 20	2.9	12.0	0.0	0.0	0.0	0.0	0.3	0.0	15.1	54.6	2.5	0.8	3.6	8.2
Av. 21	1.2	4.8	0.0	0.0	0.0	0.0	0.0	0.0	14.9	67.6	1.0	0.1	4.7	5.8
Av. 22a	3.4	12.9	0.8	0.1	0.0	0.1	0.3	0.1	16.9	51.6	4.2	0.7	3.6	5.3
Av. 22b	2.6	10.5	0.3	0.0	0.0	0.1	0.6	0.2	16.7	55.7	4.0	1.0	3.5	4.7
Av. 23	1.1	9.5	1.7	0.6	0.1	0.4	0.2	0.0	16.6	49.2	6.0	1.1	5.2	8.3

Table 10. SEM-EDS compositional data for spinels, normalized to 100%. All values are the average of four to eight spot analyses of each sample; full data is reported in the catalogue of slag samples.

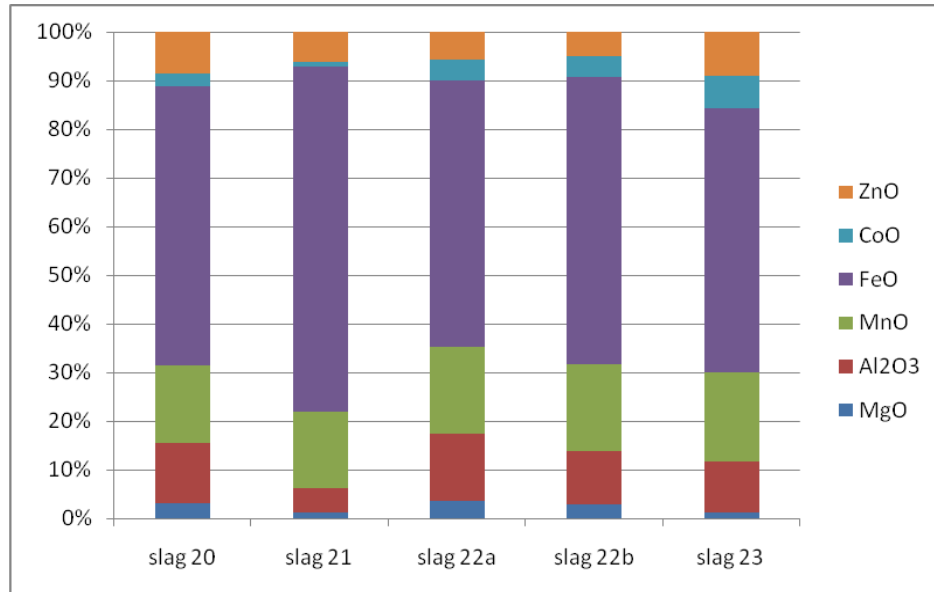


Fig. 41- Figure showing the average ratio of metal oxides forming spinels in all slag samples. All values normalized to 100%.

As seen in the tables, their trend is to form complex crystals, revealing different compositions of slightly varying ratios of tri- and divalent metal ions (Bachmann 1982: 16). The elements present in forming these crystals relate them to the franklinite (zinc iron manganese oxide) and hercynite (iron aluminium oxide) family of spinels.

Delafossite CuFeO_2 is optically recognized by its platy crystal morphology, here represented in straight lathes (Fig. 42a), and often surrounded by cuprite (Fig. 42b) and spinels (Fig. 43).

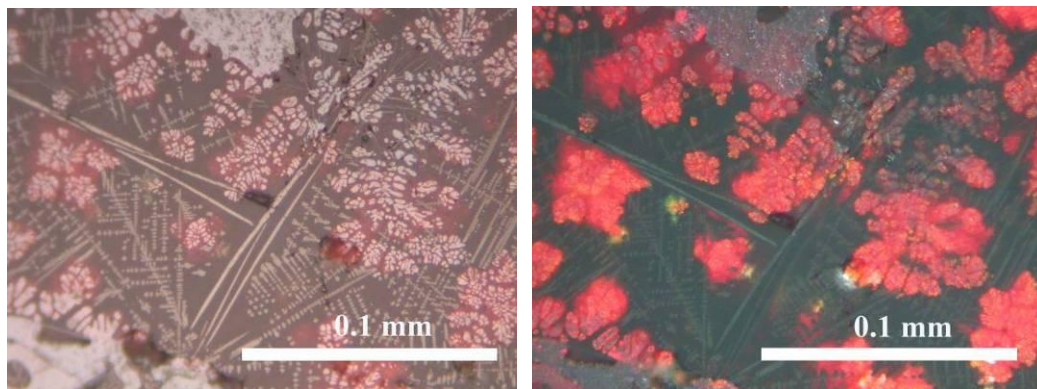


Fig. 42- a) Photomicrograph of delafossite under plane polarized light (Slag 23). Note straight lathes embedded in grey glass matrix along with various cuprite formations; b) photomicrograph of optically grey delafossite inclusions under cross polarized light (Slag 23).

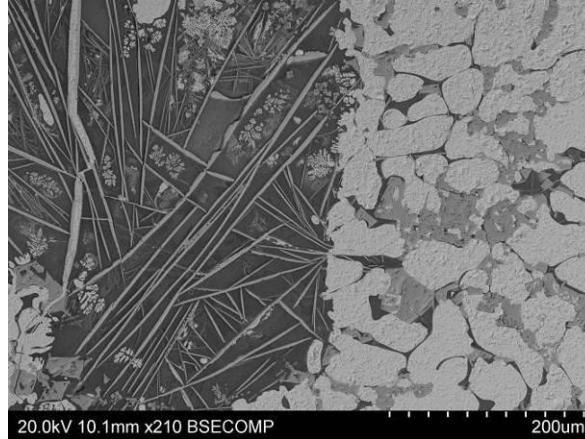


Fig. 43- Backscattered electron image of delafossite crystals surrounded with spinels and cuprite in glass matrix (Slag 21).

It also exhibits eutectoid intergrowth with cuprite, which is optically and chemically recognizable (Table 11, Fig. 44). Delafossite is believed to be typical for melting (crucible) slags, but is also known from smelting slags (Bachmann 1982). Hauptmann and co-workers (1993) outline the paragenesis of delafossite-cuprite-copper-magnetite in modern copper refining slags. However, Shugar’s (2000) accounts on Chalcolithic slags from Abu Matar add to this discussion, recognizing them as smelting slag. He emphasizes the presence of delafossite as indicative for a less reducing to partially oxidizing atmosphere during the smelting process combined with insufficient silica to form fayalite (see also Müller *et al.* 2004) ; which could suggest the same case for Belovode samples.

	Al ₂ O ₃	SiO ₂	CaO	TiO ₂	MnO	FeO	CuO
	wt %	wt %	wt %	wt %	wt %	wt %	wt %
<i>Average Slag 21</i>	0.9	0.9	0.0	0.2	2.1	42.9	53.0
<i>Average Slag 23</i>	3.3	1.7	0.6	0.8	4.5	37.3	51.9

Table 11. SEM-EDS compositional data for delafossite, normalized to 100%. All values are average of two analyses of each sample; full data is reported in the catalogue of slag samples.

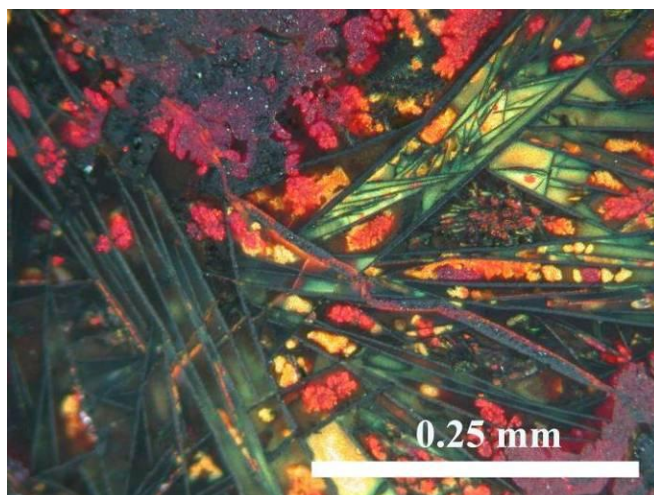


Fig. 44- Photomicrograph of delafossite under cross polarized light (Slag 21). Note straight lath in the centre inter-grown with red cuprite. Delafossite lathes are here surrounded with various formations of cuprite (red, orange/yellow and green).

Silicates

The examination of the silica-rich compounds is crucial when it comes to “fluxing” and assessing the complexity of a metallurgical process (cf. Hauptmann 2000), as well as how the addition of flux can that be distinguished from the smelting of self-fluxing ores. All silicates in the Belovode slags are found inter-grown mainly with spinels and occasional irregularly shaped copper prills, apart from bigger ones, which are badly corroded. Nevertheless, when separately analysed, they revealed two phases optically recognized as grey and dark grey (Fig. 45).

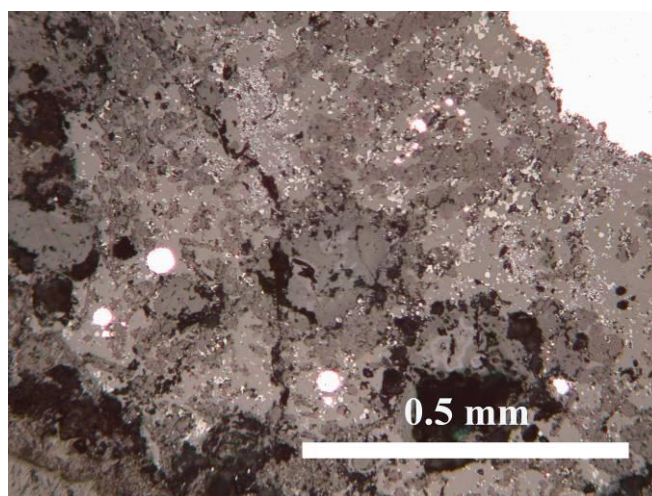


Fig. 45- Photomicrograph of silicates (glass matrix) under plane polarized light (Slag 22b). Note difference between prevailing grey substance surrounding dark grey polyhedral crystals. Bright spots are copper prills.

Silicates in slags are usually classified according to the ratio between metal oxides and silica (Bachmann 1982), and here the ratio between alumina, potash and silica in the dark grey glass revealed the formation of leucite, KAlSi_2O_6 (Table 12, Fig. 46). Optically, it is visible as polyhedral crystallization within the grey slag matrix, present in three out of five analyzed samples.

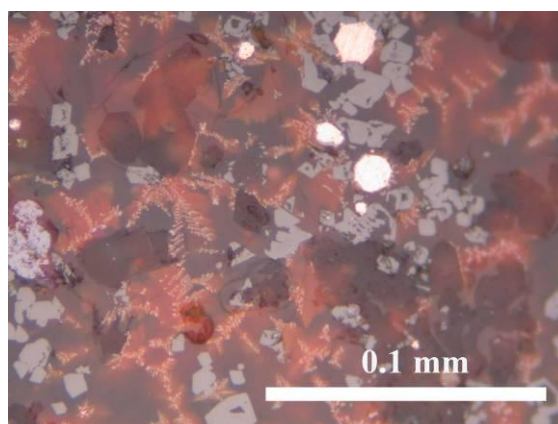


Fig. 46- Photomicrograph of dark grey transparent leucite crystals developed in glass matrix (Slag 22a). Note polyhedral formations embedded in grey matrix along with copper prills, spinels and cuprite dendrites.

	Na2O	MgO	Al2O3	SiO2	P2O5	K2O	CaO	TiO2	MnO	FeO	CoO	CuO	ZnO	BaO
	wt %	wt %	wt %	wt %	wt %	wt %	wt %	wt %	wt %	wt %	wt %	wt %	wt %	wt %
Av. 20	0.7	0.1	21.0	54.6	0.0	17.9	0.0	0.0	0.3	1.5	0.0	3.3	0.2	0.2
Av. 22a	0.0	0.0	19.4	54.1	3.2	14.5	1.3	0.0	0.1	1.4	0.0	6.0	0.0	0.1
Av. 22b	0.1	0.0	21.6	56.0	0.1	20.1	0.0	0.1	0.1	1.1	0.0	0.9	0.0	0.0

Table 12. SEM-EDS compositional data for leucite formed in glass matrix, normalized to 100%. All values are the average of four to eight analyses of each sample; full data is reported in the catalogue of slag samples.

The glass matrix of sample Slag 21 has trapezohedral crystals of similar optical appearance to leucite, but with a higher iron content (Table 13) in comparison with other samples (see also Catalogue). They could possibly indicate the formation of crystals belonging to the garnet family, morphologically similar to leucite described above. The higher readings of iron, along with manganese and zinc are probably caused by precipitation of spinel-forming oxides, found in great abundance throughout this sample.

	Na2O	MgO	Al2O3	SiO2	P2O5	K2O	CaO	TiO2	MnO	FeO	CoO	CuO	ZnO	BaO
	wt %	wt %	wt %	wt%	wt %	wt%	wt%	wt %	wt %	wt%	wt%	wt%	wt%	wt%
<i>Av.21</i>	0.0	0.0	7.5	61.7	2.8	1.4	1.4	0.2	3.6	9.6	0.0	9.5	2.2	0.0

Table 13. SEM-EDS compositional data for the optically dark grey glass matrix in the sample Slag 21, normalized to 100%. All values are average of five analyses; full data is reported in the catalogue of slag samples.

The optically grey glass matrix reveals significant readings in lime and manganese oxide, which along with its silica content could indicate glass of pyroxene type (cf. Bachmann 1982; Figs. 37a, 38a, 40a, 42, 43 and 45). The high lime content, around 15.7% in average, and the significant phosphorus content (see Table 14), are probably the result of a substantial fuel ash contribution in the smelting.

	Na2O	MgO	Al2O3	SiO2	P2O5	K2O	CaO	TiO2	MnO	FeO	CoO	CuO	ZnO	BaO
	wt%	wt%	wt%	wt%	wt%	wt%	wt%	wt%	wt%	wt%	wt%	wt%	wt%	wt%
<i>Average 20</i>	1.2	2.4	4.2	41.2	3.4	0.9	16.1	0.0	18.9	3.1	0.3	4.5	3.5	0.2
<i>Average 21</i>	0.8	1.4	6.2	42.5	3.5	2.1	12.2	0.0	14.7	8.6	0.0	4.5	3.3	0.2
<i>Average 22a</i>	0.8	3.2	6.6	37.4	5.0	2.0	19.2	0.3	12.8	3.9	0.7	6.4	1.7	0.0
<i>Average 22b</i>	1.0	3.1	5.9	37.0	4.8	1.8	20.8	0.3	13.8	4.5	0.5	4.5	2.0	0.0
<i>Average 23</i>	0.0	1.4	7.7	41.5	1.8	1.3	10.0	0.0	17.6	5.3	1.4	7.7	4.4	0.0

Table 14. SEM-EDS compositional data for the optically grey glass matrix in slag samples, normalized to 100%. All values are average of three to eleven analyses of each sample; full data is reported in the catalogue of slag samples.

Sample 21 showed a significantly higher lime content in one of the areas analyzed, possibly suggesting either more intensive reaction of the fuel or some other source of lime, such as the crucible ceramic (for detail see Catalogue).

The elevated levels of zinc and iron are possibly due to the composition of ore, along with the readings of barium and cobalt with values up to 1.2% and 2% (see Catalogue for Slag 20 and 23). Iron oxide levels are rather low, suggesting no intentional flux was added and hence the usage of self-fluxing ores. However, variable readings of iron oxide could indicate different ore sources being exploited and utilized in the metal processing in Belovode. On the other hand, the overall similar chemical composition (Fig. 47)

suggests that the same principle of ore processing was applied throughout the occupational period of this site.

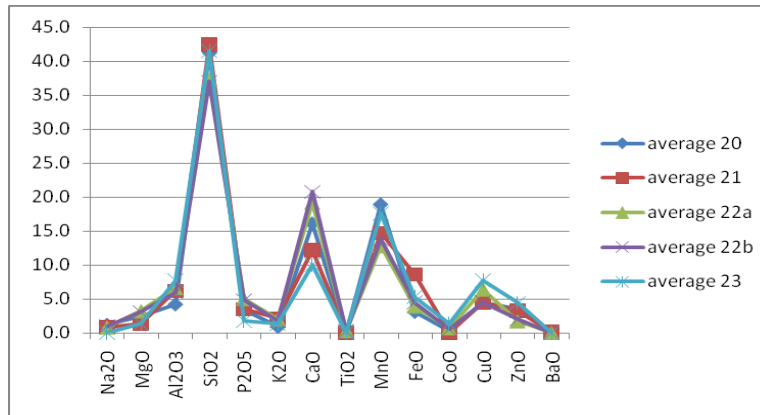


Fig. 47- Figure showing average composition of optically grey glass matrix in all samples. Note the consistent composition throughout the samples analyzed.

Metal prills

All slag samples contained numerous copper prills of various sizes, which are under reflected light microscopy conspicuous in their colour variation from bright to deep yellow (Figs. 38a, 40a, 45 and 46). They are mostly round in shape, with corrosion developing on their edges (Figs. 40a and 40b).

The fully crystallized bright α -grains formed in the eutectic of copper-copper oxide in the Slag 21 indicate smelting temperature around 1075° , as well as gradual cooling sufficient for the full formation of grains and dendrites (Fig. 48a). The characteristic red-orange internal reflection of oxide inclusions indicate presence of cuprite (Fig. 48b), which formed with less than 0.43 wt% oxygen present, around 0.22 wt% (see binary phase diagram in Appendix Figures; Neumann, Zhong and Chang 1984).

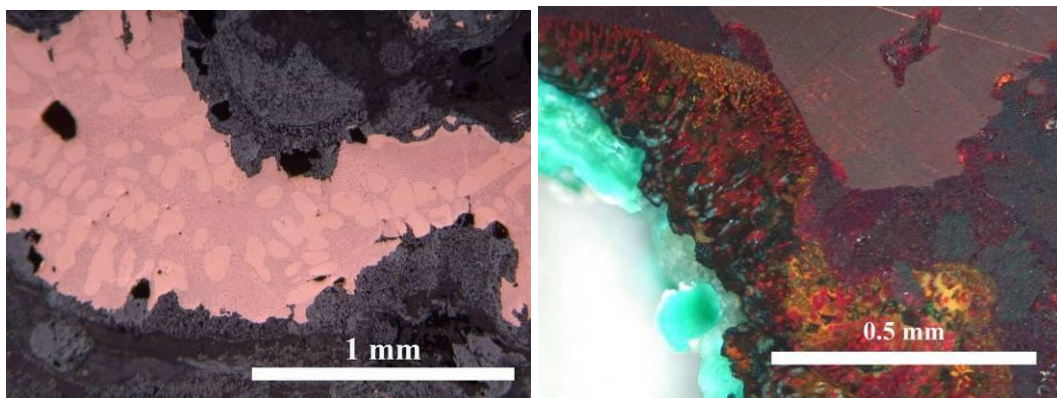


Fig. 48- a) Photomicrograph of copper metal in Slag 21 under plane polarized light. Note dendritic formation of α - grains in the copper-copper oxide eutectic; b) Photomicrograph of copper metal in Slag 21 under cross polarized light (up right). Note red internal reflections of cuprite forming eutectic in it.

EPMA confirmed the pure copper content of the α -phase, with significant impurities in form of zinc, probably on account of the ore content (Table 15). The low concentrations of iron and manganese in two samples are most likely detected by reason of spinel forming beneath the visible surface, picked within analytical volume of the instrument.

	O	Cu	Fe	Mn	S	Zn	Ba	Total
	wt%	wt%	wt%	wt%	wt%	wt%	wt%	wt%
<i>Average Slag 20</i>	0.32	99.59	0.00	0.00	0.00	0.10	0.00	97.93
<i>Average Slag 21</i>	0.44	99.47	0.00	0.00	0.01	0.08	0.00	99.05
<i>Average slag22a</i>	1.50	98.08	0.03	0.02	0.00	0.37	0.00	98.53
<i>Average Slag 22b</i>	0.22	99.69	0.00	0.00	0.00	0.09	0.00	99.17
<i>Average Slag 23</i>	0.20	99.66	0.01	0.01	0.00	0.09	0.00	98.18

Table 15. EPMA compositional data for metal prills in Belovode slag samples, normalized to 100%. All values are the average of two to four spot analyses of each sample; full data is reported in the catalogue of slag samples. Column “total” shows average analytical total prior to normalization.

Further observations include the remains of charcoal in sample 22a (Figs. 49a and 49b), identified by its characteristic cellular structure.

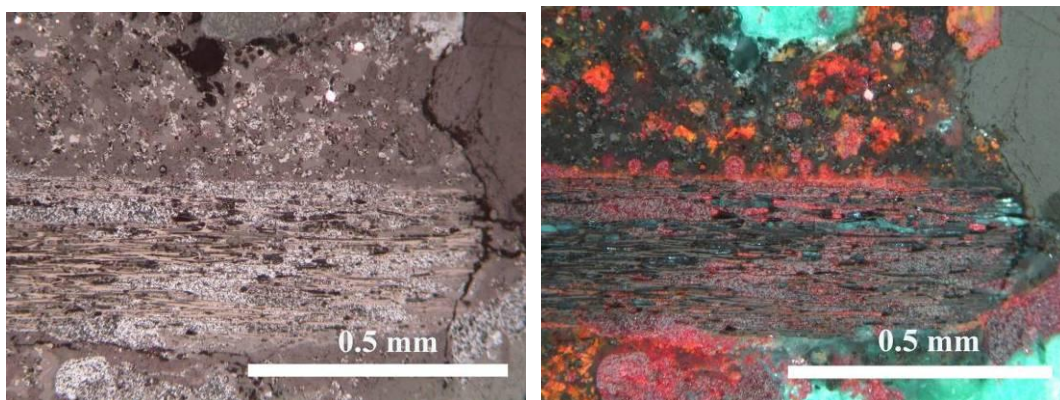


Fig. 49- a) Photomicrograph of charcoal in Slag 22a under plane polarized light; b) photomicrograph of charcoal in Slag 22a under cross polarized light.

The analyses of slag samples pointed at heterogeneous structures, which are supported with their origin from various excavation layers in Trench III in Belovode. However, despite the detected variations in composition, all samples clearly pointed at same type of ore and processes taking place, but in different events. The character of the metallurgical activity is strongly indicative as smelting, rather than melting, which is generally based on significant amount of various metal oxides in the non-cuprous part of the slag samples.

Results of Research: Analysis of Ore Samples

Geological ores

Geological ore is the term here reserved for ores originating from Ždrelo (Fig. 50), a copper mine in the vicinity of Belovode. Several lumps of ore were collected during the field survey; two of them were pressed ground and pressed into pellets and analyzed with ED-XRF (Table 16).



Fig. 50- One of the shaft-hole entrances in Ždrelo (photo by Dušan Šljivar)

The first impression one gains from the ED-XRF results is the heterogeneity of the analyzed samples, though both originate from the same ore vein. The copper oxide content varies; it is around 7 % for Ždrelo C1, and 15 % for C2. The iron oxide readings are higher in sample Ždrelo C1 than in C2, as well as levels of silica, lime and magnesia.

On the whole, both samples are rich in copper oxides, although gangue oxides (particularly silica, alumina, magnesia and iron oxide) reach substantial amounts.

This leads to the first fundamental link to the slag samples described above- the smelting of these ores would produce slag rich in all gangue elements, but not with significant amounts of cobalt oxides (see Table 7). On the other hand, although the analytical set-up is different, there is a link between slags and ores, based on qualitative compositional analyses. The quantitative relation is vague: magnesia occurs in comparable amounts for sample Ždrelo C2, but levels of iron oxides are rather low for comparison; however the alumina-silica ratio in the ores is greater in the sample Ždrelo C2, as opposed to sample C1 which appears to have a rather similar ratio with most of the slag samples.

Nevertheless, although comparable readings in gangue oxides can match certain slag samples, there is still the question of significant cobalt oxide readings in the slags that do not match these ores; which in turn could be explained by potential co-smelting of different types of ores.

	MgO	Al ₂ O ₃	SiO ₂	P ₂ O ₅	SO ₃	K ₂ O	CaO	TiO ₂	MnO	Fe ₂ O ₃	CuO	Cl	V ₂ O ₅	Cr ₂ O ₃	CoO	NiO	ZnO	As ₂ O ₃	SrO	Y	Ba	Ce	PbO	Total	
	%	%	%	%	%	%	%	%	%	%	%	ppm	ppm	ppm	ppm	ppm	ppm	ppm	ppm	ppm	ppm	ppm	ppm	ppm	%
ZdrC1	6.21	8.96	47.66	0.20	0.49	1.13	16.07	0.29	0.22	11.71	6.91	143	74	87	188	79	560	54	74	0	44	0	156	91.31	
ZdrC2	1.52	31.19	36.52	0.09	0.62	1.42	3.45	0.05	2.15	4.15	15.61	0	0	0	632	330	29232	229	100	213	0	192	1383	65.84	

Table 16. ED-XRF compositional data for ores from Ždrelo, normalized to 100%. Column “Total” shows analytical total prior to normalization.

Archaeological ores

Archaeological ore is the term reserved for ores originating from the excavation layers in Belovode. Samples presented here were selected out of more than 200 lumps of ores from the site, each representing a optically different group, recognized during the selection in the National Museum of Belgrade. All samples were analysed optically and chemically, and though originating from different trenches and excavation levels (see Catalogue in Appendix), they can be classified in two groups: oxidic and dark ores.

OXIDIC ORES

Although optically different, samples Ore 9, Ore 12 and Ore 19 reveal the dominant copper content, which characterizes the body of these minerals. The difference appears in the oolitic structures in their bodies, allowing optical discrimination of each sample prior to chemical composition.

Sample Ore 9 reveals a typical mineral structure, here distinguished by optically green colour as one of the copper carbonates, malachite. Two distinctive phases are detected: the green needle-like structure as the prevailing one, stained with light grey oolitic formations, which is recognized as the second phase (Figs. 51a and 51b).

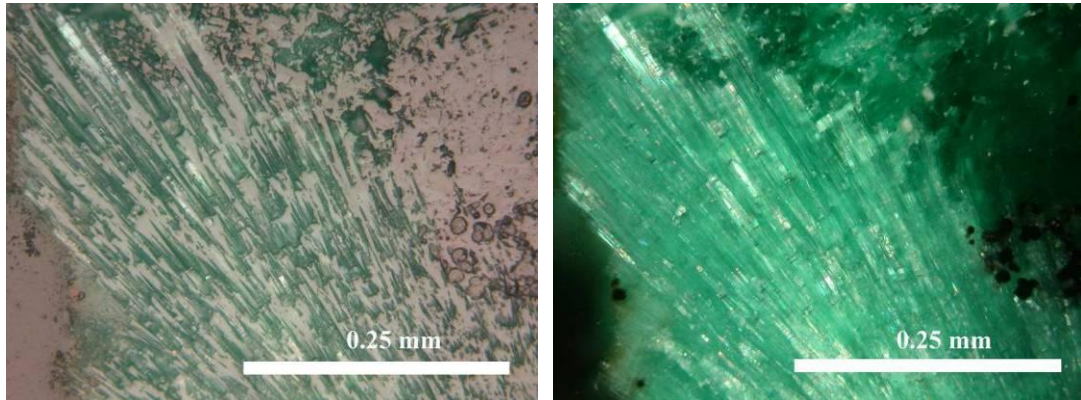


Fig. 51- a) Photomicrograph of phases in Ore 9 under plane polarized light. Note green needle-like phase with grey ooids developing in the right centre of the image; b) photomicrograph of phases in Ore 9 under cross polarized light. Note the same green structure now stained with dark phases rich in manganese oxide.

The green radiating crystals revealed chemical composition based on copper oxide, and minute concentrations of zinc oxide, around 2.7% in average (Table 17). Since copper oxide is either red (Cu_2O) or black (CuO) it is assumed that this phase is in fact copper carbonate, malachite. On the other hand, the oolitic formations in the copper-based body pointed at equal concentrations of manganese and copper oxide, along with silica, alumina and lower readings in lime and zinc oxide (Table 18).

	CuO	ZnO
	wt%	wt%
Minimum	94.7	1.6
Maximum	98.4	5.3
Average	97.3	2.7

Table 17. SEM-EDS compositional data for minimum, maximum and average values for the optically green phase in Ore 9; fully reported in the catalogue of ore samples. All values previously normalized to 100%.

	Al ₂ O ₃	SiO ₂	P ₂ O ₅	CaO	MnO	FeO	CuO	ZnO
	wt%	wt%	wt%	wt%	wt%	wt%	wt%	wt%
Minimum	3.9	18.6	1.3	2.6	26.7	1.2	29.8	0.0
Maximum	6.2	26.5	2.5	3.4	34.7	7.5	38.1	2.1
Average	4.9	21.6	1.9	3.0	30.9	3.7	33.2	0.8

Table 18. SEM-EDS compositional data for minimum, maximum and average values for the optically light grey phase in Ore 9; fully reported in the catalogue of ore samples. All values previously normalized to 100%.

Ore 12 is optically confirmed as mineral, with major green/light grey phase and optically reddish-brown oolitic structures developing in it (Figs. 52a and 52b). Green crystals revealed the copper-based structure, with minute concentrations of manganese and zinc oxides (Table 19).

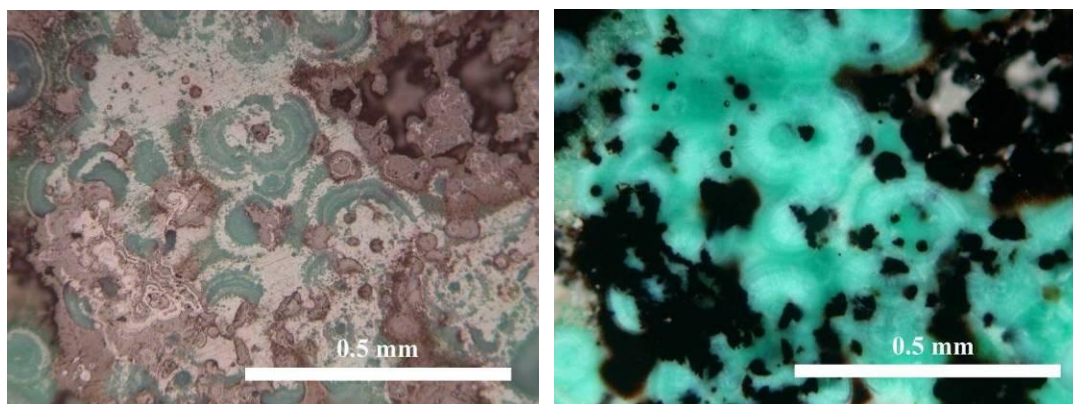


Fig. 52- a) Photomicrograph of phases in Ore 12 under plane polarized light. Note green radiating crystals as the main phase and reddish-brown oolitic structures developing in it; b) photomicrograph of phases in Ore 12 under cross polarized light. Note dark ooids staining the light green phase.

	MnO	CuO	ZnO
	wt%	wt%	wt%
Minimum	0.6	95.5	0.0
Maximum	1.4	99.3	3.9
Average	0.9	98.3	0.8

Table 19. SEM-EDS compositional data for minimum, maximum and average values for the optically green phase in Ore 12; fully reported in the catalogue of ore samples. All values previously normalized to 100%.

On the other hand, the oolitic formations pointed at a more complex structure: ooids, whose major constituents are manganese and copper oxides (Table 20) developed in the dark grey copper-silicate matrix containing significant readings of manganese oxide (Table 21, Fig. 53).

	MgO	Al2O3	SiO2	P2O5	CaO	MnO	FeO	CuO
	wt%	wt%	wt%	wt%	wt%	wt%	wt%	wt%
Minimum	0.0	0.0	13.1	0.0	2.1	24.7	0.0	37.4
Maximum	0.7	3.8	25.0	2.1	3.0	40.0	3.4	43.8
Average	0.3	1.7	18.3	1.4	2.4	34.9	0.7	40.4

Table 20. SEM-EDS compositional data for minimum, maximum and average values for the optically reddish- brown phase in Ore 12; fully reported in the catalogue of ore samples. All values previously normalized to 100%.

	Al2O3	SiO2	CaO	MnO	CuO
	wt%	wt%	wt%	wt%	wt%
Minimum	0.7	36.0	0.8	10.5	44.5
Maximum	1.3	40.2	1.2	17.1	51.4
Average	0.9	37.5	1.0	13.5	47.1

Table 21. SEM-EDS compositional data for minimum, maximum and average values for the optically dark grey phase in Ore 12; fully reported in the catalogue of ore samples. All values previously normalized to 100%.

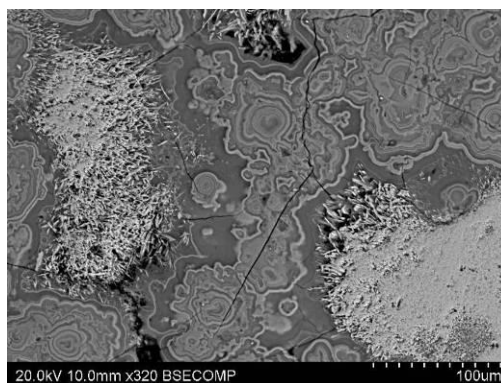


Fig. 53- Back scattered electron image of phases in Ore 12. Note grey phase developing in the dark grey matrix (compare with Tables 20 and 21). Bright crystals are copper-rich phase.

Ore 19 presented a similar mineral structure as the previous ones (Fig. 54a), whereas its chemical composition occurs has differences. The optically blue/light grey matrix consists mainly of copper oxide, with significant readings in silica and lower alumina values (Table 22). The mineralogical structure and colour of this phase indicate azurite (Fig. 54b), which is in certain areas stained with the light green copper mineral, malachite (Figs. 55a and 55b).

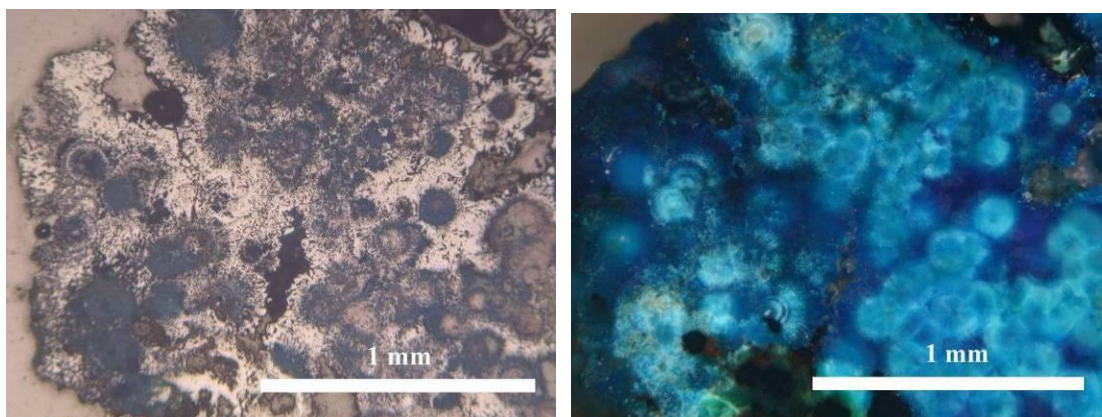


Fig. 54- a) Photomicrograph of Ore 19 under plane polarized light. Note blue/light grey phase and grey ooids developing in it; b) photomicrograph of phases in Ore 19 under cross polarized light.

	Al ₂ O ₃	SiO ₂	CuO
	wt%	wt%	wt%
Minimum	1.1	2.8	79.4
Maximum	1.7	19.0	96.1
Average	1.4	7.7	90.9

Table 22. SEM-EDS compositional data for minimum, maximum and average values for the optically dark blue phase in Ore 19; fully reported in the catalogue of ore samples. All values previously normalized to 100%.

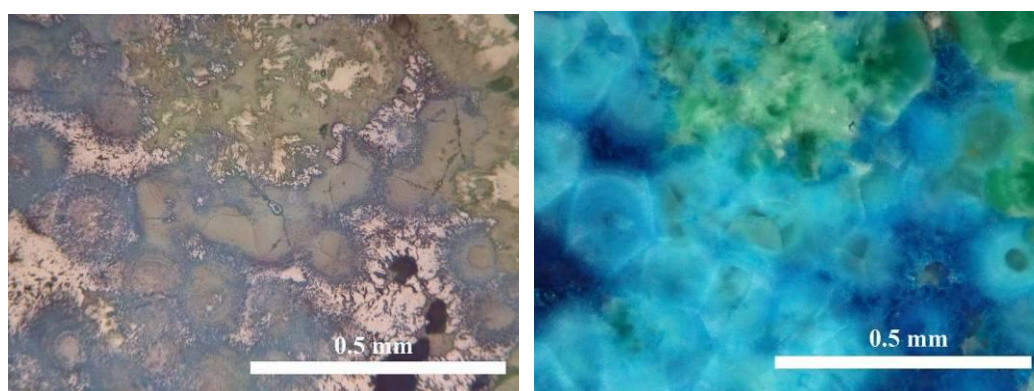


Fig. 55- a) Photomicrograph of azurite and malachite in Ore 19 under plane polarized light; b) photomicrograph of azurite and malachite in Ore 19 under cross polarized light.

The optically grey oolitic structures in the mineral body have copper oxide and silica as major components, along with significant readings in alumina and manganese oxide, around 7% and 11% in average (Table 23). These ooids developed in the dark grey matrix rich in silica and copper oxide (Table 24, Fig. 56).

	MgO	Al ₂ O ₃	SiO ₂	P ₂ O ₅	K ₂ O	CaO	MnO	FeO	CuO
	wt%	wt%	wt%	wt%	wt%	wt%	wt%	wt%	wt%
Minimum	0.0	4.3	30.6	0.0	0.0	0.9	8.6	0.0	40.5
Maximum	0.8	11.9	40.0	1.0	1.7	1.4	14.7	3.3	46.0
Average	0.1	7.2	36.5	0.8	0.4	1.1	11.7	0.9	41.3

Table 23. SEM-EDS compositional data for minimum, maximum and average values for the optically grey phase in Ore 19; fully reported in the catalogue of ore samples. All values previously normalized to 100%.

	Al ₂ O ₃	SiO ₂	K ₂ O	CaO	CuO
	wt%	wt%	wt%	wt%	wt%
Minimum	1.8	49.5	0.0	0.8	38.2
Maximum	5.5	54.9	0.6	2.9	47.7
Average	3.5	52.9	0.2	1.5	41.8

Table 24. SEM-EDS compositional data for minimum, maximum and average values for the optically dark grey phase in Ore 19; fully reported in the catalogue of ore samples. All values previously normalized to 100%.

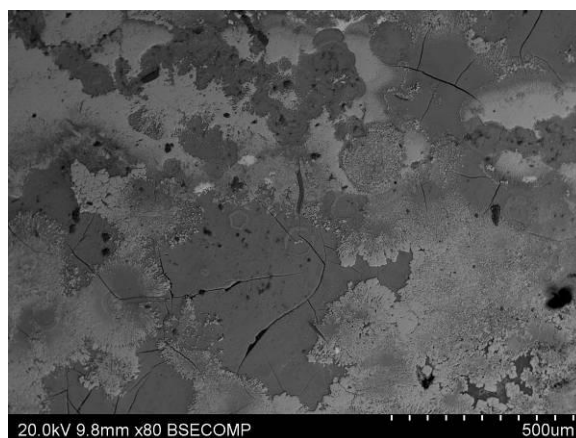


Fig. 56- Back scattered electron image of the ooids in the dark grey matrix (middle), sample Ore 19.

All samples, although with optically varying appearances, show evidence for copper oxide minerals inter-grown with secondary copper-manganese-silicon based oolitic

formations. The potential link to slag samples is mirrored in the qualitative analyses: major gangue oxides, such as manganese, zinc, aluminium and silicon-based are present in quantitatively close ratios to the one in the slags (particularly Ore 19). Other quantitative analyses (Ore 9 and 12) do not show this similar ratio of components. Moreover, the low concentrations of zinc oxide rule out these samples as the sole source for the slag formation. Also, the absence of cobalt oxide contributes to this assumption.

DARK ORES

Samples Ore 13 and Ore 17 have a similar content of sulphides in the copper-rich matrix, although having different chemical composition and optical appearance. Since both samples showed distinctive structures, and the sulphur content optically distinguished them from the oxidic ores, they are called dark ores.

Ore 13 is under plane polarized light shown as composed of grey (Fig. 57a) and green matrix (Figs. 58a and 58b), with the dark grey phase developing inside the former (Fig. 57b).

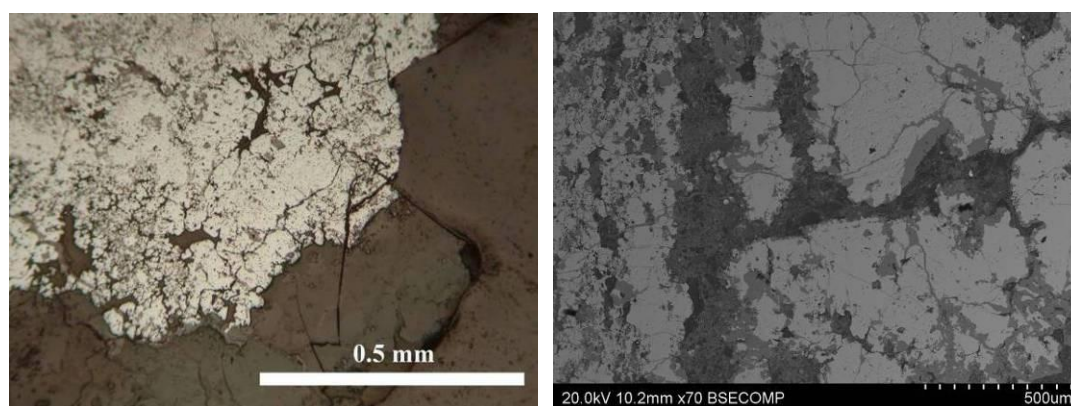


Fig. 57- a) Photomicrograph of copper-rich phase in Ore 13 under plane polarized light. Note corrosion layer in the image bottom; b) back scattered electron image of the dark grey phase (middle) developing in the copper-rich body, Ore 13.

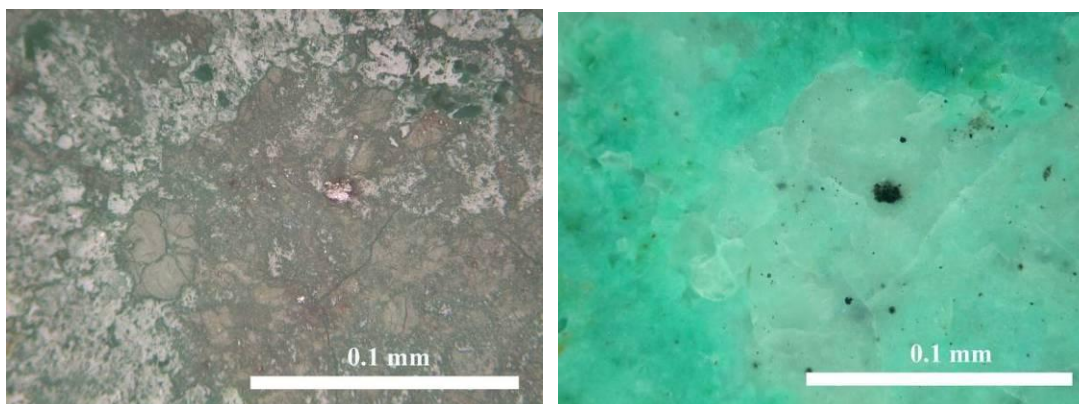


Fig. 58- a) Photomicrograph of the green phase in Ore 13 under plane polarized light; b) photomicrograph of the green phase in Ore 13 under cross polarized light.

The grey matrix has under the cross-polarized light two different reflections: the prevailing one has blue/dark strongly anisotropic reflection (Fig. 59) characteristic for tenorite (CuO); the other phase is inter-grown with the previous one, with red-orange internal reflection, typical for cuprite, Cu_2O . In addition, optically bright prills scattered across the cuprite phase suggest that copper metal is present in it, indicating their derivation from a potential heat treatment of the sample (Figs. 60a and 60b).

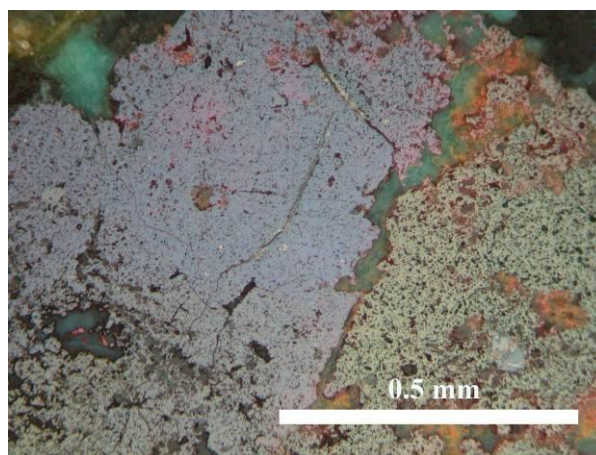


Fig. 59- Photomicrograph of the tenorite/cuprite phase in Ore 13. Note characteristic blue (tenorite) and red/orange (cuprite) reflections.

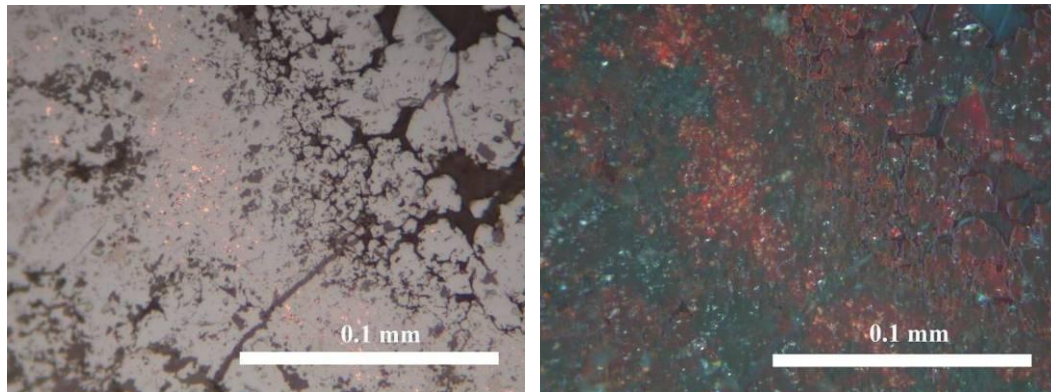


Fig. 60- a) Photomicrograph of bright (copper) prills scattered across the middle of the image under plane polarized light (Ore 13); b) photomicrograph of the same section under cross polarized light. Note difference in reflection, dark blue/red, indicating tenorite and cuprite present in this phase.

The optically dark phase developed inside the grey matrix (Fig. 57a) showed significant readings in alumina, phosphorus and copper, along with minute concentrations of magnesia and lead oxide (Table 25). Furthermore, the light grey prills scattered across this phase revealed silver sulphides (Table 26, Fig. 61), along with the grain of copper sulphide (Table 27, Fig. 62).

	MgO	Al ₂ O ₃	SiO ₂	P ₂ O ₅	SO ₃	K ₂ O	CaO	FeO	CuO	PbO
	wt%	wt%	wt%	wt%	wt%	wt%	wt%	wt%	wt%	wt%
<i>Minimum</i>	0.0	20.2	2.6	5.7	2.7	0.4	2.2	0.7	13.0	0.0
<i>Maximum</i>	1.5	33.4	41.5	16.6	12.3	1.1	4.8	1.9	54.1	7.1
<i>Average</i>	0.6	27.7	13.9	11.9	6.6	0.7	3.4	1.1	30.0	4.1

Table 25. SEM-EDS compositional data for minimum, maximum and average values for the optically dark phase in grey matrix of Ore 13; fully reported in the catalogue of ore samples. All values previously normalized to 100%.

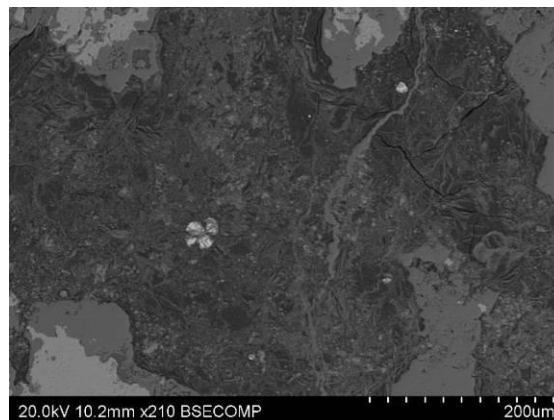


Fig. 61- Back scattered electron image of dark grey phase containing silver sulphide prills, Ore 13 (see Table 26).

	S	Cu	Ag
	at%	at%	at%
<i>Minimum</i>	19.2	5.0	49.5
<i>Maximum</i>	24.4	31.1	71.7
<i>Average</i>	21.1	16.4	62.5

Table 26. SEM-EDS compositional data for silver sulphide prills in Ore 13, given in atomic % and fully reported in the catalogue of ore samples. All values previously normalized to 100%.

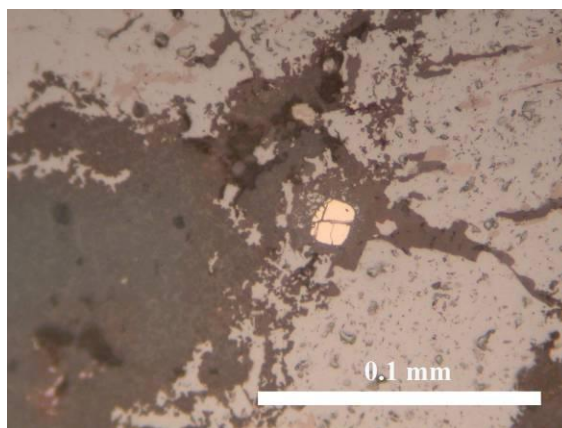


Fig. 62- Photomicrograph of the copper sulphide grain developing in the dark grey matrix, Ore 13 (see also Table 27).

	S	Cu
	at%	at%
spot 1	9.4	90.6
spot 2	11.6	88.4
Average	10.5	89.5
St. Deviation	1.6	1.6

Table 27. SEM-EDS compositional data for copper sulphide prill in Ore 13 given in atomic %. All values normalized to 100%.

The green matrix in this sample is chemically characterized by high readings in copper, along with some alumina, silica and phosphorus, suggesting corrosion product developing on top of the grey matrix (Table 28).

	Al ₂ O ₃	SiO ₂	P ₂ O ₅	CaO	CuO
	wt%	wt%	wt%	wt%	wt%
spot 1	3.3	6.5	1.1	0.5	88.6
spot 2	2.0	2.9	1.3	0.0	93.8

Table 28. SEM-EDS compositional data for the green matrix in Ore 13. All values normalized to 100%.

Nevertheless, the convoluted agglomerations of cuprite (Table 29, Fig. 63) embedded in the green matrix, resembled the cuprite in the slag samples, suggesting possible heat treatment of this sample. The presence of tenorite contributes to the assumption: this mineral is very rarely present in nature; and here most likely demonstrates the product of the heat treatment of the sample. In addition, the cuprite phase in the grey matrix containing metal prills stands in good agreement with the previous assumption (see Fig. 60a).

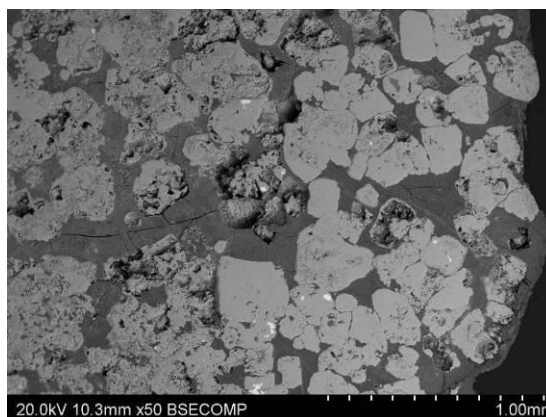


Fig. 63- Back scattered electron image of cuprite in form of convoluted agglomerations, Ore 13.

	O	Cu
	wt%	wt%
<i>Minimum</i>	10.9	79.9
<i>Maximum</i>	20.1	89.1
<i>Average</i>	13.6	86.4

Table 29. SEM-EDS compositional data for cuprite in green matrix in Ore 13; fully reported in the catalogue of ore samples. All values measured as elements and previously normalized to 100%.

The complex structure is evident in the sample Ore 17 as well: two prevailing phases, optically blue-grey and dark grey (Figs. 64a and 64b), develop around yellow (Fig. 65a) and light grey crystals (Fig. 65b).

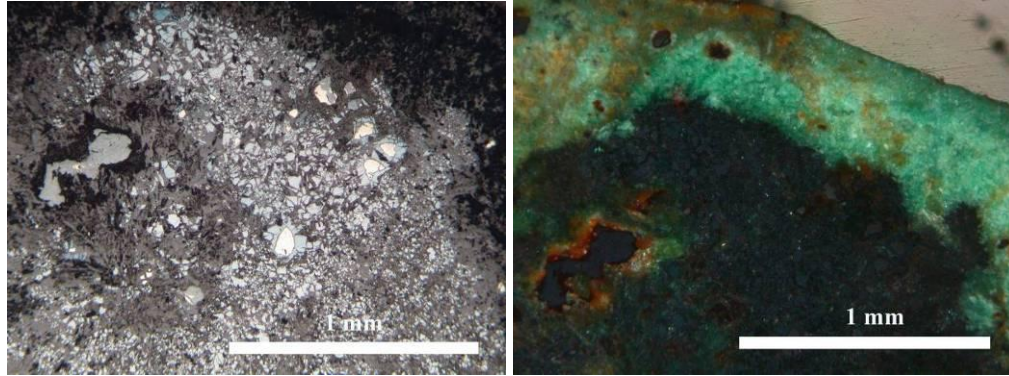


Fig. 64- a) Photomicrograph of main phases in Ore 17 under plane polarized light. Note blue-grey and dark grey phases, with yellow prills embedded in it. Blue crystals (top) are covellite; **b)** photomicrograph of the same section under cross polarized light. Note light green corrosion layer developing on rims of the sample.

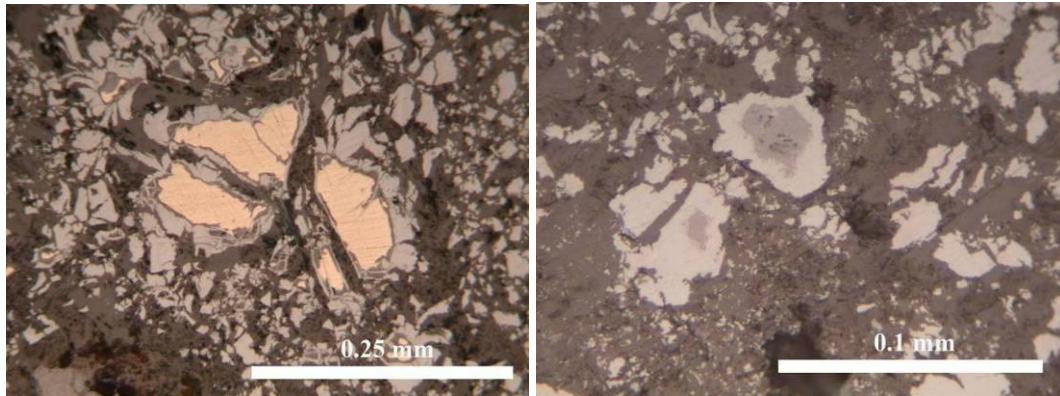


Fig. 65- a) Photomicrograph of pyrite (yellow crystals) under plane polarized light, Ore 17. Note dark mass penetrating crystals, rich in iron oxides. The light grey crystals surrounding them are chalcocite; **b)** photomicrograph of former pyrites (light grey crystals) under plane polarized light, Ore 17. Note dark mass inside the crystal, rich in iron oxide. The light grey crystals surrounding them are chalcocite.

The blue-grey phase is chemically revealed as chalcocite, Cu_2S (Table 30), which in certain parts develops into dark blue crystals of covellite, CuS (Fig. 66a). The dark grey phase is copper-rich, with low values in zinc oxide (Table 31, Fig. 65a and 65b). On the rim of the sample, this phase revealed bright particles grouped in zones, chemically revealed as silver sulphide and lead oxide crystals (Table 32, Table 33, Figs. 66b and 67).

	S	Fe	Cu
	at%	at%	at%
Minimum	35.0	0.0	61.8
Maximum	37.3	1.0	64.4
Average	35.7	0.6	63.7

Table 30. SEM-EDS compositional data for minimum, maximum and average values for chalcocite in Ore 17, given in atomic % and fully reported in the catalogue of ore samples. All values previously normalized to 100%.

The optically yellow, metal-like crystals are pyrite, FeS_2 (Table 34, Fig. 65a), which showed chemically identical composition as the light grey inclusions, despite the different optical appearance (Table 35, Fig. 65b).

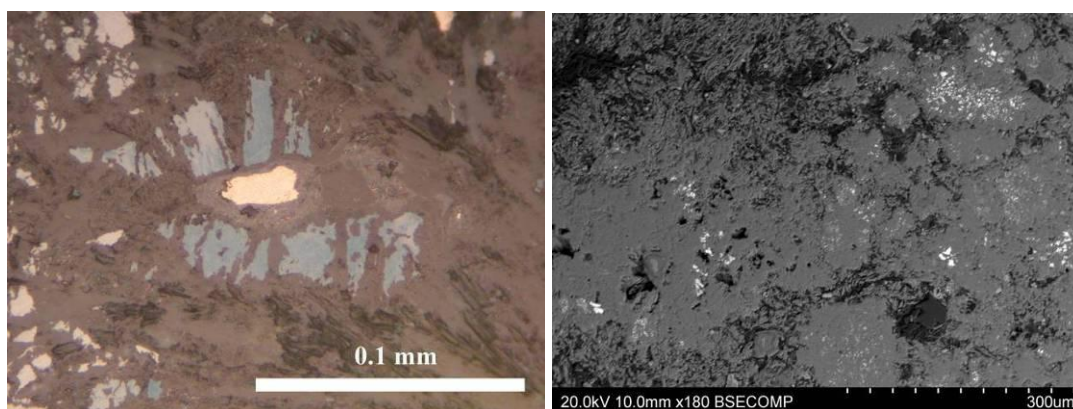


Fig. 66- a) Photomicrograph of covellite crystals (blue) surrounding pyrite (yellow) in a dark grey copper-rich phase, Ore 17; b) back scattered electron image showing bright silver sulphide particles grouping in the dark grey phase (see Table 32).

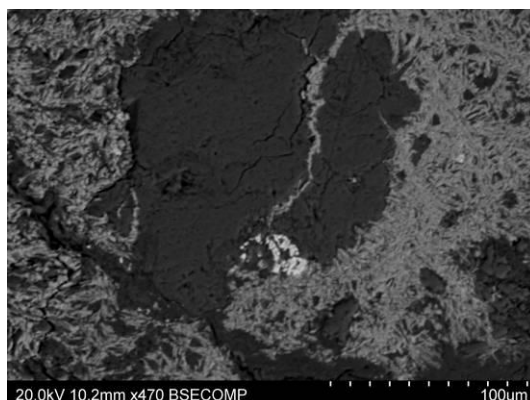


Fig. 67- Back scattered electron image of the lead oxide particle embedded in copper-rich matrix and corrosion product (dark phase), Ore 17. See Table 33.

	FeO	CuO	ZnO
	wt%	wt%	wt%
Minimum	0.0	95.2	2.4
Maximum	0.8	97.0	4.8
Average	0.5	95.8	3.7

Table 31. SEM-EDS compositional data for minimum, maximum and average values for the optically dark grey phase in Ore 17; fully reported in the catalogue of ore samples. All values previously normalized to 100%.

	Mg	S	Cu	Ag
	at%	at%	at%	at%
Minimum	0.0	19.9	5.1	50.3
Maximum	1.6	37.4	18.7	71.1
Average	0.9	27.0	10.2	61.9

Table 32. SEM-EDS compositional data for minimum, maximum and average values for silver sulphide particles in Ore 17, given in atomic % and fully reported in the catalogue of ore samples. All values previously normalized to 100%.

	Al2O3	SiO2	P2O5	SO3	K2O	CaO	FeO	CuO	PbO
	wt%	wt%	wt%	wt%	wt%	wt%	wt%	wt%	wt%
Minimum	15.6	0.0	13.7	0.0	0.0	0.0	1.1	6.2	23.4
Maximum	28.8	9.9	22.6	5.4	0.5	0.6	2.5	45.9	41.0
Average	25.1	2.6	19.8	1.2	0.1	0.2	1.8	15.1	34.0

Table 33. SEM-EDS compositional data for minimum, maximum and average values for lead oxide-rich particles in Ore 17; fully reported in the catalogue of ore samples. All values previously normalized to 100%.

	S	Fe	Cu
	at%	at%	at%
Minimum	66.8	31.6	0.7
Maximum	67.4	32.1	1.4
Average	67.1	31.9	1.0

Table 34. SEM-EDS compositional data for minimum, maximum and average values for pyrite (optically yellow) in Ore 17, given in atomic % and fully reported in the catalogue of ore samples. All values previously normalized to 100%.

	S	Fe	Cu
	at%	at%	at%
Minimum	67.0	31.8	0.5
Maximum	67.5	32.1	1.2
Average	67.1	32.0	0.9

Table 35. SEM-EDS compositional data for minimum, maximum and average values for pyrite (optically light grey) in Ore 17, given in atomic % and fully reported in the catalogue of ore samples. All values previously normalized to 100%.

These crystals are surrounded by an optically grey mass, based on iron oxides, which penetrates across and inside these crystals (Figs. 65a and 65b). The chemical composition in this case varies: yellow crystals are surrounded with iron oxide containing significant readings in copper, silica, phosphorus and arsenic (Table 36); whereas light grey crystals are penetrated by an iron-rich phase with low levels of copper oxide (Table 37).

	Al ₂ O ₃	SiO ₂	P ₂ O ₅	SO ₃	CaO	FeO	CuO	ZnO	As ₂ O ₃
	wt%	wt%	wt%	wt%	wt%	wt%	wt%	wt%	wt%
Minimum	0.0	7.1	1.2	1.0	0.0	57.2	15.4	0.0	1.0
Maximum	1.0	9.0	5.1	3.3	0.7	70.4	26.4	1.4	2.4
Average	0.3	8.0	3.4	1.8	0.5	64.1	20.0	0.3	1.5

Table 36. SEM-EDS compositional data for minimum, maximum and average values for the optically dark phase surrounding pyrite (optically yellow) in Ore 17; fully reported in the catalogue of ore samples. All values previously normalized to 100%.

	SiO ₂	SO ₃	FeO	CuO
	wt%	wt%	wt%	wt%
Minimum	2.7	0.0	89.7	6.1
Maximum	3.8	0.8	90.3	7.1
Average	3.2	0.3	90.0	6.5

Table 37. SEM-EDS compositional data for minimum, maximum and average values for the optically dark phase surrounding pyrite (optically light grey) in Ore 17; fully reported in the catalogue of ore samples. All values previously normalized to 100%.

This complex sample has a geological rather than artificial structure, mainly supported by the observation of chalcocite and pyrite crystals preserved in the copper-rich matrix. Any artificial (heat) treatment would have formed eutectic of these crystals, or their gradual development from higher to lower copper-containing sulphides (cf. Bachmann 1982), which is not detected here. On the other hand, these ores did not contribute to the formation of slag samples described above; their high iron content, along with copper sulphides, lead, silver and arsenic do not match the slag analyses (see Table 7).

The general conclusion deriving from these analyses is that none of the ores showed a composition equal to the slag samples. However, since comparable levels of certain metal and gangue oxides are found in slags and oxidic ores, one can assume that other but similar ore sources were used for copper smelting, which is as general principle recognized in practice of the early collectors and craftsmen (cf. Shugar 2000).

Results of Research: Analysis of Artefacts

The artefacts from Belovode can be divided in two groups: cold and hot worked, where the later one involves all kinds of heat treatment. Four artefacts were chosen for this study: two malachite beads, a lump of copper metal and the copper ingot. They all originate from the excavated area, except for the copper ingot, which is a surface find from the vicinity of Belovode.

Malachite beads

Both beads were studied under the Scanning Electron Microscope: the Environmental Scanning Electron Detector in VP-SEM (vacuum) mode was used for analysis of the inner surface of the fragmented one (Belovode 32), aimed to explore the technology of drilling; while the whole bead (Belovode 33) was studied for compositional analysis using Energy Dispersive Spectroscopy.

Electron optically, as well as visually, malachite beads presented a thick corrosion layer (see Catalogue in Appendix), which still preserved drilling marks on both samples (Figs. 68a and 68b).

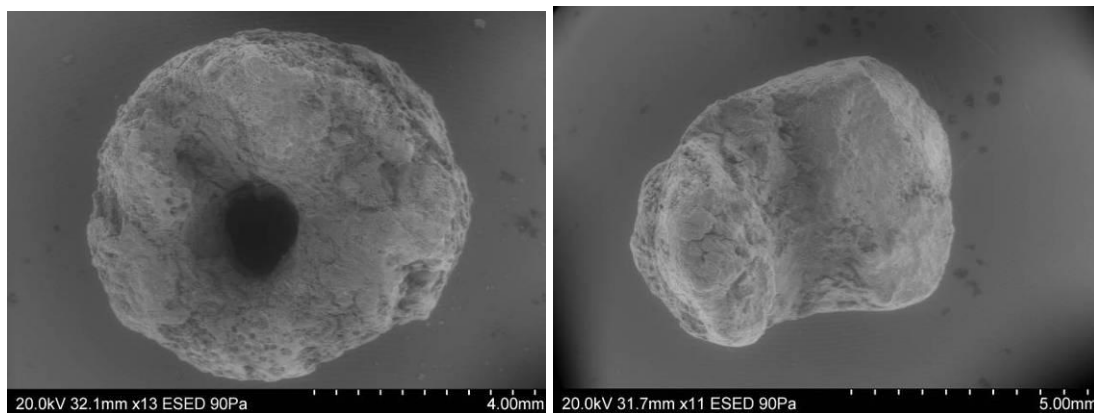


Fig. 68- a) Photomicrograph of Belovode 33 under Environmental Scanning Electron Detector. Note conical indentation (up right part of the image) leading to the drill-hole; b) Photomicrograph of Belovode 32 under Environmental Scanning Electron Detector. Note biconical shape of the drill-hole, filled with corrosion and dirt.

They are revealed as biconical indentations, indicating the shape of the tool, as well as its position and the working angle. Nevertheless, the compositional analysis of the inner

and outer surface of the fragmented bead (Belovode 32) did not discover the type of tool used (Tables 38 and 39). The readings of silica in the inner surface were similar or lower than those in the outer surface, suggesting that a stone tool was not used in this case: the flakes from the stone tool would have remained in the drill hole, which in turn would increase its silica content. On the other hand, these results suggest the usage of either wooden, bone or even metal tools, but no direct evidence has been discovered thus far.

	MgO	Al ₂ O ₃	SiO ₂	P ₂ O ₅	K ₂ O	CaO	FeO	CuO
	wt%	wt%	wt%	wt%	wt%	wt%	wt%	wt%
spot 1	1.3	13.2	29.1	0.8	1.5	1.4	3.5	49.2
spot 2	2.0	14.6	36.0	1.3	2.0	2.1	4.1	37.9
spot 3	1.9	17.3	49.4	0.0	2.2	3.8	9.9	15.6

Table 38. SEM-EDS compositional data for inner surface of the malachite bead Belovode 32 (drill hole). All data normalized to 100%.

	MgO	Al ₂ O ₃	SiO ₂	P ₂ O ₅	K ₂ O	CaO	TiO ₂	FeO	CuO
	wt%	wt%	wt%	wt%	wt%	wt%	wt%	wt%	wt%
spot 1	2.2	19.3	54.8	1.0	3.3	2.9	1.0	7.2	8.2
spot 2	2.3	18.3	48.0	0.9	2.7	7.8	0.0	5.6	14.5
spot 3	0.9	24.9	41.5	0.0	1.0	1.6	0.0	3.7	26.3

Table 39. SEM-EDS compositional data for outer surface of the malachite bead Belovode 32. All data normalized to 100%.

The optical and compositional analysis of the bead Belovode 33 revealed its typical mineral structure. Two phases are recognized: the green phase with ooids developing in it (Figs. 69a and 69b), and the dark red phase (Figs. 70a and 70b). Since revealed by its characteristic colour, the green phase clearly stands for malachite. It has a high copper content, containing also magnesia, alumina and silica, along with minute concentrations of iron and zinc oxides (Table 40).

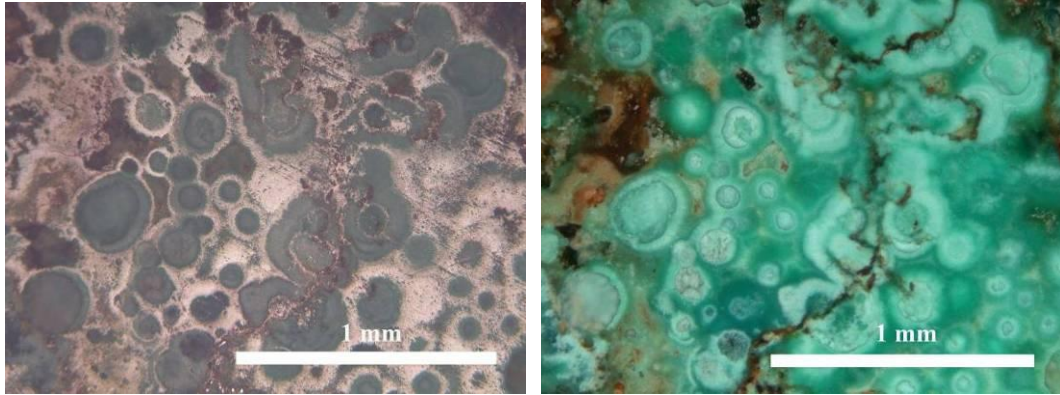


Fig. 69- a) Photomicrograph of the green phase in bead Belovode 33 under plane polarized light; b) Photomicrograph of the green phase in bead Belovode 33 under cross polarized light.

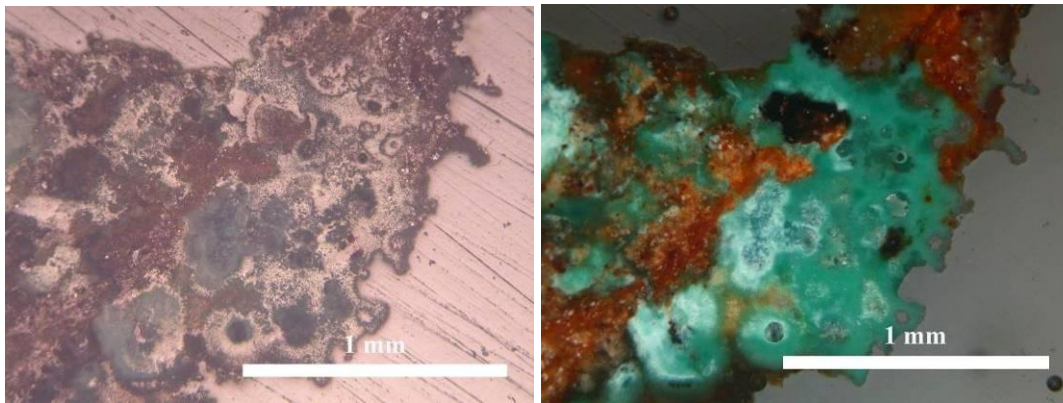


Fig. 70- a) Photomicrograph of the green and dark red phase in Belovode 33 under plane polarized light; b) Photomicrograph of the green and dark red phase in Belovode 33 under cross polarized light. Note white (quartz) inclusions in the dark red phase.

	MgO	Al ₂ O ₃	SiO ₂	P ₂ O ₅	K ₂ O	CaO	FeO	CuO	ZnO
	wt%	wt%	wt%	wt%	wt%	wt%	wt%	wt%	wt%
Minimum	1.12	1.93	2.14	0.00	0.00	0.00	0.00	73.19	0.00
Maximum	6.23	4.96	8.18	3.73	0.00	1.88	5.76	89.94	3.23
Average	3.32	3.16	4.98	1.22	0.00	0.77	1.75	83.74	1.07

Table 40. SEM-EDS compositional data for minimum, maximum and average values for the optically green phase in Belovode 33; fully reported in the catalogue of malachite beads. All values previously normalized to 100%.

The optically dark red phase is revealed as a matrix with quartz inclusions in it. The chemical analysis of the inclusion-free area pointed at high iron oxide readings, around 21% in average, along with significant levels of silica, magnesia and alumina (Table 41).

	MgO	Al ₂ O ₃	SiO ₂	P ₂ O ₅	K ₂ O	CaO	TiO ₂	FeO	CuO	ZnO
	wt%	wt%	wt%	wt%	wt%	wt%	wt%	wt%	wt%	wt%
Minimum	12.9	13.4	28.1	0.0	0.9	0.5	0.0	11.5	2.2	0.0
Maximum	20.6	19.0	46.1	6.8	6.4	4.2	3.2	33.0	3.9	1.9
Average	16.2	16.5	36.2	2.3	1.9	2.0	0.5	20.8	2.8	0.8

Table 41. SEM-EDS compositional data for minimum, maximum and average values for the optically dark red phase in Belovode 33; fully reported in the catalogue of malachite beads. All values previously normalized to 100%.

However, it is important to emphasize that neither optical nor chemical analysis have demonstrated any heat treatment applied in the processing of malachite beads from Belovode. This is also partly caused by the corrosion layer developing on their surface, hence removing any marks of potential heating, as well as shaping techniques, like hammering or polishing. It is also very unlikely that they are corroded metal beads recrystallized as malachite. From the evidence presented, it is indicative that these beads were cold-worked, and according to its shape, further used as pieces of jewellery.

Copper metal lump

A lump of corroded copper metal (Belovode 14) was found associated with ores and initially thought to represent copper mineral, mainly by reason of its amorphous shape (see Catalogue in Appendix). The sample was studied both optically and chemically, revealing a single phase in its body. The optically bright yellow matrix pointed at characteristic copper metal colour (Figs. 71a and 72b), which was further confirmed by SEM-EDS analysis (Table 42).

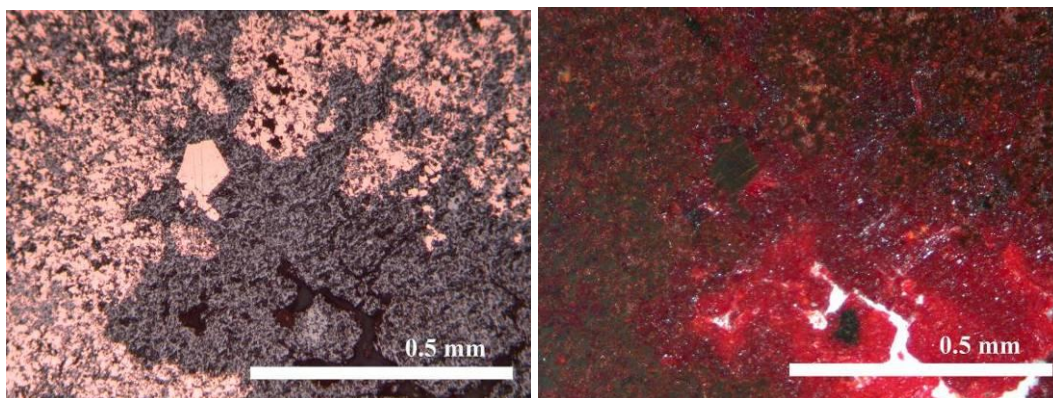


Fig. 71- a) Photomicrograph of the optically bright yellow phase (copper) with grey corrosion crystals developing in it, taken under plane polarized light; b) photomicrograph of the copper-rich phase (note internal reflection) under cross polarized light (Belovode 14).

	O	Cu
	wt%	wt%
spot 1	0.7	99.3
spot 2	0.8	99.2
area 1	0.8	99.2

Table 42. SEM-EDS compositional data of the optically bright yellow phase in Belovode 14. All results measured as elements and normalized to 100%.

The metal matrix is revealed as heavily corroded; the grey crystals developed in approximately half of the total volumes of the copper metal present (Figs. 72a and 72b). The grey crystals have a dark red/orange colour under cross polarized light, suggesting the presence of cuprite. The abundance of porosity holes present on the polished surface of this sample suggested intensive reaction with the air while cooling, which could be an indication of discarding of this piece of molten metal while being hot. This in turn can also explain the development of corrosion products inside the body of the sample.

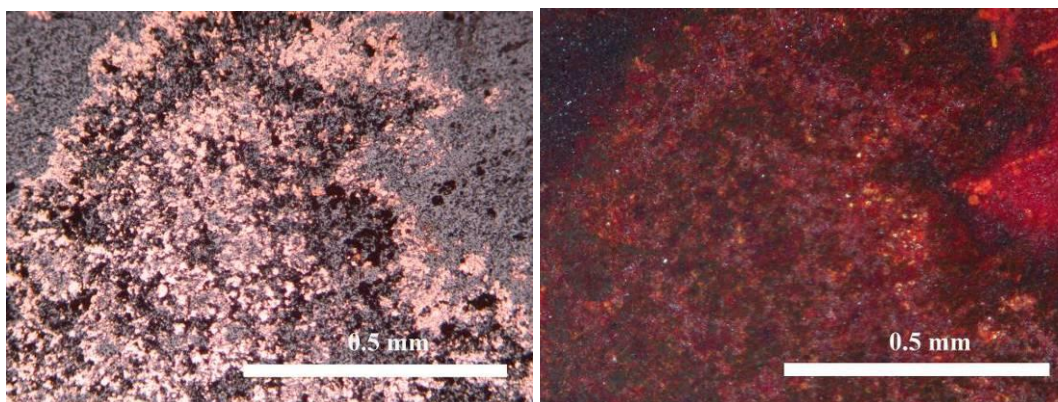


Fig. 72- a) Photomicrograph of the corroded copper phase in Belovode 14, taken under plane polarized light. Note porosity holes (black) scattered across the image; b) photomicrograph of the corroded copper phase in Belovode 14, taken under cross polarized light.

The thick layer of light-green corrosion is due to post-depositional processes, developing here in two chemically distinctive layers (Fig. 73a and 73b). The first layer showed high readings in copper, with minute concentrations of iron oxide and silica (Table 43), while the second one appeared as richer in both iron oxide and silica, and particularly phosphorus (Table 44).

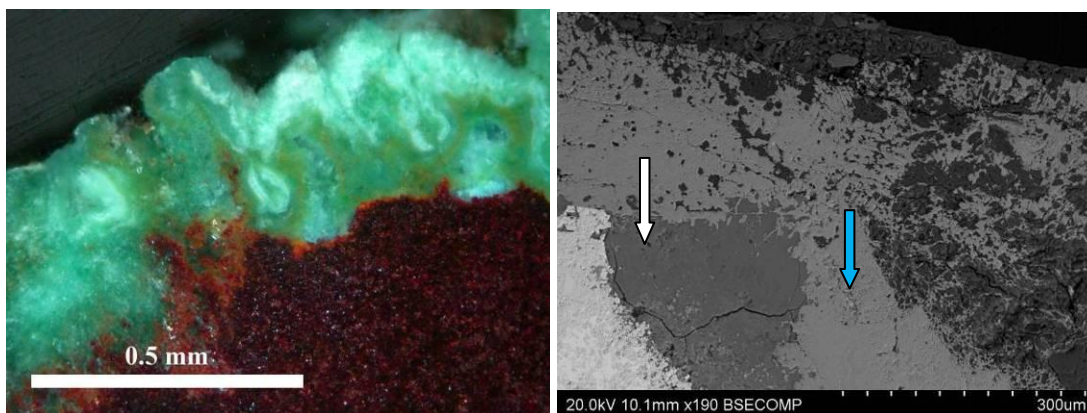


Fig. 73- a) Photomicrograph of the light green corrosion product on Belovode 14, taken under cross polarized light; b) back scattered electron image of the corrosion products, Belovode 14. Note grey (first) and light grey layer (second) interrupted by the dark grey deposit (dirt). Only two first layers are shown in Tables 43 and 44 (first layer: white arrow; second layer: blue arrow).

	Al ₂ O ₃	SiO ₂	P ₂ O ₅	CaO	CuO
	wt%	wt%	wt%	wt%	wt%
Minimum	0.0	43.1	0.0	0.6	45.1
Maximum	1.0	53.3	5.9	1.0	52.2
Average	0.5	47.9	2.0	0.7	49.0

Table 43. SEM-EDS compositional data for minimum, maximum and average values for the first layer of corrosion (Belovode 14); fully reported in the catalogue of artefacts. All values previously normalized to 100%.

	Al ₂ O ₃	SiO ₂	P ₂ O ₅	CaO	CuO
	wt%	wt%	wt%	wt%	wt%
<i>Minimum</i>	0.0	0.0	31.0	0.8	63.5
<i>Maximum</i>	0.0	2.7	31.8	2.8	67.4
<i>Average</i>	0.0	1.6	31.5	1.5	65.4

Table 44. SEM-EDS compositional data for minimum, maximum and average values for the second layer of corrosion (Belovode 14); fully reported in the catalogue of artefacts. All values previously normalized to 100%.

According to the evidence discussed, it is assumed that a lump of molten copper was discarded from further processing and exposed to intensive reaction with the air. Hence, the corrosion products could have developed in the porosity holes created during the rapid cooling. The presence of the silica-rich grain could attest the presence of gangue material, potentially indicating smelting rather than melting process performed in this case. Nevertheless, the scarce evidence of the metal present, as well as the volume of the artefact does not offer sufficient information to strengthen the assumption. With the

results presented, the sample can be ascribed to the assemblage of technological debris from pyrometallurgical activities on Belovode.

Copper ingot

The bun-shaped ingot is a surface find from the vicinity of the settlement, hence assumed to originate from metallurgical activities in Belovode. It was discovered well preserved, with a light green layer developed on its surface (see Catalogue in Appendix). A sample 4 mm in length was carefully removed from the object, using a diamond saw (Fig. 74), and analyzed as a longitudinal section embedded in paraloid B72.



Fig. 74- Image of the ingot showing sampled section. Note the drill hole in the middle of the left image made by villagers from Belovode.

This method was applied to facilitate releasing of the sample for further analysis, like trace element and lead-isotope, both conducted in Mannheim (see Chapter 2). The sample was firstly tested for micro-hardness, and then observed in unetched condition under polarizing microscope, in order to show the range and type of phases present. It was then etched with aqueous ferric chloride solution consisted of FeCl_3 (10 gr), HCl (30 ml) and H_2O (120 ml), as described by Scott (1991: 72). The etchant was used to make the grain boundaries visible, as well as their inner structure, hence indicating the

working technology applied. After optical microscopy, chemical analysis was conducted using SEM-EDS.

The sample itself reveals a single phase, metal body, with corrosion products developing on its edges (Fig. 75a). The optically bright yellow phase showed residual as-cast structure, preserved in the microstructure of the copper-copper oxide eutectic with α -grains of copper. The grains are optically characterized by their highly reflective bright yellow colour (Table 45), embedded in the eutectic structure with grey crystals and identical bright yellow matrix as the metal grains (Fig. 75b). These crystals under cross-polarized light showed bright red internal reflections, characteristic for cuprite, which is also confirmed by compositional analysis (Table 46).

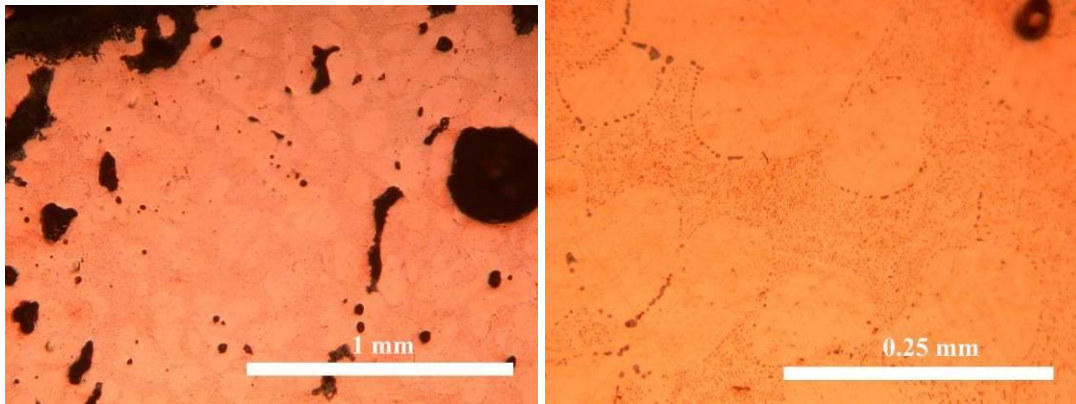


Fig. 75- a) Photomicrograph of the unetched Belovode 34 under plane polarized light. Note bright α grains embedded in eutectic, covering half of the volume of this section. The dark spots on the image are porosity holes, with the exception of corrosion products developing in the edge of the sample (up right); b) photomicrograph of unetched Belovode 34 under plane polarized light. Note bright α grains embedded in eutectic, which formed strings of grey crystals (cuprite) around them.

	O	Cu
	wt%	wt%
Minimum	0.8	98.9
Maximum	1.1	99.2
Average	0.9	99.1

Table 45. SEM-EDS compositional data for minimum, maximum and average values for α grains in Belovode 34; fully reported in the catalogue of artefacts. All values measured as elements and previously normalized to 100%.

	O	Cu
	wt%	wt%
Minimum	10.6	87.6
Maximum	12.4	89.5
Average	11.3	88.7

Table 46. SEM-EDS compositional data for minimum, maximum and average values for cuprite in Belovode 34; fully reported in the catalogue of artefacts. All values measured as elements and previously normalized to 100%.

Since the presence of eutectic covers approximately half of the volume in this sample, it indicates around 0.2 wt% oxygen present, thus pointing at the temperature achieved around 1075° (compare with the Cu-O phase diagram in Appendix Figures; Neumann, Zhong and Chang 1984).

Once etched, the sample showed crystallized structure of the fully-grown grains in the copper-copper oxide eutectic, showing negative evidence for further working on this object after casting (Figs. 76a and 76b). The grains are presented in both dendritic and round form, and the average size is estimated to be around 0.1 mm (Fig. 77).

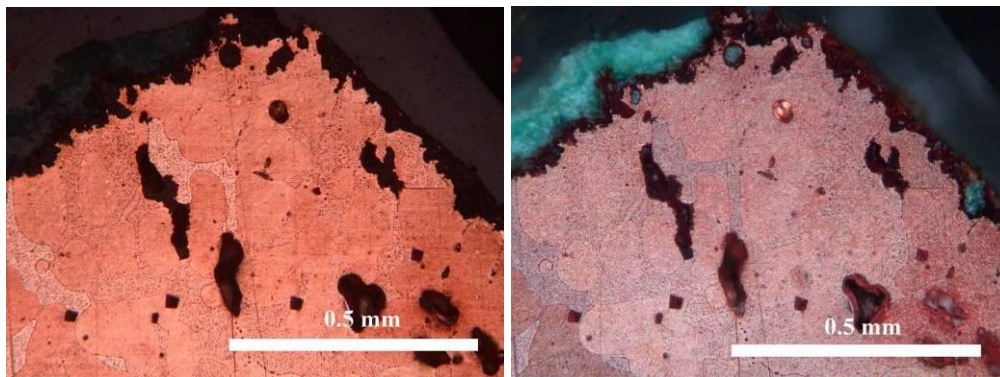


Fig. 76- Photomicrograph of Belovode 34 under plane polarized light, etched with ferric chloride. Note the α grains fully crystallized, and no indications of further work on this sample; b) photomicrograph of Belovode 34 under cross polarized light, etched with ferric chloride. Note red internal reflections of cuprite in the eutectic.

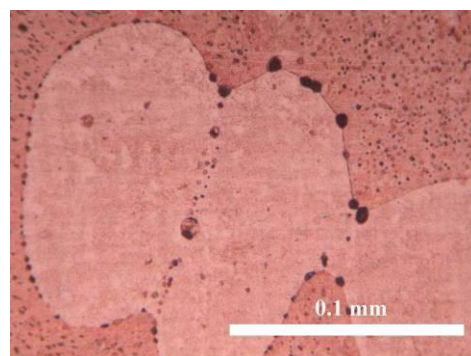


Fig. 77- Photomicrograph of Belovode 34 under plane polarized light, etched with ferric chloride. Note the size of the grain embedded in eutectic.

The average value of 63 Hv for hardness of the ingot is usually recognized as characteristic for pure copper both worked and annealed (cf. Scott 1991: 82). On the other hand, the undistorted large grain structure suggests that no finishing work was performed on the object. Since hardness values, ranging from 56 Hv to 75 Hv (see Fig. 78), appear to be higher than expected from a microstructure with no marks of final work, it is likely that the presence of oxide crystals (cuprite) could have increased the hardness of artefact in question (Lechtman 1996).

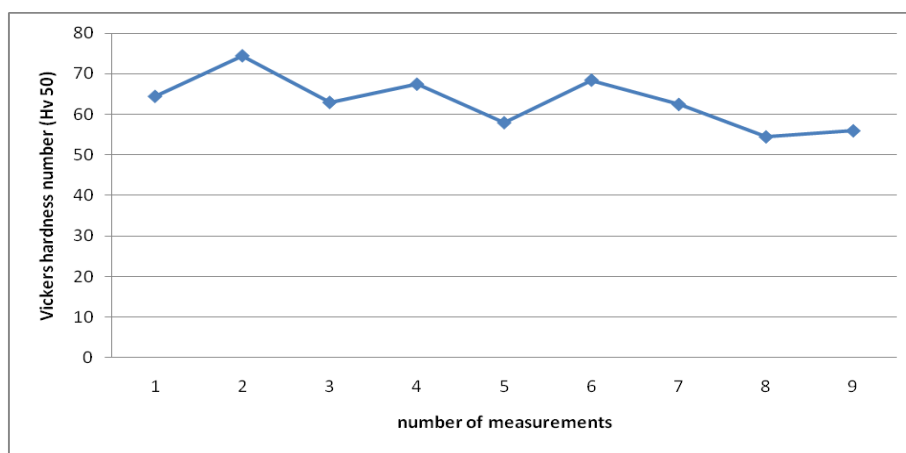


Fig. 78- Figure showing the Hv values taken along the sequence of Belovode 34 (nine measurements). The average Hv value is 63.

The surface of the object both macroscopically and microscopically appears to be only slightly affected by corrosion (Figs. 79a and 79b). The corrosion layer has two optically and chemically distinctive phases (Tables 47 and 48). The major component of the optically red primary phase is copper oxide, followed with concentrations of phosphorus, iron oxide and lime. The optically light green corrosion layer has lower concentration of copper oxide, and significant readings in iron oxide, sulphur and silica.

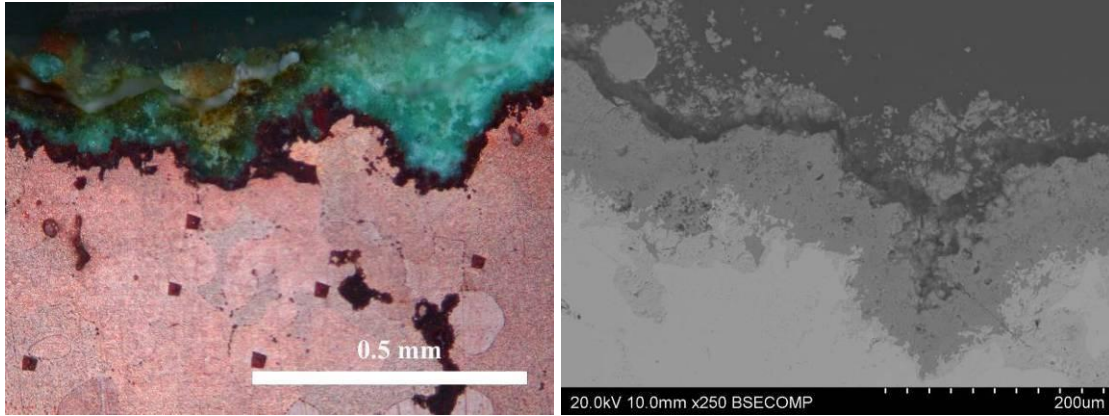


Fig. 79- a) Photomicrograph of the metal body and corrosion in Belovode 34 under cross polarized light, etched with ferric chloride. Note red layer rich in cuprite (the first phase) and the light green one (the second phase); b) back scattered electron image of corrosion products in Belovode 34. Note bright grey metal body, light grey and dark grey corrosion layers, as well as dirt on top of them.

	SiO ₂	P ₂ O ₅	SO ₃	CaO	FeO	CuO
	wt%	wt%	wt%	wt%	wt%	wt%
Minimum	0.0	1.3	0.0	0.0	0.0	91.8
Maximum	2.3	2.7	0.9	0.8	3.7	98.7
Average	1.0	2.0	0.5	0.5	1.1	94.9

Table 47. SEM-EDS compositional data for minimum, maximum and average values for the first layer of corrosion in Belovode 34; fully reported in the catalogue of artefacts. All values previously normalized to 100%.

	SiO ₂	P ₂ O ₅	SO ₃	CaO	FeO	CuO
	wt%	wt%	wt%	wt%	wt%	wt%
Average	4.3	1.7	3.3	1.1	19.4	70.2

Table 48. SEM-EDS compositional data for average values for the second layer of corrosion in Belovode 34; fully reported in the catalogue of artefacts. All values previously normalized to 100%.

Regarding the pure copper composition of this object, it is assumed that the ingot could have been made either from melted native or smelted high-purity copper. The presence of porosity holes throughout the sample suggests intensive reaction with the atmosphere, potentially indicating an open-mould casting. The shape of the object (see Catalogue) reveals flat surface on one side, but not the shrink-hole indentation, which would be expected in open-mould casting. However, the lack of feeders and casting seams can contribute to this assumption. These bi-valve formations are usually removed with hammering and subsequent polishing, and the lack of any finishing work on the sample strengthens the hypothesis of this ingot being cast in an open mould.

Results of Research: Analysis of Ceramics

The ceramic sherds analyzed in this section were collected either by reason of the distinctive white lagging found on the inside and outside surface of their walls (Belovode 29 and 30), or the green mass adhered to their outer walls (Belovode 26). Since all of them were found in the context of the potential workshop or courtyard of a house yielding a shallow pit associated with lumps of copper ores, they were chosen for further study on the likely relation with metallurgical activities on the site (see Catalogue in Appendix).

Four samples in total were prepared for the analysis: ED-XRF was used for qualitative assessment of the compositional difference between the outside and inside walls of three sherds, while optical microscopy and SEM-EDS were aimed for detailed study on the structure and composition of four samples. All samples will be described in two groups; the first one refers to the ceramic sherd with green mass adhered to its outer walls, and the second one covers three samples indicating usage of crushed bone for padding of the walls.

Belovode 26

The bulk chemical ED-XRF analysis of the outer walls of Belovode 26 pointed at high readings in copper and manganese oxides, as opposed to the composition of inner walls (Table 49 in Appendix Tables, Fig. 80). They go together with minute concentrations of zinc (200 ppm), cobalt (88 ppm) and nickel (154 ppm) oxides, pointing at the crushed ore content. The composition of the inner walls is rich in alumina-silicates, showing no traces of metallurgical activities in this vessel.

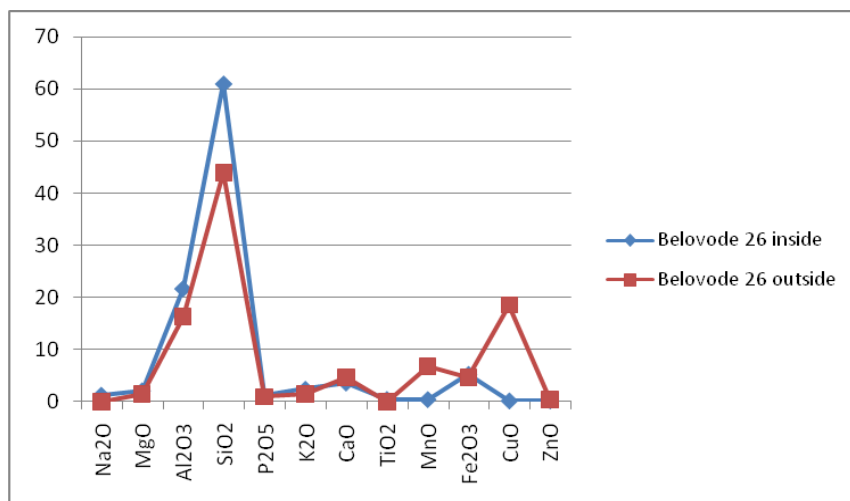


Fig. 80- ED-XRF compositional data for the inside and outside walls of Belovode 26 (major oxides presented). Note elevated readings in copper oxide in the outer walls.

The ceramic fabric is optically bright red, well kneaded and tempered with very abundant quartz grains and crushed calcite, amounting to around 40 vol%; they are mostly still angular and measuring up to 0.5 mm across (Figs. 81a and 81b).

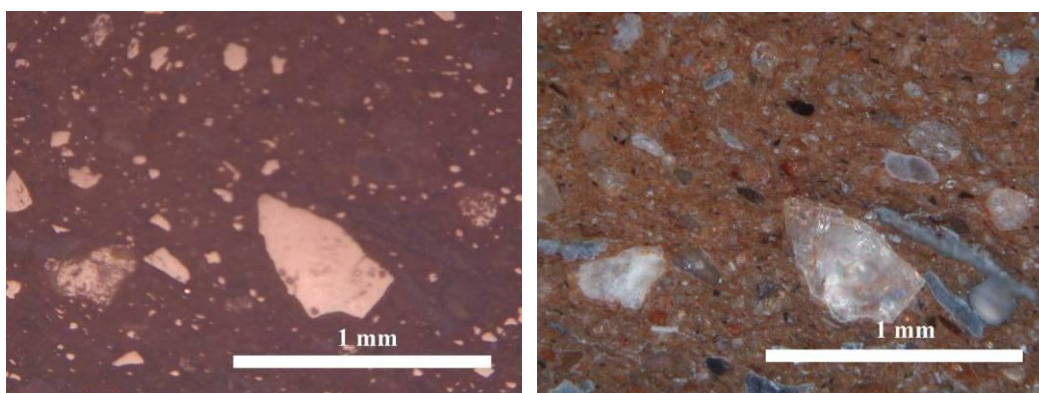


Fig. 81- a) Photomicrograph of the fabric in Belovode 26 under plane polarized light. Note white quartz as the major temper; b) Photomicrograph of the fabric in Belovode 26 under cross polarized light. Note crushed calcite (grey crystals) near quartz grains, as tempering material.

The orientation of clay minerals is parallel to the surfaces; the pores tend to be elongated, indicating low firing temperature of the vessel. The dense paste looks “dry”, but firm and far from collapsing. The SEM-EDS analysis of the ceramic body revealed alumina and silica as the major components, in the average ratio 1: 4, with significant amounts of magnesia and iron oxide (Table 50). These results are also comparable with

the ones gained from ED-XRF, on the qualitative basis (see Table 49 in Appendix Tables).

	Na ₂ O	MgO	Al ₂ O ₃	SiO ₂	P ₂ O ₅	K ₂ O	CaO	TiO ₂	MnO	FeO	CuO
	wt%	wt%	wt%	wt%	wt%	wt%	wt%	wt%	wt%	wt%	wt%
Minimum	0.5	1.6	14.5	60.6	0.6	3.1	1.8	0.7	0.0	5.2	0.0
Maximum	2.9	2.3	19.1	64.8	1.0	3.8	6.8	1.0	0.0	7.4	1.1
Average	1.0	2.0	17.4	63.4	0.9	3.5	4.2	0.8	0.0	6.7	0.3

Table 50. SEM-EDS compositional analysis of minimum, maximum and average values of body of Belovode 26; fully reported in the catalogue of ceramic artefacts. All results previously normalized to 100%.

The green lump of ore particles adhered to the outer walls of this sherd revealed characteristic light green crystals of malachite, mixed with the oolitic structures of similar optical appearance; all are embedded in a dark grey matrix abundant in silica grains (Figs. 82, 83a and 83b).

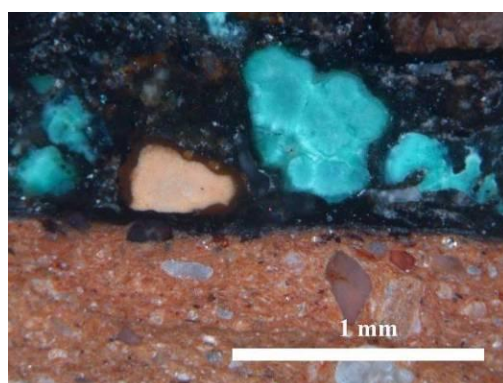


Fig. 82- Photomicrograph of the ore-rich layer adhered on outer walls of Belovode 26 under cross polarized light. Note light green crystal with convoluted agglomerations inside it and white quartz grain embedded in the dark grey matrix.

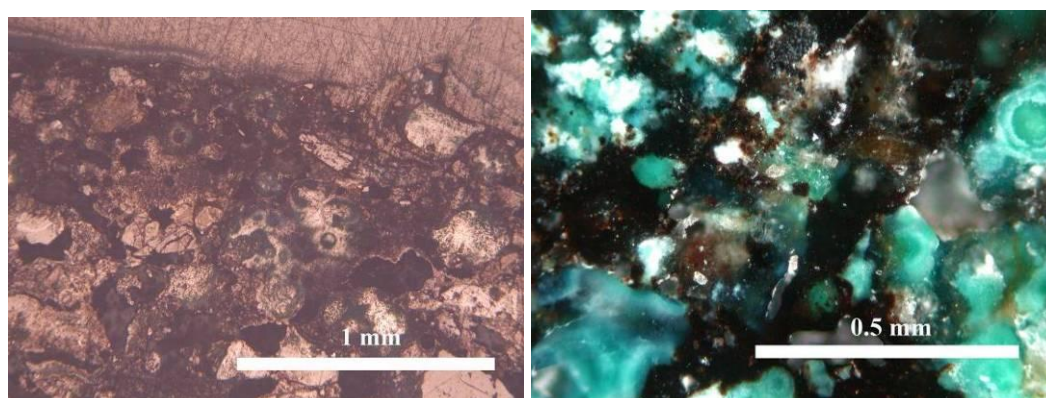


Fig. 83- a) Photomicrograph of the ore-rich layer adhered on outer walls of Belovode 26 under plane polarized light; b) photomicrograph of the ore-rich layer adhered on outer walls of Belovode 26 under cross polarized light. Note green ooids embedded in the dark grey matrix.

The light green crystals near the ceramic wall are optically identified as a grouping of convoluted agglomerations, which under the electron microscopy show bright phases rich in copper oxide (Table 51, Fig. 84a).

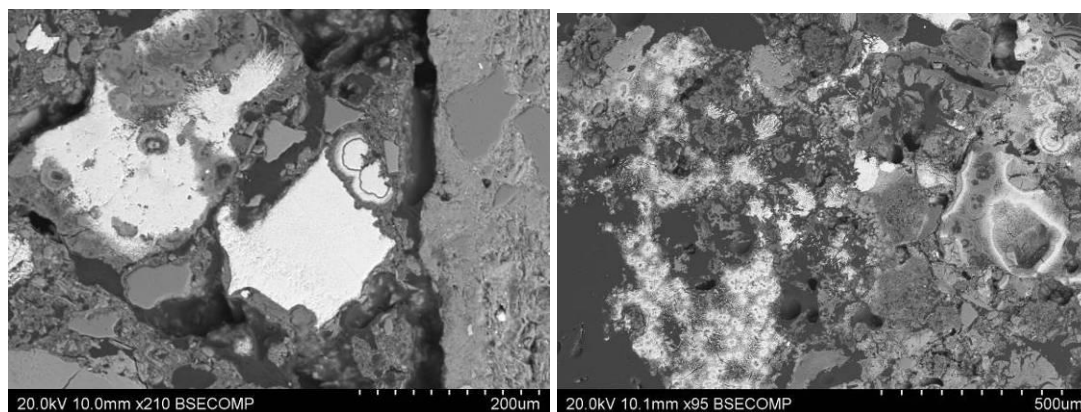


Fig. 84- a) Backscattered electron image of the corroded copper metal (bright); b) back scattered electron image of the geological copper ore (bright ooids).

	O	Cu
	wt%	wt%
spot 1	35.6	64.4
spot 2	35.6	64.4
spot 3	35.5	64.5

Table 51. SEM-EDS compositional analysis of copper phase in the adhered ore-rich layer in Belovode 26. All results are measured as elements and normalized to 100%.

The bright phase is indicative for molten copper, rather than geological ore, which is revealed in the upper parts of this layer (Fig. 84b). The geological copper has both distinctive structure, and chemical composition: ooids rich in copper contain minute concentrations of zinc and manganese oxides (Table 52). The optically green oolitic structures also include grey phases with elevated levels of manganese and lime, with copper oxide as the major component (see Figs. 83a and 84b, Table 53).

	SiO ₂	CaO	MnO	FeO	CuO	ZnO
	wt%	wt%	wt%	wt%	wt%	wt%
Minimum	0.0	0.0	0.0	0.0	94.1	0.0
Maximum	1.5	0.8	2.4	1.1	98.0	5.3
Average	0.9	0.4	0.5	0.6	96.3	1.3

Table 52. SEM-EDS compositional analysis of minimum, maximum and average values of the oolitic structures in the adhered ore-rich layer in Belovode 26; fully reported in the catalogue of ceramic artefacts. All results previously normalized to 100%.

	Al ₂ O ₃	SiO ₂	P ₂ O ₅	CaO	MnO	FeO	CuO
	wt%	wt%	wt%	wt%	wt%	wt%	wt%
Average	1.7	4.4	1.0	12.6	16.1	0.9	63.3

Table 53. SEM-EDS compositional analysis of average values of the optically grey phase in the oolitic structures, found within the adhered ore-rich layer in Belovode 26; fully reported in the catalogue of ceramic artefacts. All results previously normalized to 100%.

In addition, the presence of charcoal (Fig. 85, Table 54) confirms the assumption of the heat treatment this copper-rich mass underwent. Nevertheless, since no marks of the elevated temperature have been detected on the inner surface of the ceramic sherd, there is no indication for this vessel being used as a crucible.

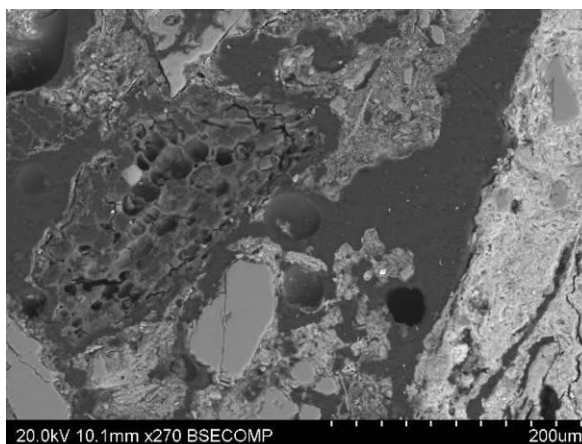


Fig. 85- Backscattered electron image of the piece of charcoal embedded in the ore-rich layer adhered to outer walls of Belovode 26.

	P ₂ O ₅	SO ₃	K ₂ O	CaO	CuO
	wt%	wt%	wt%	wt%	wt%
spot 1	0.0	7.0	0.0	63.7	29.4
spot 2	3.2	0.0	2.0	64.8	30.0
Average	1.6	3.5	1.0	64.2	29.7
St. deviation	2.3	4.9	1.4	0.8	0.4

Table 54. SEM-EDS compositional analysis of charcoal in the adhered ore-rich layer in Belovode 26. All results normalized to 100%.

Bearing in mind that the ceramic sherd originates from the potential workshop space, this adherence is rather ascribed to post-depositional processes leading to bonding of this mass to the outer walls; where the evidence for heating could only strengthen the assumption of a workshop being the most likely context for this find.

Belovode 29 and Belovode 30

The bulk chemical ED-XRF analysis of the outside walls of both Belovode 29 and 30 showed elevated concentrations of silica and iron oxide, as opposed to the composition of inside walls (Tables 55 and 56 in Appendix Tables, Figs. 86a and 86b).

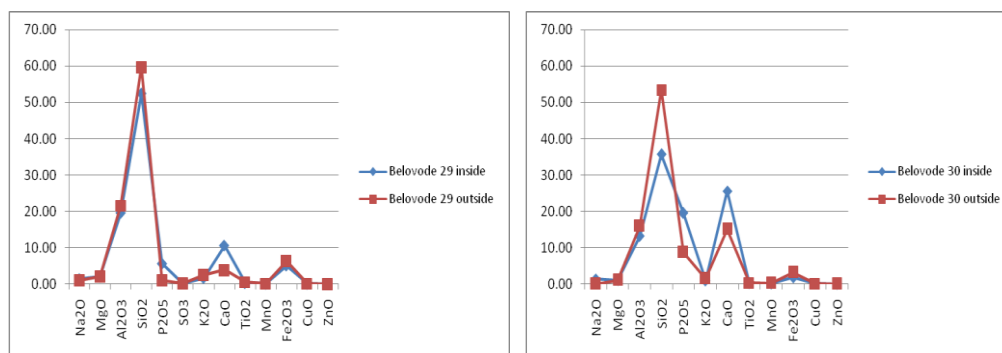


Fig. 86- a) ED-XRF compositional data for the inside and outside walls of Belovode 29 (major oxides presented). Note high readings in calcium oxide and phosphorus, particularly in the inside walls; **b)** ED-XRF compositional data for the inside and outside walls of Belovode 30 (major oxides presented). Note high readings in calcium oxide and phosphorus, particularly in the inside walls.

Both samples revealed higher readings in calcium and phosphorus in the inside surface as opposed to the outer; however the concentration of phosphorus appear to be even higher in the inside walls of Belovode 30 (see Table 56 in Appendix Tables).

The three samples analyzed in total (Belovode 29, Belovode 30ch and Belovode 30wh) have a similar fabric: it is optically dark brown, well kneaded and tempered with very abundant quartz (Fig. 87a) and crushed calcite (Belovode 30ch and 30wh), amounting to around 50 vol% (Fig. 87b). Most of the quartz grains lost their angularity, indicating the reaction with the surrounding matrix during the firing process.

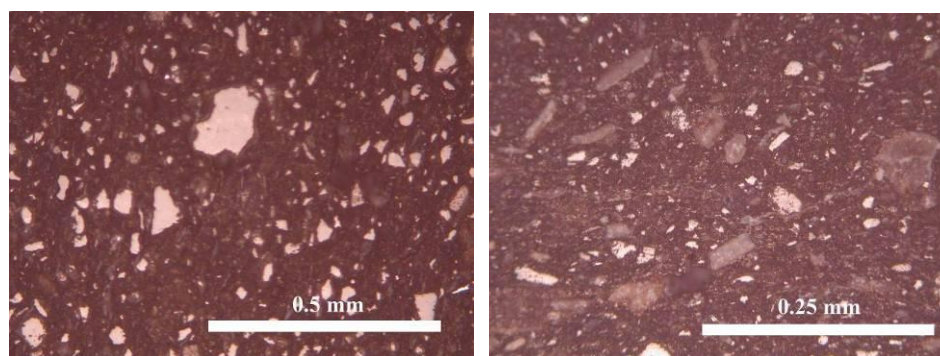


Fig. 87- a) Photomicrograph of the fabric in Belovode 29 under plane polarized light. Note white quartz as the major temperer; **b)** Photomicrograph of the fabric in Belovode 30ch under plane polarized light. Note quartz and calcite as the major tempering material.

Expansion voids surround the quartz grains, together with elongated open cracks along the fabric, particularly in the samples Belovode 30ch and 30wh (Fig. 88a). Belovode 30 presented greater variety of the tempered materials, which include more organic substances, such as shells or bones (Figs. 88b and 89).

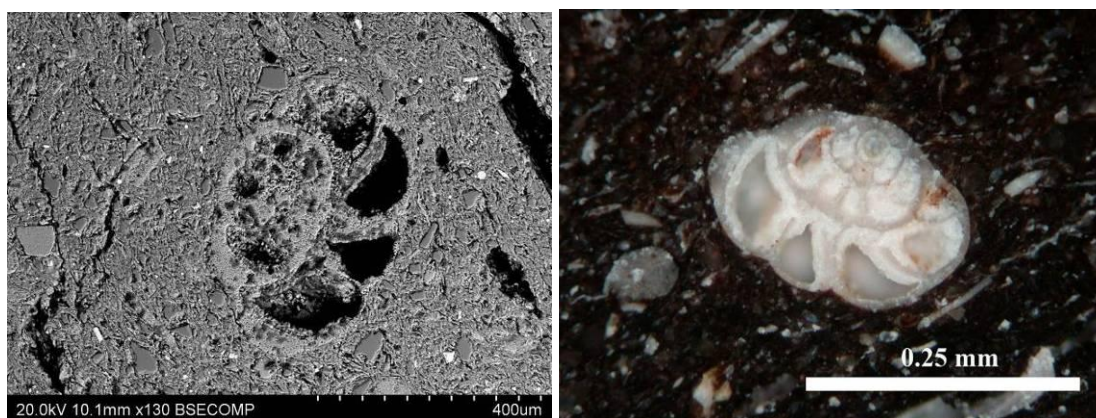


Fig. 88- a) Back scattered electron image of the fabric in Belovode 30wh. Note cracks in the fabric (up right) and shell as tempering material; b) photomicrograph of the shell included as tempering material in the fabric of Belovode 30, taken under cross polarized light.

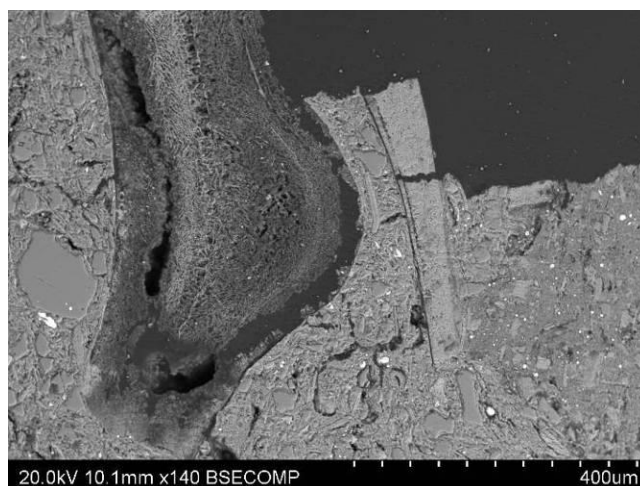


Fig. 89- Back scattered electron image of bone used as tempering material in the fabric of Belovode 30.

The orientation of clay minerals is parallel to the surfaces; however the pores are mainly found elongated, pointing towards low firing temperature of these vessels. The dense paste gives the “dry” impression, with little indication of potential collapsing. The SEM-EDS analysis of ceramic bodies revealed the same alumina to silica ratio (1:4 in

average) as in Belovode 26, followed by significant amounts of iron oxide, magnesia and potash (Tables 57, 58 and 59).

	Na2O	MgO	Al2O3	SiO2	P2O5	K2O	CaO	TiO2	FeO
	wt%	wt%	wt%	wt%	wt%	wt%	wt%	wt%	wt%
Minimum	0.6	0.6	12.0	63.5	0.0	2.1	1.0	0.0	2.1
Maximum	5.2	2.2	19.3	78.1	1.3	4.2	2.1	1.7	7.9
Average	2.1	1.6	17.1	67.4	0.3	3.1	1.6	0.7	6.0

Table 57. SEM-EDS compositional analysis of minimum, maximum and average values of body of Belovode 29; fully reported in the catalogue of ceramic artefacts. All results previously normalized to 100%.

	Na2O	MgO	Al2O3	SiO2	P2O5	K2O	CaO	TiO2	MnO	FeO
	wt%	wt%	wt%	wt%	wt%	wt%	wt%	wt%	wt%	wt%
Minimum	0.0	1.5	13.5	53.5	0.7	2.7	2.8	0.5	0.0	4.2
Maximum	1.4	2.2	19.4	67.0	2.4	5.2	14.2	1.0	2.3	7.4
Average	0.7	1.8	16.4	62.5	1.3	3.4	6.9	0.7	0.2	6.0

Table 58. SEM-EDS compositional analysis of minimum, maximum and average values of body of Belovode 30ch; fully reported in the catalogue of ceramic artefacts. All results previously normalized to 100%.

	Na2O	MgO	Al2O3	SiO2	P2O5	K2O	CaO	TiO2	MnO	FeO
	wt%	wt%	wt%	wt%	wt%	wt%	wt%	wt%	wt%	wt%
Minimum	0.0	1.6	15.4	53.3	0.6	3.0	3.2	0.6	0.0	6.1
Maximum	1.3	3.2	20.8	64.1	2.0	4.6	10.5	2.4	0.0	8.2
Average	0.8	2.1	17.0	60.6	1.4	3.5	6.7	1.0	0.0	6.9

Table 59. SEM-EDS compositional analysis of minimum, maximum and average values of body of Belovode 30wh; fully reported in the catalogue of ceramic artefacts. All results previously normalized to 100%.

SEM-EDS analysis are confirmed with microscopic observation (Figs. 90a, 90b, 91a and 91b), revealing high readings of calcium and phosphorus in the average ratio of approximately 55:45 wt% (see Catalogue in Appendix).

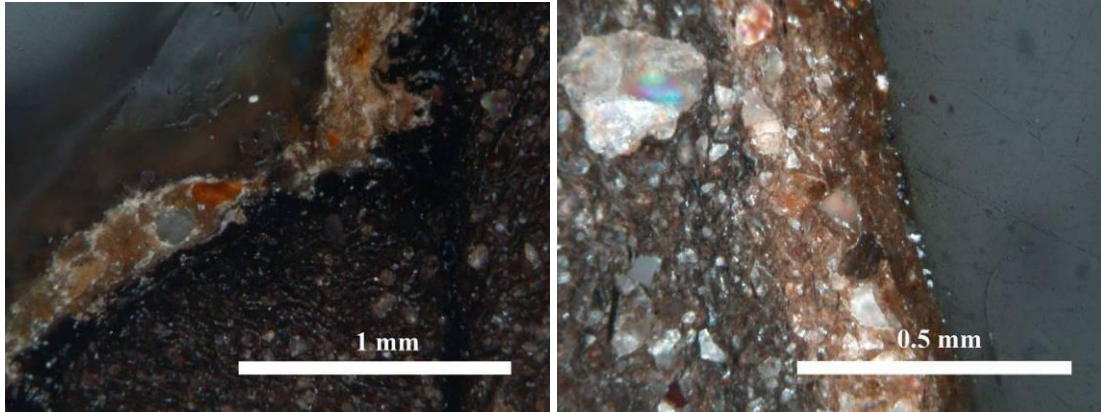


Fig. 90- a) Photomicrograph of the calcium phosphate lagging on the outside walls of Belovode 29 under cross polarized light. Note quartz inclusions embedded in the lagging; b) photomicrograph of the bone ash lagging on the inside walls of Belovode 29 under cross polarized light. Note quartz inclusions embedded in the lagging.

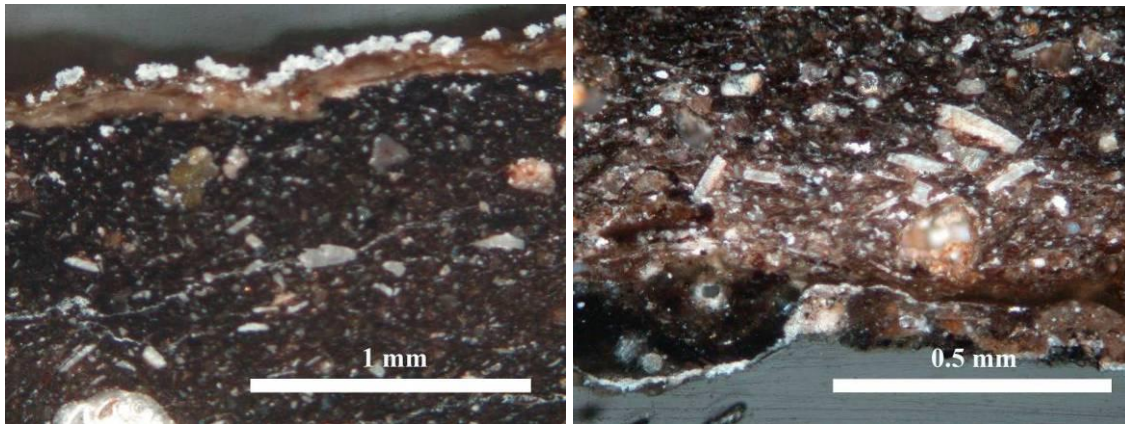


Fig. 91- a) Photomicrograph of the calcium phosphate lagging on the inside walls of Belovode 30wh under cross polarized light; b) photomicrograph of the bone ash lagging on the outside walls of Belovode 30wh under cross polarized light.

All laggings appear thick and dense, particularly in the inside walls (Figs. 92a and 92b) of all three samples, whereas the outer layers revealed a cellular structure of the bone adhered to the bottom/outer walls of the vessel (Belovode 30ch and 30wh; Figs. 93a and 93b).

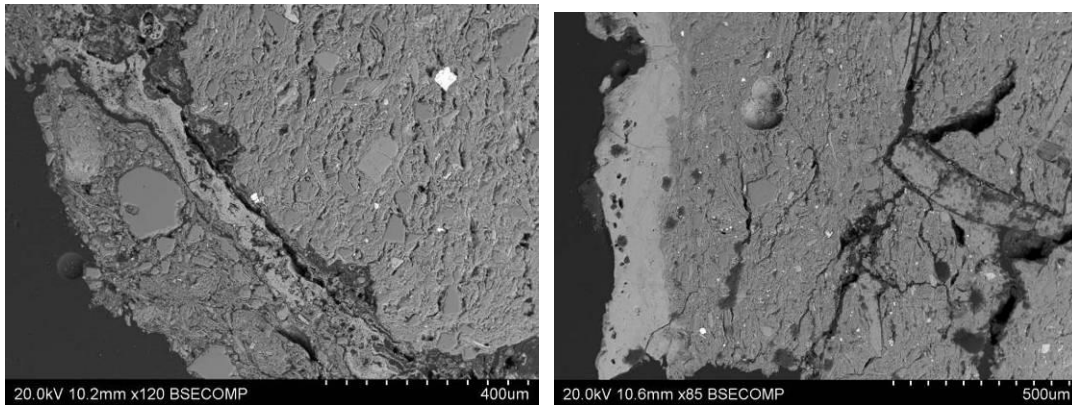


Fig. 92- a) Back scattered electron image of the calcium phosphate lagging (light grey) on the outside walls of Belovode 29. Note the layer of dirt on top of it; b) back scattered electron image of the calcium phosphate lagging (light grey) on the inside walls of Belovode 30.

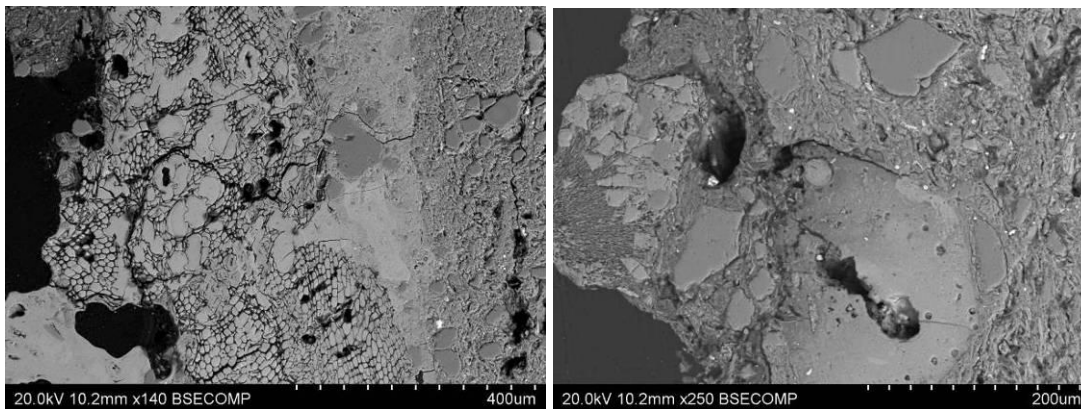


Fig. 93- Back scattered electron image of the calcium phosphate lagging on the outside walls of Belovode 30ch. Note cellular structure of the charcoal filled with calcium phosphate; b) Back scattered electron image of the calcium phosphate lagging on the outside walls of Belovode 30wh. Note cellular structure of the charcoal filled with calcium phosphate.

The laggings on the inside walls of Belovode 30 are free of inclusions, whereas in Belovode 29 the quartz grains are found embedded in it. However, the outside laggings are shown as less consistent: apart from the layer of dirt, the calcium phosphate layer is found to fill in the cellular structure of the remaining charcoal. This is under cross polarized light presented as black phase with cellular structure (Fig. 94); the chemical composition also confirms this assumption.

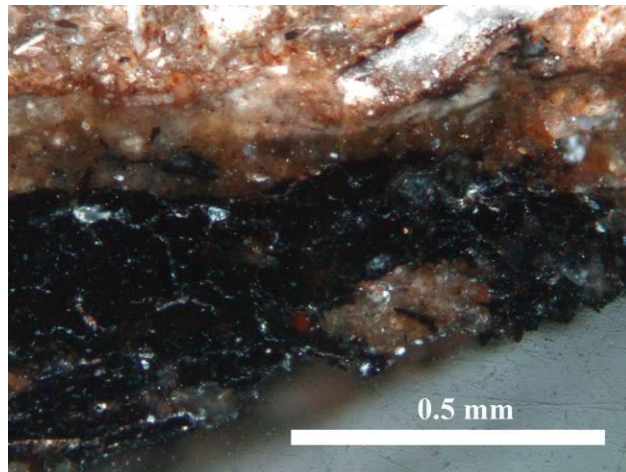


Fig. 94- Photomicrograph of the charcoal filled with calcium phosphate in the bottom of Belovode 30ch under cross polarized light.

Metallurgical activities are revealed in the inner section of Belovode 29: the layer of crushed ore rich in copper content and significant amounts of zinc oxide (Table 60, Fig. 95), indicate potential beneficiation of copper ores in this vessel. The layer itself is presented with metal-rich particles, with no indication of thermal treatment applied.

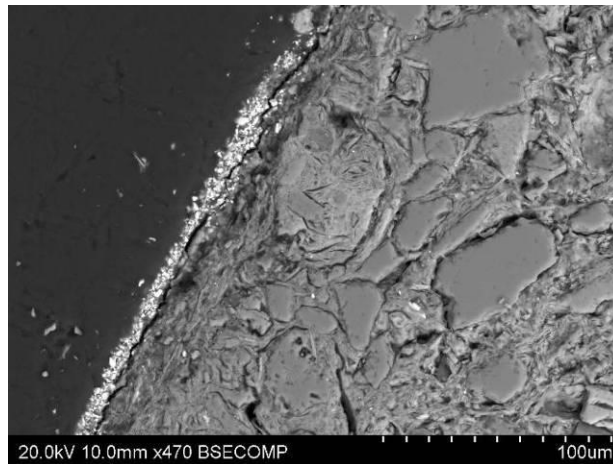


Fig. 95- Back scattered electron image of the crushed ore layer on the inside walls of Belovode 29.

	Al ₂ O ₃	SiO ₂	SO ₃	K ₂ O	CaO	FeO	CuO	ZnO
	wt%	wt%	wt%	wt%	wt%	wt%	wt%	wt%
Minimum	0.0	1.6	0.0	0.0	0.0	0.7	88.6	3.1
Maximum	1.9	3.9	1.8	0.0	1.4	1.3	91.6	3.9
Average	1.4	3.0	0.7	0.0	0.6	1.0	89.9	3.5

Table 60. SEM-EDS compositional analysis of minimum, maximum and average values of the crushed ore layer on the inside walls of Belovode 29; fully reported in the catalogue of ceramic artefacts. All results previously normalized to 100%.

It is important to emphasize that none of the analyzed ceramic sherds have shown traces of activities related to the smelting of copper ores. However, the calcium phosphate laggings could potentially indicate their relation to metallurgy: they appear as an interior of refractories in pre-Hispanic metallurgy in the Northwest Argentina, believed to facilitate the casting, increase the firmness of crucible and protect it from the erosive action of the metal (González and Gluzman 2007). On the other hand, this is the sole case known in archaeometallurgy, and chronologically comes rather late for comparison: from 9th to 15th AD.

Nevertheless, although no further indications for smelting activities have been found on these sherds, their context could potentially indicate their function. All sherds were found in the workshop, or courtyard of a house containing a shallow pit assumed to be used for smelting activities (Šljivar, Jacanović and Kuzmanović- Cvetković 2006); this can be indicative for their potential association with metallurgical activities on the site. The layer of crushed ore in one of the sherds points towards storage function, where the emphasis should be set on its deposition on top of the bone-ash lagging.

Nevertheless, the calcium phosphate laggings could have been also used as good refractory in cooking (cf. Keller and Stern 1999), or other domestic purposes; and despite the lack of firm evidence for their relation to metallurgical activities, this occurrence can be treated as a very specific in the Vinča culture pottery assemblage.

Provenance studies: Lead isotope and trace element analysis

Altogether 14 samples were analyzed for their lead isotope ratio with ICP-MS, selected on the basis of representativeness of analyzed archaeological material. The sample belonging to copper ingot Belovode 34 was additionally studied for the trace element composition, with the same analytical set-up (see Chapter 2). The aim of these analyses was to explore the provenance and inter-relation of all materials indicating metallurgical activities in Belovode, with particular emphasis on the association of the copper ingot with the excavated assemblage.

The isotope abundance ratios of lead in all investigated metal artefacts are summarized in Table 61, and depicted in Fig. 96. The most striking result is the tight grouping of all samples in three assemblages, based on the distinctive lead isotope ratios:

- Group A (Belovode 13, Belovode 17, Belovode 32 and Belovode 34) represents artefacts: malachite bead and ingot, and sulphidic ores, one of which was assumed to be thermally treated; the lead isotope abundances ratio shows grouping of data points around $^{208}\text{Pb}/^{206}\text{Pb} \approx 2.076$, $^{207}\text{Pb}/^{206}\text{Pb} \approx 0.843$ and $^{206}\text{Pb}/^{204}\text{Pb} \approx 18.490$;
- Group B (Belovode 12, Ždrelo 1 C1, Ždrelo 2 C2, Ždrelo 2) stands for archaeological ore and geological ores from the mine in the vicinity of Belovode; the lead isotope abundances ratio shows grouping of data points around $^{208}\text{Pb}/^{206}\text{Pb} \approx 2.072$, $^{207}\text{Pb}/^{206}\text{Pb} \approx 0.839$ and $^{206}\text{Pb}/^{204}\text{Pb} \approx 18.611$;
- Group C (Belovode 20, Belovode 21, Belovode 22 and Belovode 23) exhibits slag samples, here grouped as a distinctive field, although appearing drawn out across the diagram; the lead isotope abundances ratio shows grouping of data points around $^{208}\text{Pb}/^{206}\text{Pb} \approx 2.045$, $^{207}\text{Pb}/^{206}\text{Pb} \approx 0.827$ and $^{206}\text{Pb}/^{204}\text{Pb} \approx 18.918$;

Group	Sample	Pb (ppm)	$^{208}\text{Pb}/^{206}\text{Pb}$	$^{207}\text{Pb}/^{206}\text{Pb}$	$^{206}\text{Pb}/^{204}\text{Pb}$
A	ŽDRelo 1 C1	727.8	2.0735	0.83991	18.620
A	ŽDRelo 1 C2	1286.6	2.0713	0.83931	18.617
A	ŽDRelo 2	1116.1	2.0730	0.83988	18.623
A	Belovode 12	5.7	2.0693	0.83947	18.585
B	Belovode 13	9.0	2.0771	0.84338	18.480
B	Belovode 17	253.7	2.0754	0.84249	18.491
B	Belovode 32	94.3	2.0751	0.84252	18.490
B	Belovode 34	4.4	2.0773	0.84348	18.499
C	Belovode 20	3.2	2.0610	0.83512	18.675
C	Belovode 21	4.3	2.0550	0.83089	18.831
C	Belovode 22	1.2	2.0546	0.83065	18.870
C	Belovode 23	1.6	2.0088	0.81254	19.296

Table 61. Lead isotope abundance ratios in material from Belovode and Ždrelo.

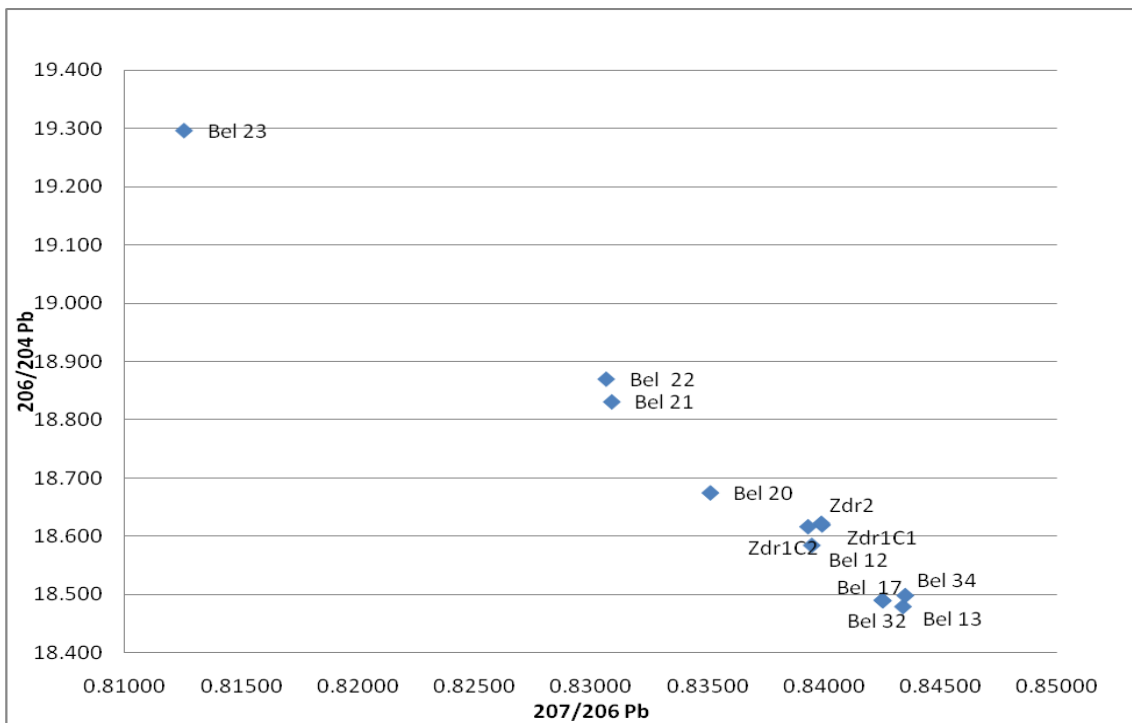
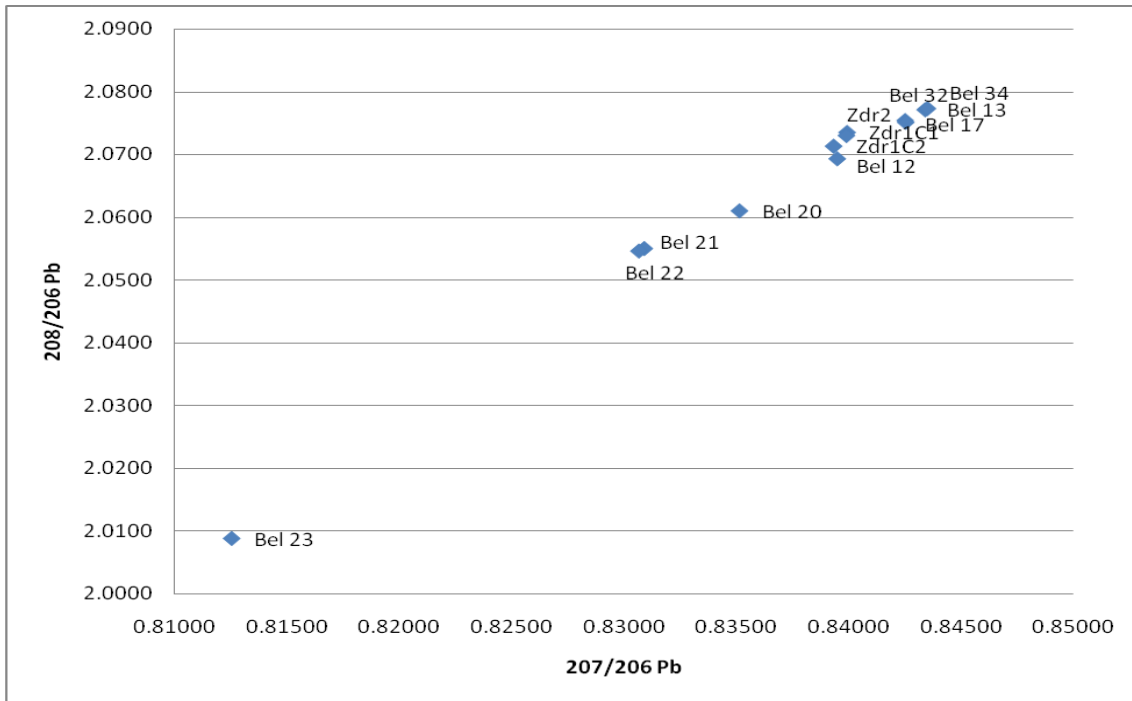


Fig. 96- Lead isotope abundance ratios in samples from Belovode and Ždrelo. Labels are abbreviated as follows: Bel=Belovode, Zdr=Ždrelo.

Variations in this order are routinely found among ores even from single deposits, both in Serbia (Pernicka *et al.* 1993) and Bulgaria (Pernicka *et al.* 1997); thus, the particular grouping of materials is here assumed to derive from the same ore source. To locate this source, the lead isotope abundance ratios of ore deposits from Serbia and Bulgaria were searched for the agreement with the lead isotope signatures in material from Belovode.

In Serbia, the database includes ores and slags from Eastern Serbia (Majdanpek, Rudnik, Rudna Glava and minor adjacent outcrops) and Čadinje in Southwest Serbia (Pernicka *et al.* 1993; Table 62, Fig. 97).

In the neighbouring country, the database is divided into three main metallogenic zones: The Balkan, The Srednogorje and the Rhodope zone, which are, though adjacent to the Eastern Serbian copper belt, not genetically related to this region (Pernicka *et al.* 1997; Table 63, Fig. 98). Only data falling within or near the field of Belovode and Ždrelo samples are further discussed and presented in this study.

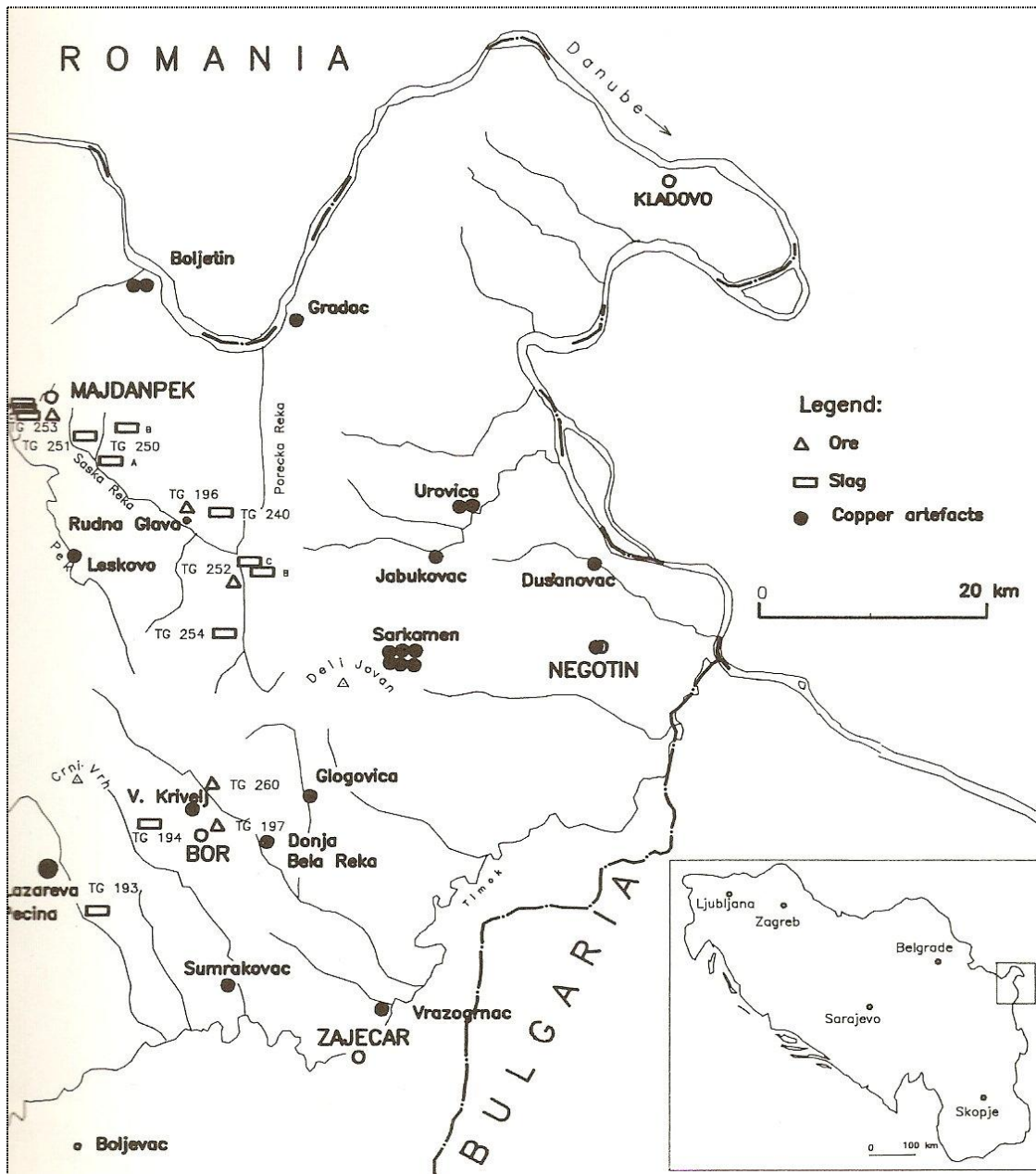


Fig. 97- Locations of ore and slag samples from Eastern Serbia (after Pernicka *et al.* 1993: 39, Fig. 18).

Label	Sample	Location	Region	Description	$^{208}\text{Pb}/^{206}\text{Pb}$	$^{207}\text{Pb}/^{206}\text{Pb}$	$^{206}\text{Pb}/^{204}\text{Pb}$
HDM	TG 193 A	Beljevina	SRB	cu slag	2.0539	0.8342	18.7200
HDM	TG196	Rudna Glava	SRB	cu ore mal	2.0374	0.8319	18.7800
HDM	TG196-1	Rudna Glava	SRB	cu ore (magn, chalc, mal)	1.5448	0.6346	25.2060
HDM	TG 196-2	Rudna Glava	SRB	cu ore mal	2.0466	0.8372	18.6600
HDM	tg 196-2g-1	Rudna Glava	SRB	cu ore (mal, azur)	1.0507	0.4525	36.6350
HDM	TG 196-2g-2	Rudna Glava	SRB	cu ore (chalc, mal)	1.9548	0.7974	19.6690
HDM	TG 196-2g-3	Rudna Glava	SRB	cu ore (mal)	1.5461	0.6067	26.3720
HDM	TG 196-2g-4	Rudna Glava	SRB	cu ore (mal)	2.0493	0.8388	18.6600
HDM	TG 196-3	Rudna Glava	SRB	cu ore (mal)	2.0409	0.8327	18.7890
HDM	TG 196-4	Rudna Glava	SRB	cu ore (mal)	1.8599	0.7515	20.9900
HDM	TG 196-4.3	Rudna Glava	SRB	cu ore (chpyr.mal.azur)	1.8791	0.7552	20.8640
HDM	TG 196 A	Rudna Glava	SRB	cu ore (chpyr.mal.azur)	1.6961	0.6830	23.2710
HDM	TG 196 B	Rudna Glava	SRB	cu ore (magn, chalc)	1.8239	0.7483	21.0590
HDM	RUDNA 1	Rudna Glava	SRB	cu ore (mal)	1.8846	0.7665	20.6120
HDM	RUDNA 2	Rudna Glava	SRB	cu ore (mal)	1.9339	0.7846	20.0130
HDM	RUDNA 3	Rudna Glava	SRB	cu ore (mal)	1.9935	0.8119	19.3020
HDM	RUDNA 4	Rudna Glava	SRB	cu ore (mal)	0.6723	0.3089	57.1560
HDM	RUDNA 5	Rudna Glava	SRB	cu ore (mal)	1.9535	0.7801	20.1180
GALE	RG1	RUDNA GLAVA 1	SRB	cu ore	2.07572	0.84975	18.3400
GALE	RG2	RUDNA GLAVA 2	SRB	cu ore	2.07802	0.85069	18.3270
GALE	RG3	RUDNA GLAVA 3	SRB	cu ore	2.08345	0.85226	18.3230
GALE	RG4	RUDNA GLAVA 4	SRB	cu ore	2.07952	0.85223	18.3360
HDM	TG 240	Velika Brestovica	SRB	cu slag	2.0587	0.8320	18.8180
HDM	TG 249 A	Rudnik	SRB	cu ore (mal)	2.0770	0.8384	18.6730
HDM	TG 249 AA	Rudnik	SRB	pb-zn ore (gal, sphal, pyr, chpyr)	2.0783	0.8387	18.6860
HDM	TG 249 B	Rudnik	SRB	cu slag	2.0783	0.8383	18.6720
HDM	TG 249 BB	Rudnik	SRB	pb-zn ore (gal, sphal, pyr, chpyr)	2.0793	0.8387	18.6890
HDM	TG 249 D	Rudnik	SRB	cu slag	2.0788	0.8388	18.6850
HDM	TG 249 EE	Rudnik	SRB	cu ore (chpyr)	2.0783	0.8387	18.6770
HDM	TG 249 F	Rudnik	SRB	pb-zn slag	2.0788	0.8384	18.6920
HDM	TG 249 FF	Rudnik	SRB	pb-zn ore (gal, sphal, pyr, chpyr)	2.0770	0.8385	18.6610
HDM	TG 249 G	Rudnik	SRB	pb-zn slag	2.0796	0.8386	18.6830
HDM	TG 249 O-1	Rudnik	SRB	cu ore (chpyr, mal)	2.0770	0.8383	18.6770
HDM	TG 249 O-2	Rudnik	SRB	cu slag	2.0785	0.8388	18.6760
HDM	TG 249 T	Rudnik	SRB	cu slag	2.0786	0.8387	18.6810
HDM	TG 249 Y	Rudnik	SRB	cu slag	2.0801	0.8391	18.7100
HDM	TG 252 A	Crnajka	SRB	fe ore	1.7186	0.7061	22.4490
HDM	TG 252 B	Crnajka	SRB	cu slag	2.0762	0.8378	18.6860
HDM	TG 252 B-1	Crnajka	SRB	cu slag	1.9225	0.7807	20.1540
HDM	TG 252 B-2	Crnajka	SRB	cu slag	2.0183	0.8217	19.0490
HDM	TG 252 B-3	Crnajka	SRB	cu slag	1.6375	0.6707	23.7570
HDM	TG 252 C-1	Crnajka	SRB	cu slag	1.4754	0.6110	26.1290
HDM	TG 252 C-2	Crnajka	SRB	cu slag	0.8906	0.3883	43.7300
HDM	TG 253 A-1	Majdanpek	SRB	cu slag, met. Cu	2.0783	0.8440	18.4610
HDM	TG 253 A-2	Majdanpek	SRB	oxidic cu ore	2.0753	0.8443	18.4600
HDM	TG 253 B	Majdanpek	SRB	cu slag, met. Cu	2.0763	0.8443	18.4700
HDM	TG 253 C	Majdanpek	SRB	cu slag	2.0781	0.8437	18.4910
HDM	TG 253 E-1	HDM 1472	SRB	native cu	2.0832	0.8451	18.4700
HDM	TG 253 E-2	Majdanpek	SRB	cu ore (cupr)	2.0750	0.8428	18.4830
HDM	TG 253 F	Majdanpek	SRB	cu ore (mal, azur)	2.0780	0.8440	18.4350
HDM	TG 253 G	Majdanpek	SRB	cu ore (chpyr)	2.0752	0.8427	18.4890
HDM	TG 268 (HDM1476)	Čadinje	SRB	native cu	2.0914	0.8505	18.4020
HDM	TG 268 A	Čadinje	SRB	sulfidic ore (gal, pyr)	2.0017	0.8117	19.3340
HDM	TG 268 D	Čadinje	SRB	cu ore (native cu, cupr)	2.0949	0.8527	18.3530
HDM	TG 268 F	Čadinje	SRB	cu ore (chpyr, pyr)	2.0946	0.8517	18.3840

Table 62. Lead isotope abundance ratios in ores and slags from Serbia (selected data). The region is abbreviated as SRB= Serbia; ore minerals are abbreviated as follows: azur=azurite, born=bornite, chalc= chalcocite; chpyr=chalcopyrite, cov=covelline, enarg=enargite, gal=galena, mal=malachite, pyr=pyrite, sphal=sphalerite (HDM after Pernicka *et al.* 1993: 26-27, Tab. 8; GALE after Gale *et al.* 1991: 58, Tab. 5.2).

Label	Sample	Location	Region	$^{208}\text{Pb}/^{206}\text{Pb}$	$^{207}\text{Pb}/^{206}\text{Pb}$
HDM	BG-17	Ai Bunar	THR	2.08290	0.84410
HDM	BG-17e	Ai Bunar	THR	2.08360	0.84440
HDM	BG-17f	Ai Bunar	THR	2.08360	0.84450
HDM	BG-17g	Ai Bunar	THR	2.08230	0.84420
HDM	BG-17h	Ai Bunar	THR	2.08300	0.84420
HDM	BG-17i	Ai Bunar	THR	2.08240	0.84410
GALE	AB1	Ai Bunar	THR	2.08110	0.84831
GALE	AB1a	Ai Bunar	THR	2.08712	0.84597
GALE	AB2	Ai Bunar	THR	2.07908	0.84368
GALE	AB2a	Ai Bunar	THR	2.07965	0.84360
GALE	AB4	Ai Bunar	THR	2.08051	0.84398
GALE	AB5	Ai Bunar	THR	2.08119	0.84396
GALE	AB5a	Ai Bunar	THR	2.08191	0.84437
GALE	75	Ai Bunar	THR	2.08105	0.84421
GALE	77D	Ai Bunar	THR	2.08162	0.84391
GALE	78C	Ai Bunar	THR	2.08134	0.84398
GALE	79	Ai Bunar	THR	2.08570	0.84581
HDM	BG-9a	Elacite	WB	2.08410	0.84040
HDM	BG-9b	Elacite	WB	2.05960	0.83610
A&V	39	Elacite	WB	2.08060	0.84320
HDM	BG-10a	Car Assen	WB	2.06090	0.83400
A&V	44	Medni Rid-Varli Brjag	BSC	2.06630	0.83690
HDM	BG-1b	Medni Rid	BSC	2.06450	0.83590
HDM	BG-1c	Medni Rid	BSC	2.07450	0.84500
HDM	BG-7a	Rosen	BSC	2.07210	0.84010
HDM	BG-7b	Rosen -Centrum	BSC	1.94510	0.79280
HDM	BG-7c	Rosen -Sarneško kladence	BSC	2.06050	0.83520
HDM	BG-7d	Rosen -Sarneško kladence	BSC	2.06540	0.83710
HDM	BG-6a	Zidarovo	BSC	2.06640	0.83660
HDM	BG-6b	Zidarovo	BSC	2.07540	0.8421
HDM	BG-6c	Zidarovo	BSC	2.06660	0.83770
A&V	42.1	Zidarovo, Ūrta	BSC	2.07570	0.84110
A&V	42.2	Zidarovo, Ūrta	BSC	2.06770	0.83750
A&V	42.3	Zidarovo, Ūrta	BSC	2.07180	0.83850

Table 63. Lead isotope abundance ratios of copper ores from Bulgaria (selected data). Regions are abbreviated as follows: BSC= Black Sea Coast, THR= Bulgarian Thrace, WB= western Bulgaria (A&V after Amov and Văkova 1994: tab. 1; HDM after Pernicka *et al.* 1997, 168, Tab. 168; GALE after Gale *et al.* 1991: 58, Tab. 5.1)

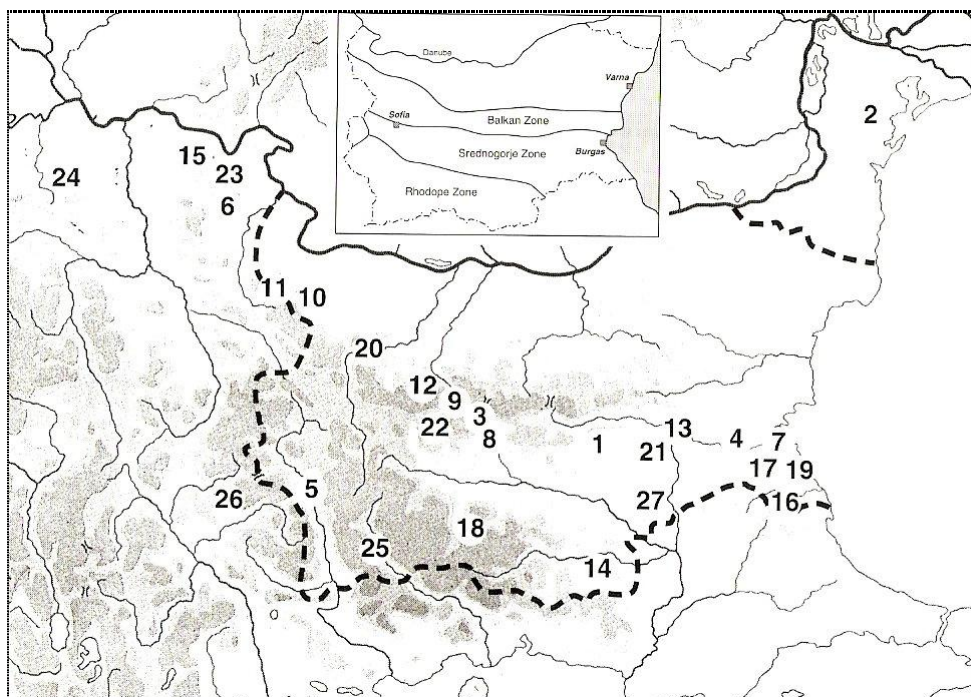


Fig. 98- Mineralized regions of Bulgaria and Eastern Serbia, with locations of analyzed ore deposits. Selected areas presented in this study: 1-Ai Bunar; 8- Car Assen; 12-Elacite; 15-Majdanpek; 17-Medni Rid, Rosen, Zidarovo; 23-Rudna Glava; 24- Rudnik (after Pernicka *et al.* 1997: 83, Fig. 14).

Of the utmost importance for the interpretation of provenance based on lead isotope abundance ratios is the observation made during the analysis of ore sources: it was shown that the lead isotope signatures in ores and slags from Rudnik or Majdanpek are indistinguishable (Pernicka *et al.* 1993: 29). This implies that any lead from other sources but copper minerals did not cause detectable change in the isotopic composition. Therefore, the studies utilizing the relative abundance of lead isotopes appear to be well justified in tracking the source from copper metal, ore or copper-based glass, without compromising inferences from lead in extraneous sources.

The provenance of material from Belovode: lead isotope analysis

The distribution of Belovode Group A (Fig. 99) material falls tightly into the range of the Majdanpek field (Eastern Serbia), showing also similar isotopy with a sample from Zidarovo (Srednogerje metallogenic zone).

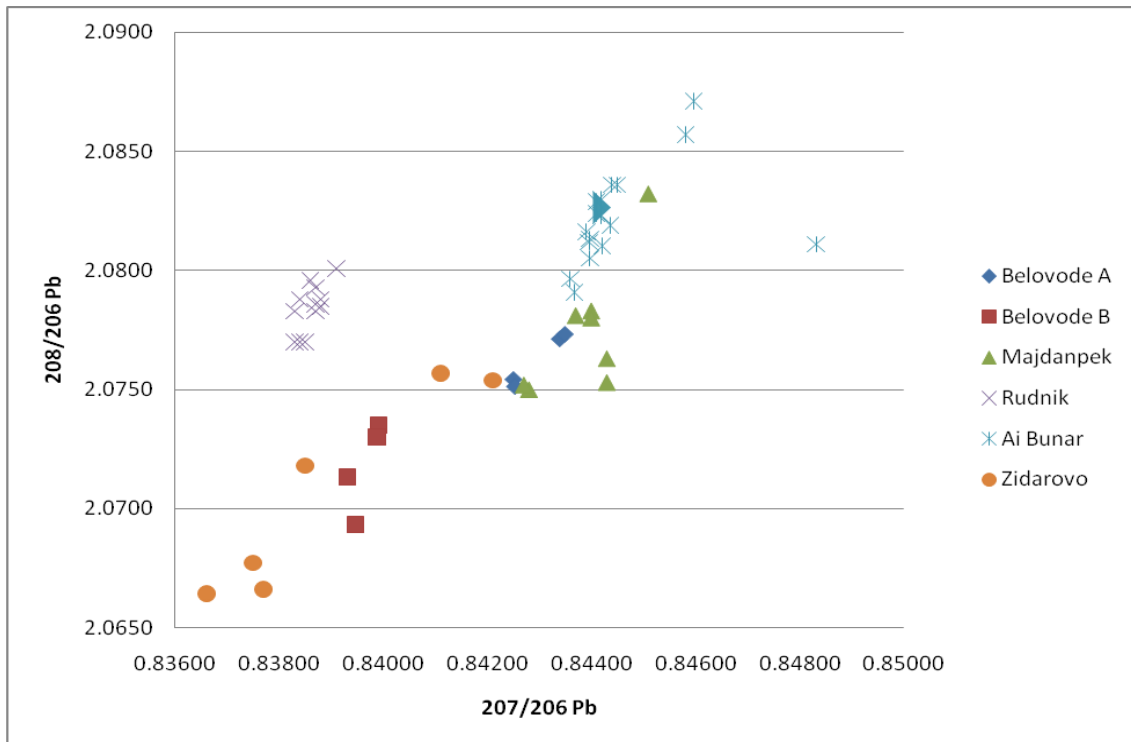


Fig. 99- Lead isotope abundance ratios in Belovode Group A and Group B in relation to Serbian and Bulgarian copper ores, native copper and copper slags.

The deposit of *Majdanpek* belongs to a Cu/Mo porphyry-type copper mineralization, with the principal ore mineral being chalcopyrite accompanied by bornite, covellite, chalcocite and rarely tetrahedrite. The part above the primary sulphides is oxidic zone, well developed with the oxidic minerals cuprite, malachite, less azurite and sporadically with native copper (Pernicka *et al.* 1993: 43). The earliest archaeometallurgical field evidence originate from the Roman and medieval period; however the findings of grooved stone tools made of andesite and easy access to native copper and oxidic ores made scholars to assume earlier activities (cf. Doelter 1916; Simić 1951).

The *Zidarovo* ore field also has some overlap with Belovode A. It is located near the Black Sea Coast, on the western slopes of the Medni Rid ridge, a rich copper deposit in Eastern Bulgaria. It is classified as vein-type hydrothermal ore deposit, with outcrops containing native copper, malachite and bornite. Numerous old workings are known since slag piles have been found in the area, although many have been destroyed by the modern mining operations (Pernicka *et al.* 1997).

The Group A did not show matching lead isotope signatures with Rudnik and Ai Bunar, both of them confirmed to present evidence for prehistoric mining dating back to c. 5000 BC (Jovanović 1963, Černych 1978b).

Ždrelo, the mine discovered in the vicinity of Belovode showed similar lead isotope abundance with the ore sample Belovode 12 (Group B). According to its isotopy, this source falls within the Zidarovo field, though no directly matching lead isotope abundance ratios have been detected.

The distinctive scatter of the Belovode Group C (Fig. 100) shows a high correspondence with *Rudna Glava*, and minor outcrops/slag heaps in *Crnajka*, *Velika Brestovica* and *Beljevina*, and *Čadinje*, a source located in Southwest Serbia. The dense correspondence of data in Fig. 100 resulted with presenting this match only with selected data for Rudna Glava and Crnajka (ratio $^{208}\text{Pb}/^{206}\text{Pb} \geq 1.9935$), avoiding the long “tail” in the previous diagram (see Fig. 101).

The lead isotope abundance ratios in the Belovode Group C show distinctive isotopic field parallel with the field of Rudna Glava, with one on-spot match of Rudna Glava sample with Belovode Slag 23 in the $^{207}\text{Pb}/^{206}\text{Pb}$: $^{206}\text{Pb}/^{204}\text{Pb}$ ratio figure. The same situation is revealed with both Crnajka and Čadinje, each matching one Belovode slag sample in the $^{207}\text{Pb}/^{206}\text{Pb}$: $^{206}\text{Pb}/^{204}\text{Pb}$ ratio figure. Velika Brestovica and Beljevina also falls within the field of Belovode slag samples. In addition, the ore sources from Bulgaria, Car Assen, Elacite, Rosen and Medni Rid demonstrated the correspondence in lead isotope abundance ratios with the single slag sample, Belovode 20 (Fig. 102).

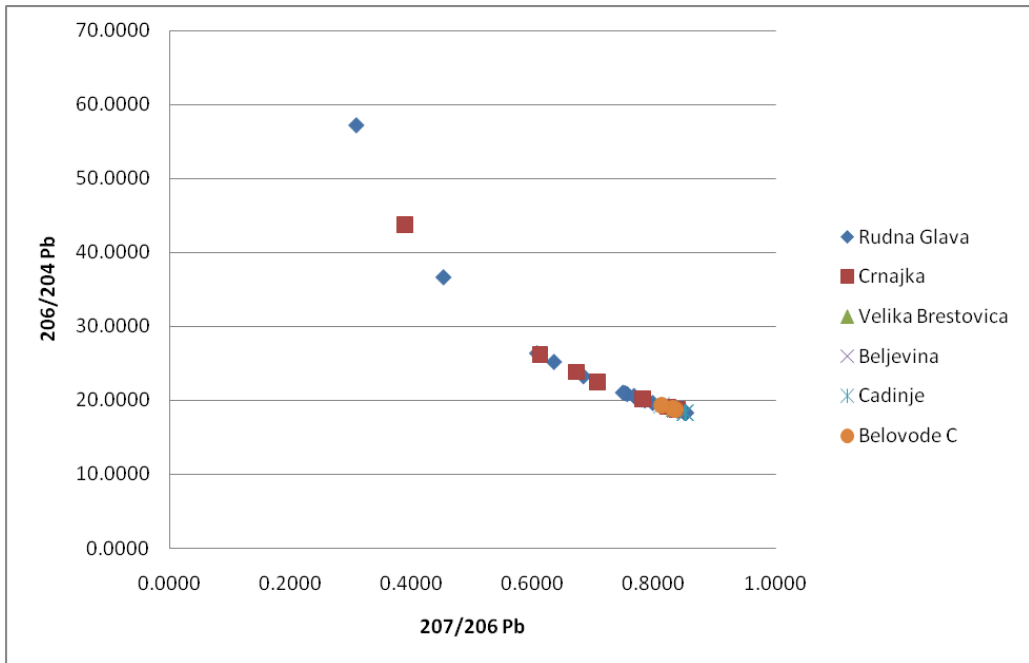
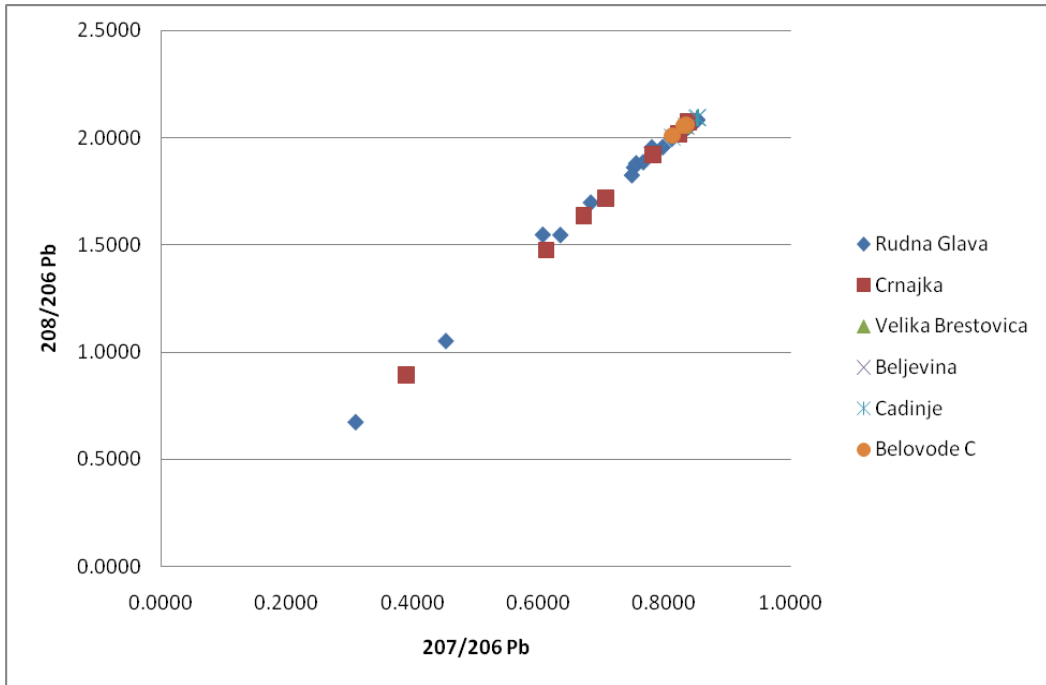


Fig. 100- Lead isotope abundance ratios of Belovode Group C in relation to Serbian copper ores, native copper and copper slags.

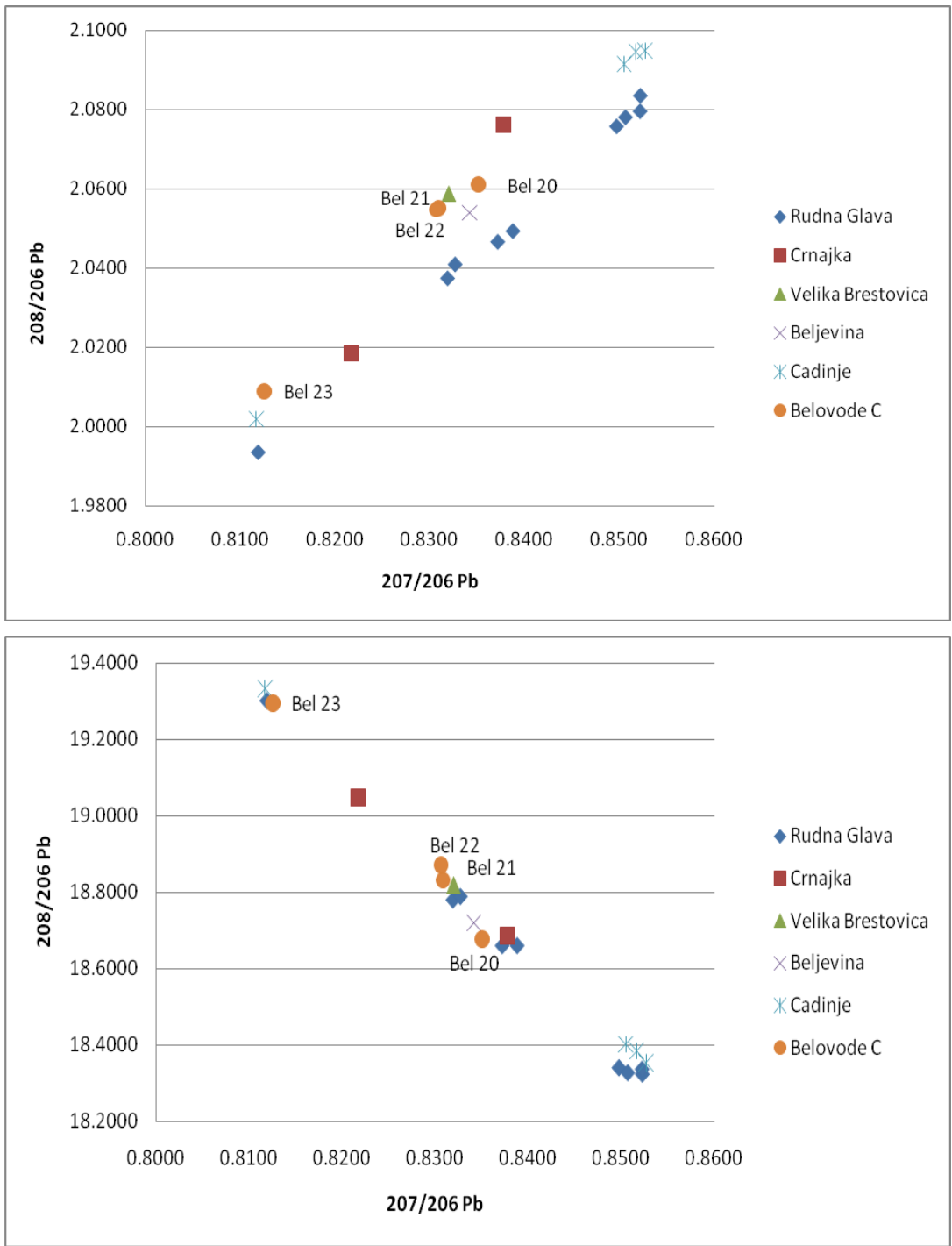


Fig. 101- Lead isotope abundance ratios of Belovode Group C in relation to Serbian copper ores, native copper and copper slags (selected data for Rudna Glava and Crnajka).

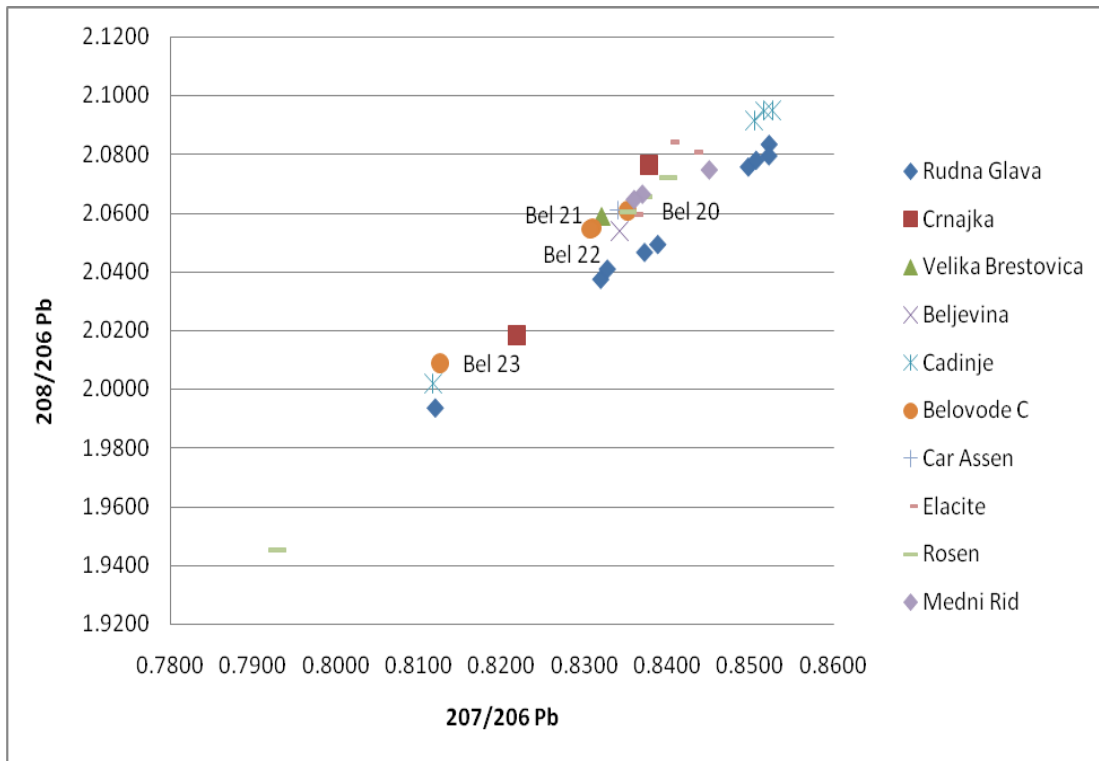


Fig. 102- Lead isotope abundance ratios of Belovode Group C in relation to Serbian and Bulgarian copper ores, native copper and copper slags.

The extreme variations in the isotope abundance ratios in the ores from *Rudna Glava* are interpreted as a result of their radiogenic character; which is claimed not to affect the reliability of tracking copper-based artefacts back to this source (Pernicka *et al.* 1993: 29, 51-52). The scatter seen here is not restricted to the copper minerals from the present-day outcrops, but also observed among ores coming from the prehistoric mine shafts, documented to be exploited from the early phases of the Vinča culture (Jovanović 1971; 1982). The deposit, located 20 km southeast from Majdanpek, is embedded in metamorphic rocks, with dominant ore mineral magnetite associated with chalcopyrite and pyrrhotine. The prehistoric mine shafts were situated within easy access to oxidized copper minerals, in a 20 m thick gossan that developed in the marble. In the following periods, these mines were exploited for iron by Romans, as well as in modern times.

Similar radiogenic variation is observed for *Crnajka*, which is by its geological origin close to Rudna Glava. It consists of magnetite, chalcopyrite and various secondary

copper minerals, which were assumed to be exploited no earlier than the Roman period (Pernicka *et al.* 1993). *Velika Brestovica* and *Beljevina* are not represented with mines, but slag heaps discarded along the rivers' valley. These slags were mainly based on sulphidic ores, and the technology of smelting pointed towards origins from Roman or medieval times.

Čadinje is an occurrence of mixed sulphide ores located near Prijepolje in southwestern Serbia, with predominant content of galena and pyrite. Ancient mining is known from the vicinity of this location, in Jarmovac (Davies 1937).

Car Assen and *Elacite* represent two copper deposits from Panagjurište, the largest copper district in the Srednogorje metallogenic zone. Car Assen has massive sulphidic deposits, followed with native copper, also detected in Elacite. The upper layers of these deposits have been almost completely removed by open-cast mining, and no old workings were found preserved thus far (Pernicka *et al.* 1997).

Both *Medni Rid* and *Rosen* are located in the Burgas district, close to the Black Sea Coast. They are classified as vein-type hydrothermal copper deposits; Rosen ore veins contain primarily chalcopyrite and pyrite, with some cobalt and molybdenum minerals, which are not present in Medni Rid. These copper deposits were exploited in the past, with no firm indication of the exact period, since potential evidence has been destroyed by modern mining (Pernicka *et al.* 1997).

The comparison of the lead isotope composition of Belovode samples with the similar material from Selevac, Pločnik and Medvednjak (Table 64, Fig. 103) shows in the first instance a conspicuous grouplet of Belovode, Selevac and Medvednjak samples above the Majdanpek field, similar in isotopy with two pieces from this source. Also, one of the samples from Selevac falls within the field of Ždrelo mine. The isotopy of Selevac samples was already discussed by Pernicka *et al.* (1993), due to the lead isotope scatter over the diagram; nonetheless, it could indicate the wider area of potential exploitation.

Sample	Site	Type	Region	$^{208}\text{Pb}/^{206}\text{Pb}$	$^{207}\text{Pb}/^{206}\text{Pb}$
HDM 1481	Selevac	malachite	SRB	2.0328	0.8236
HDM 1482	Selevac	malachite	SRB	2.0552	0.8311
HDM 1483	Selevac	cu prill	SRB	2.0422	0.8244
HDM 1484	Selevac	malachite	SRB	2.0739	0.8420
HDM 1485	Selevac	malachite	SRB	2.0749	0.8422
HDM 1486	Selevac	malachite	SRB	2.0734	0.8420
HDM 1487	Selevac	malachite	SRB	2.0762	0.8429
HDM 1488	Selevac	malachite	SRB	2.0672	0.8340
HDM 1489	Selevac	malachite	SRB	2.0735	0.8416
HDM 1490	Selevac	malachite	SRB	2.0615	0.8332
HDM 1491	Selevac	malachite	SRB	2.0731	0.8440
HDM 1492	Selevac	malachite	SRB	2.0657	0.8350
HDM 1493	Selevac	malachite	SRB	2.0681	0.8349
HDM 1494	Selevac	cu prill	SRB	2.0441	0.8253
HDM 1495	Selevac	malachite	SRB	2.0718	0.8401
HDM 1403	Medvednjak	malachite	SRB	2.0760	0.8429
HDM 1404	Medvednjak	malachite	SRB	2.0554	0.8300
HDM 1496	Gomolava	bracelet	SRB	2.0777	0.8457
HDM 1555	Pločnik	chisel	SRB	2.0812	0.8433
HDM 1556	Pločnik	flat axe	SRB	2.0836	0.8442
HDM 1557	Pločnik	flat axe	SRB	2.0825	0.8439
HDM 1558	Pločnik	hammer axe	SRB	2.0518	0.8268
HDM 1559	Pločnik	hammer axe	SRB	2.0574	0.8304
HDM 1560	Pločnik	chisel	SRB	2.0657	0.8331
HDM 1561	Pločnik	chisel	SRB	2.0629	0.8336
HDM 1562	Pločnik	chisel	SRB	2.0775	0.8403
HDM 1563	Pločnik	chisel	SRB	2.0748	0.8386
HDM 1564	Pločnik	chisel	SRB	2.0840	0.8443
HDM 1565	Pločnik	chisel	SRB	2.0844	0.8443
HDM 1566	Pločnik	chisel	SRB	2.0751	0.8405
HDM 1567	Pločnik	chisel	SRB	2.0836	0.8442
HDM 1568	Pločnik	chisel	SRB	2.0585	0.8307
HDM 1569	Pločnik	chisel	SRB	2.0831	0.8439
HDM 1570	Pločnik	chisel	SRB	2.0650	0.8352
HDM 1571	Pločnik	hammer axe	SRB	2.0824	0.8436
HDM 1969	Durankulak	malachite bead	BSC	2.0677	0.8351
HDM 1970	Durankulak	malachite bead	BSC	2.0679	0.8337
HDM 2004	Durankulak	malachite bead	BSC	2.0513	0.8298
HDM 2209	Durankulak	malachite bead	BSC	2.0757	0.8390
HDM 2210	Durankulak	malachite bead	BSC	2.0729	0.8368
HDM 2211	Durankulak	malachite bead	BSC	2.0692	0.8360
HDM 2212	Durankulak	malachite bead	BSC	2.0754	0.8364
HDM 1975	Durankulak	malachite bead	BSC	2.0824	0.8440
HDM 2005	Durankulak	finger ring	BSC	2.0339	0.8241

Table 64. Lead isotope abundance ratios in Late Neolithic/Early Chalcolithic artefacts from Selevac, Medvednjak, Gomolava, Pločnik and Durankulak. Regions are abbreviated as follows: SRB= Serbia, BSC=Black Sea Coast (after Pernicka *et al.* 1993: 18, 24, Tab. 5, Tab. 7; Pernicka *et al.* 1993: 161, Tab. A4).

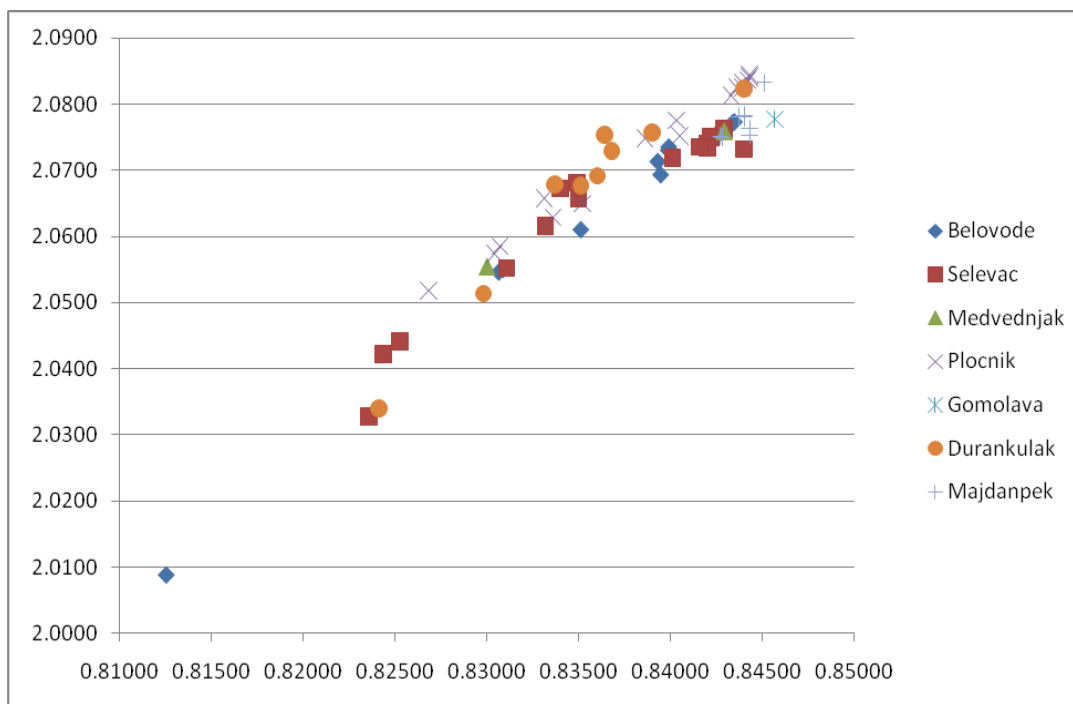


Fig. 103- Lead isotope abundance ratios in samples from Belovode and Ždrelo in relation to Late Neolithic/Early Chalcolithic artefacts from the Balkans.

The chronologically contemporary artefacts from Durankulak are presented here by reason of demonstrating the closest values to Serbian samples; nevertheless, no match with Belovode findings was observed, except for a few Selevac and Pločnik artefacts, pointing at a potential common source.

The provenance of copper ingot from Belovode: trace element analysis

For a discussion on provenance of metals, elements like Co, Ni, As, Sb, Ag and Au (generally all siderophile and chalcophile elements) are considered to represent the potential source with high probability, as opposed to Cr, Zn, U, Th and Hg which volatilize or concentrate in the slag during smelting (Pernicka *et al.* 1993). The pure copper composition of ingot Belovode 34 led to the assumption that it was made of smelted native copper or high purity copper ore; where the production steps would have required maximum two steps (smelting/melting and casting). Hence, the ratio of elements shown in Table 65 would predict similar ratios of the siderophile and

chalchopile elements in ingot and its potential source. Majdanpek, already identified as a potential source for the ingot by the lead isotope ratios is as well confirmed with trace element data (see Fig. 104).

	Co	Ni	As	Mo	Sb	Au	Pb	Bi	Te
	ppm	ppm	ppm	ppm	ppm	ppm	ppm	ppm	ppm
Belovode 34	< 1	16.29	31.07	< 1	6.68	1.29	4.44	< 1	3.91

Table 65. ICP-MS trace element data for copper ingot Belovode 34. All results given in ppm ($\mu\text{g/g}$).

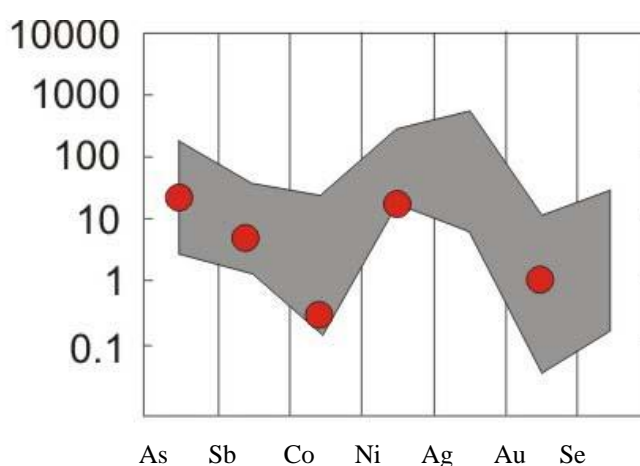


Fig. 104- Figure showing trace element data falling into pattern of Majdanpek ore deposits (pers. comm. with Prof. E. Pernicka; see also Pernicka *et al.* 1993: 32-33, Tab. 9).

Concerning the issue of the particular type of copper ore used, it is noteworthy that the abundance of cobalt and nickel are used to distinguish artefacts made of native or smelted copper, where particularly low readings in nickel appear to be a useful marker element for distinguishing artefacts made of native copper (Fig. 105; cf. Hauptmann *et al.* 1992; Pernicka *et al.* 1993; Pernicka *et al.* 1997). The single analysis in this case can not distinguish this artefact as made of native copper; however, it falls within the range of the native copper composition from the Balkans, thus indicating the possible source.

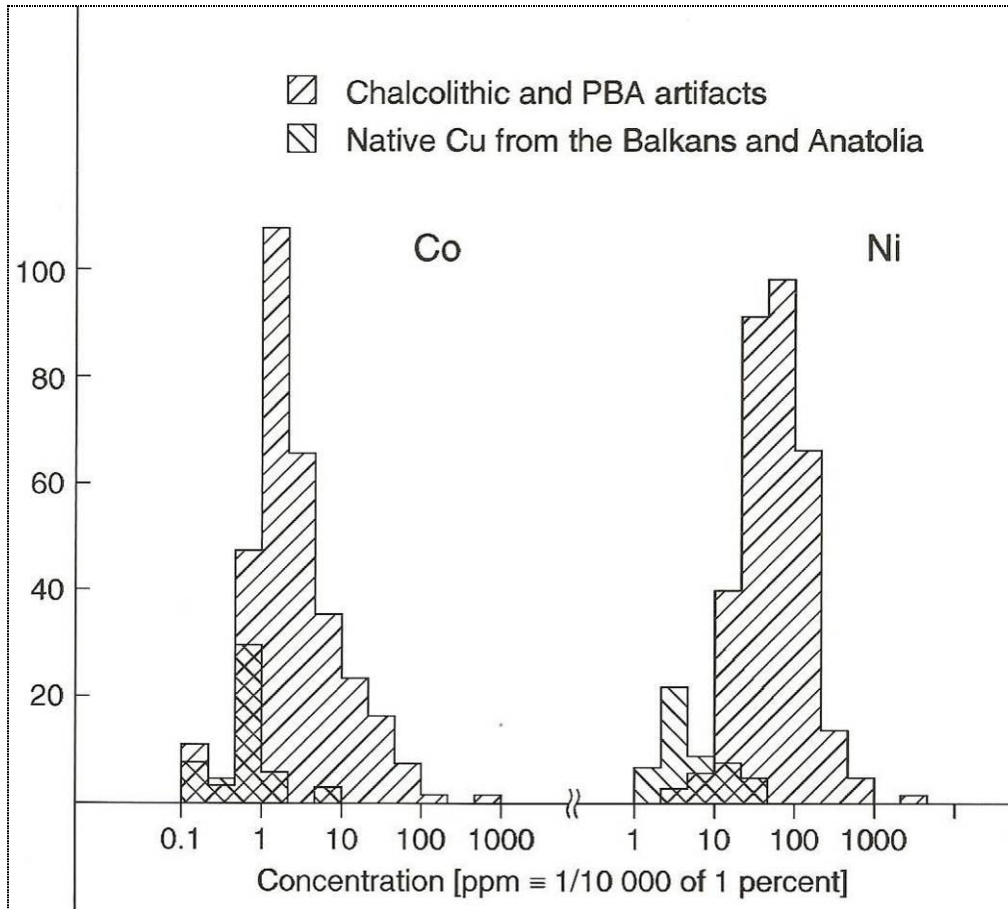


Fig. 105- Concentrations of Co and Ni in native copper from the Balkans and Anatolia in comparison with Chalcolithic and Proto (Early) Bronze Age (PBA) artefacts in Bulgaria (vast majority is smelted). Note lower concentrations of Co and Ni in the native copper (*after Pernicka et al. 1997: 124, Fig. 23*).

Discussion on provenance of samples from Belovode

The most important conclusion arising from the lead isotope analysis of Belovode ores, slags and artefacts is that this material is consistent with its origins from the Balkans, particularly Serbian ore deposits. The various isotopy of studied samples indicates no single deposit used, and justifies their grouping in three assemblages, all with their individual signature.

At this point, we should briefly consider the question whether the observed spread of lead isotope composition for the objects excavated in Belovode is indicative for widespread mixing of copper ores or of smelted metals. No indications in the archaeological record- such as scrap metal, or the short supply of metal in the Chalcolithic is known thus far. In addition, the grouping of trace element data into discrete clusters found by Chernykh (1978a) argues against widespread mixing that would diffuse such chemical differences (cf. Gale *et al.* 2003). Nevertheless, the mixing of ores should be assumed within a certain region, particularly in the early periods, where the introduction of extractive metallurgy should have been followed by experiments with various types of copper ores.

Belovode Group A has Majdanpek ore field as the most likely source for these samples. For Belovode 34 this source is confirmed with the distinctive trace element data, which combined with similar isotopic signature, clearly designates that the ingot originates from Belovode. This deposit could be the origin of few artefacts from Selevac and Medvednjak, suggesting the existence of prehistoric mine(s) yet not known to the archaeological record. Group B, which generally matches the small outcrop Ždrelo, indicates that the Belovode and possibly Selevac inhabitants may have drawn from this deposit.

Nonetheless, Group C indicates three potential areas of exploitation: Rudna Glava with adjacent ore deposits in Serbia, Panagjurište, and Burgas district in Bulgaria. As already shown above, Rudna Glava would be a viable source to have yielded metal for smelting in Belovode; particularly regarding sample Belovode 23 that is presented with radiogenic lead ratio $^{208}\text{Pb}/^{206}\text{Pb} < 2.050$ (cf. Pernicka *et al.* 1997). Nevertheless, the assignment is not unique: the adjacent outcrops, such as Crnajka or Velika Brestovica,

also closely match Belovode slags. Čadinje as well shows one distinctive match with Belovode 23; on the other hand, the rest of the ores from this source cluster away from Belovode slags, which contributes to ruling out this deposit, particularly bearing in mind its geographical position.

With Bulgarian data on hand, one of the slag samples, Belovode 20, falls within the indicated field of four deposits from Bulgaria. Plausible arguments make it unlikely that East Bulgaria was the source region for artefacts in copper-rich Eastern Serbia; however, West Bulgaria could have been one of the sources for the Belovode 20 slag sample.

It is, in any case, apparent that no single deposit supplied Belovode; the evidence presented attest the earliest exploitation of Rudna Glava, or at least the adjacent regions with similar isotopy. On the other hand, the importance of Rudna Glava deposit is confirmed in the later Chalcolithic period in the Balkans: several Durankulak and Varna artefacts fall into the Rudna Glava field (Dimitrov 2002: 131, abb. 152; Todorova 2002; Iliev *et al.* 2007), suggesting the intensive exploitation and wide distribution of artefacts made from ores in this source.

Hence, acknowledging the record for exploitation of Rudna Glava in the Chalcolithic period and the lead isotope abundance ratios of slag from Belovode that falls within the isotopic field of this mine, the likely interpretation is that Rudna Glava was exploited throughout the occupational period of Belovode. This, however, was not exclusive, but allowed also acquisition of ores from adjacent regions which is clearly indicated by the varying isotopic signature of ores, slags and artefacts from this site.

It is important to outline the smelting experiment with the ore from Rudna Glava (Table 66), conducted under reducing conditions in a furnace and with flux added (Tylecote 1982). The chemical compositions of ore, slag and metal acquired out of this smelt do not correspond with the composition of Belovode slag samples (see also Table 7).

	Mn	Fe	Co	Ni	Cu	Zn	As	Ag	Cd	Sn	Sb	Au	Pb	Bi
	wt%	wt%	wt%	wt%	wt%	wt%	wt%	wt%	wt%	wt%	wt%	wt%	wt%	wt%
ore	0.360	5.1	0.075	0.075	17.0	0.019	0.075	0.0002	0.002	0.000	0.018	0.003	0.040	0.003
slag	0.180	30.5	0.009	0.008	1.5	0.009	0.110	0.0002	0.005	0.000	0.022	0.002	0.000	0.002
metal	0.000	35.5	0.190	0.230	63.0	0.050	0.180	0.054	0.000	0.000	0.100	0.005	0.015	0.007

Table 66. Analyses of copper ore from Rudna Glava and the products of smelt (*after* Tylecote 1982: 118, Tab.2)

On the other hand, the trace element analysis conducted on 19 ore samples from Rudna Glava (Table 67) reveals different concentrations in comparison with Tylecote's experiment: Co and Ni are present in lower concentrations, Fe appeared to be two times higher, as well as Zn, while readings in Sb are less significant than in the previous analysis (5ppm to 180ppm in Table 66).

sample	origin	Cu	Sn	As	Sb	Co	Ni	Ag	Au	Fe	Zn	Se	Te	U	Th
		%	ppm	ppm	ppm	ppm	ppm	ppm	ppm	%	ppm	ppm	ppm	ppm	ppm
196-2g-1	2	5	<70	52	7.4	145	130	6.6	0.26	18.0	304	2.8	34	25	13.2
196-2g-4	2	39	<40	72	7.8	1800	330	2.6	0.27	1.3	1030	<1.5	42	<42	6.9
196-2g-3	2	18	<80	120	6.5	455	219	40.0	12.30	11.2	330	4.1	<10	55	5.3
196-3.1	2	3	<60	81	11.0	106	36	11.0	0.21	13.7	221	2.0	15	<15	8.1
196-4.1	3	10	<70	78	12.0	202	49	8.0	0.17	11.8	134	<0.7	100	90	0.9
196-4.2	3	18	<70	217	21.0	470	130	6.3	0.21	9.0	293	0.9	<10	84	1.6
196-4.4	3	31	<50	85	4.8	1230	410	3.3	0.17	1.7	610	<1.5	86	90	6.6
196-4NH	3	9	<60	71	2.0	17	31	78.0	0.27	50.0	138	12.7	18	8	2.3
196-4H	3	20	<60	11	4.6	294	145	4.8	0.13	7.4	298	0.4	19	17	0.3
196-87	3	7	<20	142	1.9	41	28	52.0	0.63	39.0	139	8.7	24	16	10.9
196	1	41	<30	63	0.5	610	330	4.5	0.50	10.6	1320	1.5	8	8	0.7
196-1	1	3	<40	11	2.0	104	108	20.0	1.76	21.0	160	5.0	11	6	1.5
196-2	2	1	<30	18	8.7	55	32	6.4	0.24	9.8	165	2.1	48	44	1.4
196-2g I	2	37	<60	75	2.6	1180	289	11.3	1.17	3.9	870	0.9	23	25	6.1
196-2g II	2	47	<60	62	1.0	1130	288	2.1	0.19	0.7	750	<0.5	13	14	2.3
196-2g III	2	4	<30	21	1.2	83	107	7.8	1.29	8.8	213	2.7	22	18	2.3
196-2g IV	2	12	<40	23	2.4	55	62	56.0	0.74	16.0	148	8.9	20	11	4.5
196-6.10m	2	42	<70	45	1.4	1470	236	2.1	0.17	0.9	790	<0.6	6	10	2.6
196-3	2	1	<40	17	2.4	38	15	5.0	0.15	11.6	146	1.1	13	11	3.9

Table 67. Chemical composition of ore samples from Rudna Glava. Column "origin" stands for following categories: 1- outcropping ore; 2- ancient shaft filling; 3- ore dump (*after* Pernicka *et al.* 1993: 32-33, Tab. 9)

The data presented here stand in contrast to each other; presumably, the trustworthy ones should be statistically more reliable. However, in order to strengthen the assumption of Belovode slag samples originating from ores from Rudna Glava, or other adjacent sources, trace element analysis of these samples should be conducted and considered to complement the diagrams of lead isotope abundance ratios presented above.

It is also noteworthy that different mineral deposits were exploited for smelting and jewellery (bead) making, suggesting the specific skills and technological knowledge of early craftsmen from Belovode. Consequently, this should be strong indication for early craft specialization in the settlement, allowing also assumption of different productions taking place in it, thus strengthening its metallurgical character.

Discussion and conclusion

Summary and wider discussion

The data presented above has indicated that smelting in Belovode took place as early as the last quarter of the 6th millennium BC, hence revealing the earliest documented evidence in the Old World. In Belovode, the concentration of slag samples in the trench situated at the outskirts of the site is particularly useful as an indicator for working process *in situ*; suggesting the existence of a workshop.

All slag samples are found to be consistent in their structure and composition, indicating that the same principle of extracting metal was utilized throughout the occupational period of Belovode. It also implies rather consistent type of ores used in each smelt, which thus far have not been detected with the precise chemical composition indicated above (Table 7, Fig. 34). Nevertheless, the lead isotope analysis indicated that more than one ore source was exploited for the metallurgical activities in Belovode: slag samples are particularly interesting since presenting an on-spot match with the lead isotope signature of Rudna Glava, the well-known prehistoric mine. This particular lead isotope abundance ratio is characteristic for the adjacent sources as well (Crnajka, Velika Brestovica), which fall within the isotopic field of slag from Belovode. In addition, one of the samples indicated an ore source from West Bulgaria, hence indicating the presence of a developed network of raw materials procurement at Belovode. It is also important to emphasize that this sample (Belovode 20) belongs to the latest excavation level, thus possibly indicating a change in the management of copper exploitation in the area, which apart from the change in the technological sphere could demonstrate certain modifications on the social level, too.

Nonetheless, the variety of copper ores found in the site shows the attempts of early craftsmen to experiment with the material from different sources and possibly explore their technological/material advantages. Namely, all slags in Belovode are Mn-rich silicate slags, which are known to have a major technological advantage compared with the formation of the more common fayalite slag (Hauptmann 2003). The divalent Mn has a much larger range of stability than the divalent Fe, meaning that Mn-silicate slag

may be formed under more oxidising condition than a fayalitic slag. Hence, the presence of manganese oxide, and of lime and alumina as well, helps to keep the slag fluid under most smelting conditions. Technologically speaking, during the smelting process, the amount of oxygen or the CO/CO₂ ratio could change considerably without affecting the slag formation (Hauptmann 2003). The temperature required for such process is around 1100°, which is here confirmed with the phase diagram (Fig. 36).

The emphasis set on the material properties of Mn-silicate slags lies in the following: the chemical analyses of major and trace elements of ores from Rudna Glava did not show significant Mn content (Tables 66 and 67) which would correspond with the composition of slag from Belovode, although the isotopy appears to confirm their origin from this location or the adjacent outcrops. However, the abundance of Mn content in the oxidic ores from Ore 9, 12 and 19 would encourage the assumption of similar samples being added to the smelting process, once this had been recognized as technologically opportune to cope with the unstable smelting conditions. Furthermore, one of these Mn-rich ores was found in Trench III, where all the slag samples originate from. The significant amounts of Co, Ni and Zn (all above 100 ppm) in the ores from Rudna Glava, mixed with Mn content in the oxidic ores could possibly designate the source for slags; nevertheless, the quantity of the evidence presented is too scarce, and requests more samples and analysis for reconstructing the technological choice indicated here.

The mixing of ores in order to improve the quality and quantity of extracted metal is a practice known from the Chalcolithic period in Palestine, from Abu Matar (Shugar 2000). On the other hand, it is important to emphasize that no large-scale mixing of ores was recognized in the lead isotope abundance ratios in the Chalcolithic artefacts and ore deposits in the Balkans (Черных 1978a; Pernicka *et al.* 1993; Pernicka *et al.* 1997; Gale *et al.* 2003). Ore samples are rather assumed to be mixed from within a single large copper-rich area, which in turn did not influence the distinctive isotopy of each larger zone in the Balkans.

The isotopy of ores and artefacts from Belovode confirmed a range of deposits exploited from its inhabitants, where the vast majority falls in the isotopic field of Eastern Serbian copper deposits (see Figs. 99-102). One of the earliest exploited sources, Majdanpek,

was much more enriched in polymetallic sulphide ore bodies than in native or oxidic copper; yet, two ore samples and artefacts from Belovode seem to originate from this deposit. The lead isotopy of Ždrelo, the mine discovered in the vicinity of Belovode, also showed a match with the sample from the site, hence strongly indicating that yet another mine was exploited at the end of the 6th millennium BC.

Nevertheless, although metallurgical activities in Belovode are based on several ore sources, it is less than 5 gr of slag samples in total that are being discussed in this research. The so-called “slagless” process is characteristic for early metallurgy (Craddock 2001). The ephemeral evidence is mainly due to the technology of early smelting activities: the process would last only a very few hours, some of the copper mineral would have been reduced to metal, some would have formed a slaggy material containing copper oxides and iron, but much of the rest would just have calcined; in such way the debris would be almost indistinguishable in the archaeological record (Craddock 2001). However, the level of technical uniformity of the smelting process throughout could suggest an organised production, whether large scale or small scale, but yet regulated production is difficult to assess at this stage, especially as so little is known about copper production in the 6th millennium BC. It is important to highlight that the production was carried out in the settlement, as expected for the earliest copper smelting (Hauptmann, Bachmann and Maddin 1996). The smelt most likely took place in a crucible, considering the intensive oxidation confirmed in the structure of slags, as well as the early date. Regarding the charge in the smelt, the elevated lime content, around 16% in average, is recognized as a substantial fuel ash contribution (Table 7); an origin of the lime from the crucible fabric is ruled out because of the proportionally low lime content in ceramics sherds from the site, generally understood in the early periods as no different from the technical ware. In addition, the efficiency of the smelting process can not be estimated, since no similar processes are known from that time; yet, the consistent temperature achieved throughout the occupational period could suggest routine mastery of the technological knowledge.

The character of Belovode is very much determined by the various assemblages of ores, slags and artefacts as a metallurgical settlement. Furthermore, the location on the windy plateau, near the water and fuel source and the most important- ore deposits, contributes to the assumption that this settlement developed in response to environmental conditions, where social, economic and political factors played a significant role as well (cf. Gosselain 1992; Lemmonier 1992). The Vinča culture in whole occupied the area abundant in ore deposits over a whole millenium, where nearly 400 settlements were found settled within easy access to them (Chapman 1981). Belovode itself flourished during the early phases of this culture, and was abandoned at the beginning of the Gradac phase. The potential “intrusion” of ore from deposits in West Bulgaria in the last stage of the site may tell about a change on the technological level that could reflect social changes and decisions made about abandonment of the site. Although the ore deposits seem not to be exhausted, since they were further exploited in the Late and Final Chalcolithic (Pernicka *et al.* 1993; Gale *et al.* 2003), they could have become economically no longer viable and cause the permanent abandonment of Belovode. This occurrence is, however, characteristic for most of the metallurgical settlements in the Vinča culture: the layers of great fire and permanent abandonment of settlements occur throughout the inhabited region; due to its complexity, this issue is beyond the scope of this research and will not be discussed here.

Nonetheless, Belovode as such provides evidence for a small-scale economic system, where the *chaîne opératoire* can be broken down to the main activities of mining and exploitation, raw material acquisition and the production itself (cf. Stöllner 2003). Throughout the 500 years of occupation it was undoubtedly contributing or stimulating the change of economic systems within the Vinča culture and in the surrounding areas. For several decades, it has generally been accepted that metal production and control over it had a major impact on the development of stratified societies as well as on urbanization in general (cf. Childe 1950; Renfrew 1967; Pernicka 1990; Yener 2000). With the evidence of the permanent living and working structures where smelting took place, and near-by places where raw material was extracted, Belovode offers a record for

the craft specialization in the Vinča culture, one of the indications of complex society developing in the Balkans at the end of the 6th millennium BC.

The archaeological records of the development of complex societies thus far were mainly constrained to the Anatolian and Near Eastern cultures, particularly regarding the advent of pyrometallurgy in these regions. Presenting the earliest documented evidence for metallurgy in the Old World, the Vinča culture expands the indicated area of the emergence of early civilizations over the Bosphorus and Dardanelli bridges to the Balkans. The relations of the Vinča culture to Anatolia in particular have been discussed at length: the emergence of the black burnished ware is seen as the trend dominating these cultures in the mid-6th millennium BC, appearing along with the development of pyrometallurgical activities (Özdoğan 1993). This trend is also recognized with the Maritsa, Pre-Cucuteni and Gumelnitsa cultures; all of which revealed evidence for the early metallurgical activities within a unique zone labelled as the Balkan metallurgical province (Черных 1978a; Chernykh 2002). The evidence presented above indicates a clear necessity that current views on the development of metallurgy in the Old World have to be revised, particularly concerning the issue of cultural homogeneity, which could suggest the reasoning behind the cultural and geographical route the early metallurgical societies underwent when they spread over Europe.

Directions for further research

There are several ways for extending this study, in order to fully understand the technological choices: first and foremost, the relation of the slag samples with Rudna Glava and the adjacent outcrops should be compared on the level of trace element analysis, which in turn would strengthen the assumption on the origins of ores smelted in Belovode. Furthermore, the composition of ceramics from this study should be compared with the local pottery, which should particularly regard the question of the calcium phosphate lagging, and whether certain clays were being specially selected for this type of pottery. In addition, a greater consideration of the ore collection has to be taken into account, mainly by reason of more specific identification of number of sources used. It would be particularly significant to identify ore deposits for bead

production and metallurgy, respectively. Having shown the evidence for their origins from various ore sources in the vicinity of Belovode, it would be important to explore material properties of these deposits, which in turn could suggest whether different technological choices might point towards social specialization at the site.

Hopefully, though, this study will have provided a starting point for gaining a greater understanding of the complexities of copper ore production in the Early Chalcolithic, not only on a technical basis, but also in terms of economic and social aspects and interactions; not only within the Vinča culture, but also on the inter-regional level.

Conclusion

Overall, this study has demonstrated the organized and consistent copper production throughout the occupational period in Belovode, which involved specialized skills of craftsmen at a time copper is understood to represent an emerging crucial commodity. By documenting aspects of both the technical and the cultural processes of copper production on this site, it has provided a glimpse into what was surely an established technology before the collapse of the Vinča culture. This allows assumptions on the existence of a developed society, highly organized and with broad influence in what is later termed the emergence of early states in the Old World.

Bibliography

Antonović, D. 2003. Copper processing in Vinča: new contributions to the thesis about metallurgical character of Vinča culture. *Starinar* (Belgrade) 52: 27-45.

Antonović, D. 2006. Malachite finds in Vinča culture: Evidence of Early Copper Metallurgy in Serbia. *Journal of Metallurgy* (Belgrade): 85-92.

Amov, B. G. and Văkova, V. N. 1994. A summary of lead isotope data for ore deposits in Bulgaria. In *Проблеми на най-ранната металургия* (eds. H. Todorova and Popov, P.). Sofia.

Archive of the Department of Prehistory, National Museum Belgrade.

Bachmann, H. G. 1982. *The Identifications of Slags from Archaeological Sites*. London: Institute of Archaeology.

Bailey, D.W. 2000. *Balkan Prehistory*. London and New York: Routledge.

Bognar-Kutzian, I. 1976. On the origins of early copper-processing in Europe. Pp 69-76 in *To Illustrate the Monuments* (ed. J. V. S. Megaw). London: Thames and Hudson.

Borić, D. 2007. The Earliest Copper Mining in Europe: New Radiometric Evidence. Paper presented on *Early Balkan Metallurgy Workshop*, June 11th, 2007, UCL Institute of Archaeology, London.

Brukner, B. 1980. Naselje vinčanske grupe na Gomolavi- neolitski i eneolitski sloj (The Vinča Culture Settlement in Gomolava- Neolithic and Eneolithic layers, in Serbian). *Rad vođovđanskih muzeja* (Novi Sad) 26: 5-55.

Черных, Е.Н. 1978а. *Горное дело и металургия в древнейшей Болгарии* (*Mining and Metallurgy in ancient Bulgaria*, in Bulgarian). София: Болгарской Академии Наук.

Černych, E.N. 1978b. Aibunar- a Balkan copper mine of the fourth millennium BC. *Proceedings of the Prehistoric Society* 44: 203-217.

Chernykh, E.N. 2002. Some of the most important aspects and problems of early metal age studying. Pp. 25-31 in *The Beginnings of Metallurgy in the Old World*, band 1, (eds. E.Pernicka and M.Bartelheim). Rahden/Westf.: Verlag Marie Leidorf GmbH.

Chernykh, E.N., Lebedeva, E.Y., Zhurbin, I.V., López-García, P., López-Sáez, J.A. and Martínez-Navarette, M.I. 2002. Kargaly II. *Gorny-The Late Bronze Age Settlement: Topography, lithology, stratigraphy: Household, manufacturing and sacral structures: Relative and absolute chronology*. Moscow.

Chapman, J. 1981. *The Vinča culture of South-East Europe*. Oxford: BAR. International Series 117.

Chapman, J. and Tylecote, R. 1983. Early Copper in the Balkans. *Proceedings of the Prehistoric Society* 49: 373-379.

Childe, V.G. 1944. Archaeological Ages as Technological Stages. *Journal of the Royal Anthropological Institute of Great Britain and Ireland* 74: 7-24.

Childe, V.G. 1950. The Urban Revolution. *Town Planning Review* 21: 3-17.

Craddock, P.T. 1995. *Early Metal Mining and Production*. Edinburgh: Edinburgh University Press.

Craddock, P.T. 2001. From Hearth to Furnace: Evidences for the Earliest Metal Smelting Technologies in the Eastern Mediterranean. *Paleorient* 26/2: 151-165.

Čović, B. 1961. Rezultati sondiranja na preistorijskom naselju u Gornjoj Tuzli (*The Excavation Results from Prehistoric Settlement Gornja Tuzla*, in Serbian). *Glasnik Zemaljskog Muzeja u Sarajevu* (Sarajevo) XV-XVI: 79-139.

Davies, O. 1937. Ancient mining in the central Balkans. *Revue Internationale des Etudes Balkaniques* 1/5: 405-418.

Dimitrov, K. 2002. Die Metallfunde aus den Gräberfeldern von Durankulak. Pp 127-158 in *Durankulak- Die Prähistorischen Gräberfelder* (hrsg. H. Todorova). Sofia: The Bulgarian Academy of Sciences.

Doelter, C. 1916. *Die Mineralschätze der Balkanländer und Kleinasiens*. Stuttgart: Enke.

Dokov, R., Vassilef, L., Staikov, M., Simov, S. and Panayotov, A. 1989. *Metallogenic Map of Bulgaria*. Sofia.

Esin, U. 1969. *Kuantitativ Spektral Analiz Yardimiyla Anadolu'da Baslangicidan Asur Kolonilieri Cagina Kadar akir ve Tunc Madenciligi*. Istanbul: Tas Matabaasi.

Gale, N. H., Stos-Gale, Z. A., Lilov, P., Dimitrov, M. and Todorov, T. 1991. Recent Studies of Eneolithic copper ores and artefacts in Bulgaria. Pp. 49-76 in *Découverte du Métal* (eds. J.-P. Mohen and C. Éluère). Paris: Picard.

Gale, N. H., Stos-Gale, Z. A., Raduncheva, A., Panayotov, I., Ivanov, I., Lilov, P. and Todorov, T. 2003. Early Metallurgy in Bulgaria. Pp. 122-173 in *Mining and Metal Production Through the Ages* (eds. P. Craddock and J. Lang). London: The British Museum Press.

Galović, R. 1975. Neolitska ritualna grupa iz Smederevske Palanke (*The Neolithic Ritual Assemblage from Smederevska Palanka*, in Serbian). *Zbornik Narodnog Muzeja* (Belgrade) 8: 21-30.

Gavela, B. 1956-1957. Eneolitska naselja u Grivcu (*Eneolithic Settlements in Grivac*, in Serbian). *Starinar* (Belgrade): 237-268.

Garašanin, M. 1950. Sekire sa otvorom za držalje u Umetničkom Muzeju u Belgradeu (*Shaft-hole axes in the Art Museum in Belgrade*, in Serbian). *Muzeji* (Belgrade) 5: 87-105.

Garašanin, M. 1973. *Praistorija na tlu Srbije* (*The Prehistory in Serbia*, in Serbian). Belgrade: Srpska Knjizevna Zadruga.

Garašanin, M. 1979. Centralnobalkanska zona (*The Central Balkan Area*, in Serbian). Pp. 79- 212 in *Praistorija Jugoslavenskih Zemalja* (ed. A. Benac). Sarajevo: Svjetlost.

Garašanin, M. 1991. Der Übergang vom Neolithikum zur Frühen Bronzezeit auf dem Balkan und an der unteren Donau. Pp 136-141 in *Die Kupferzeit als historische Epoche*, Symposium Saarbrücken und Otzenhausen, 6.11.-13.11.1988 (hrsg. J. Lichardus and R. Echt). Bonn.

Garašanin, M. 1994-1995. Die Gradac-Stufe der Vinča-Gruppe und der Beginn des Aeneolithikums. *Dacia* 38-39: 9-17.

Gaul, H. 1942. Possibilities of Prehistoric Metallurgy in the East Balkan Peninsula. *American Journal of Archaeology* 46: 400-409.

Gimbutas, M. 1974. Obre and its place in old Europe. *Wissenschaftliche Mitteilungen des Bosnisch- Herzegowinischen Landesmuseum* 4(4): 5-13.

Gimbutas, M. (ed.) 1976. *Neolithic Macedonia as Reflected by Excavations at Anza*. Los Angeles: Institute of Archaeology, University of California.

Glumac, P. 1983. An Archaeometallurgical Study of the Materials from Selevac. *Zbornik Narodnog Muzeja* (Belgrade) 11(1): 135-141.

Glumac, P. 1988. Copper Mineral Finds from Divostin. Pp 457- 462 in *Divostin and the Neolithic of Central Serbia* (eds. D. Srejić and A. McPharron). Pittsburgh/Kragujevac: University of Pittsburgh/Narodni muzej Kragujevac.

Glumac, P. and Tringham, R. 1990. The Exploitation of Copper Minerals. Pp 549-563 in *Selevac, A Neolithic Village in Yugoslavia*, (eds. R.Tringham and D.Krstić). Los Angeles: University of California.

Glumac, P. D. and Todd, J.A. 1991. Early Metallurgy in Southeast Europe: the Evidence for Production. Pp. 7-19 in *Recent Trends in Archaeometallurgical Research, MASCA Research Papers in Science and Archaeology, vol.8, part I* (ed. P.D. Glumac). Philadelphia: University of Pennsylvania.

González, L. R. and Gluzman, G. G. 2007. Prehistoric Metallurgy in Northwest Andes (South-American Andes). In *Archaeometallurgy in Europe II*, CD of preprints, paper 236.

Gosselain, O. 1992. Technology and Style: Potters and Pottery among the Bafia of Cameroon. *Man* 27: 259-286.

Grbić, M. 1929. *Pločnik, Eine Prähistorische Ansiedlung aus der Kupferzeit*. Belgrad: Nationalmuseum in Belgrad.

Hartmann, A. and Sangmeister, E. 1972. The Study of Prehistoric Metallurgy. *Angewandte Chemie* 11 (7).

Hauptmann, A. 1989. The Earliest Periods of Copper Metallurgy in Feinan/Jordan. Pp 119-135 in *Old World Metallurgy, Der Anschnitt, Beiheft 7* (eds. A. Hauptmann, E. Pernicka and G.A. Wagner). Bochum: Deutsches Bergbau-Museum.

Hauptmann, A. 2000. *Zur frühen Metallurgie des Kupfers in Fenan/Jordanien*, Der Anschnitt, Beiheft 11. Bochum: Deutsches Bergbau-Museum.

Hauptmann, A. 2003. Developments in Copper Metallurgy During the Fourth and Third Millennia BC at Feinan, Jordan. Pp. 90-100 in *Mining and Metal Production Through the Ages* (eds. P. Craddock and J. Lang). London: The British Museum Press.

Hauptmann, A., Begemann, F., Heitkemper, E., Pernicka, E. and Schmitt-Strecker, S. 1992. Early Copper Produced at Feinan, Wadi Araba, Jordan: The Composition of Ores and Copper. *Archaeomaterials* 6: 1-33.

Hauptmann, A., Lutz, J., Pernicka, E. and Yalçın, Ü. 1993. Zur Technologie der frühesten Kupferhüttung im östlichen Mittelmeerraum. Pp 541-572 in *Between the Rivers and Over the Mountains, Archaeologica et Mesopotamica, Alba Palmieri Dedicata* (ed. M. Frangipane, A. Hauptmann, M. Liverani, P. Matthiae and M. Mellink). Rome: Dipartimento di Scienze Storiche Archeologiche e Antropologiche dell'Antichità, Università di Roma "La Sapienza".

Hauptmann, A., Bachmann, H.-G. and Maddin, R. 1996. Chalcolithic Copper Smelting: New Evidence from excavations at Wadi Fidan 4. Pp. 3- 10 in *Archaeometry '94* (eds. S. Demirci, A. M. Özer and G. D. Summers). Ankara: Tübitak.

Iliev, I., Dimitrov, K., Kuleff, I. and Pernicka E. 2007. Archaeometallurgical Studies on Eneolithic Copper Artefacts from Northeast Bulgaria. In *Archaeometallurgy in Europe II*, CD of preprints, paper 99.

Janković, S. 1967. *Metalogenetske epohe i rudonosna područja Jugoslavije (Metallogenetic epoch and ore deposits in Yugoslavia, in Serbian)*. Bor: Institut rudarstva i metalurgije.

Jovanović, B. 1961. Stratigrafija naselja Vinčanske grupe kod Kosovske Mitrovice (Stratigraphy of Vinča Culture Settlement near Kosovska Mitrovica, in Serbian). *Glasnik Muzeja Kosova i Metohije (Priština)* VI: 9-78.

Jovanović, B. 1971. *Metalurgija eneolitskog perioda Jugoslavije (Metallurgy of the Eneolithic period in Yugoslavia, in Serbian)*. Belgrade: Arheološki institut.

Jovanović, B. 1982. *Rudna Glava, najstarije rudarstvo bakra na centralnom Balkanu (Rudna Glava, the Oldest Copper Mining in the Balkans, in Serbian)*. Belgrade, Bor: Archaeological Institute, Museum of Mining and Metallurgy.

Jovanović, B. 1983. Mali Šturac- ein neues prähistorisches Kupferbergwerk in Zentralserbien. *Der Anschnitt* 4-5: 177-179.

Jovanović, B. 1984. Bakarni minerali sa naselja vinčanske grupe 'Fafos' kod Titove Mitrovice (Copper minerals from Vinča Culture Settlement "Fafos" near Titova Mitrovica, in Serbian). *Glasnik Muzeja Kosova (Priština)* XIII-XIV: 13-16.

Jovanović, B. 1993. Archaeological comment to E. Pernicka's et al. "Eneolithic and Early Bronze Age copper artefacts from the Balkans and their relation to Serbian copper ores". *Prähistorische Zeitschrift* 68: 55-57.

Jovanović, D. 2001. *Zlato i bakar istočne Srbije (Gold and Copper in Eastern Serbia, in Serbian)*. Belgrade: Srpsko društvo za istoriju nauke i Arheološki institut SANU.

Jović, V. 1996. Mineralogical study of malachite and azurite from the Belovode locality (Veliko Laole). *Préhistoire Européene* 8: 191-196.

Junghans, S., Sangmeister, E. and Schröder, M. 1968. *Kupfer und Bronze in der frühen Metallzeit Europas*, Studien zu den Anfängen der Metallurgie, band 2. Berlin: Gebr. Mann.

Jurišić, A. 1959. Velika Gradina u Staparima, Praistorijsko Naselje (Velika Gradina in Stapani, the Prehistoric Settlement, in Serbian). *Starinar* (Belgrade) 9-10: 367-368.

Jurišić, A. 1960. Gradine zapadne Srbije (The Settlements in Western Serbia, in Serbian). *Arheološko društvo Jugoslavije, Praistorijska sekcija I, Ohrid*: 95-97.

Keller, C. and Stern, W. B. 1999. Rückstände in Kochgefäßen - Zum Phänomen der Knochenasche, *Jahrbuch des Oberösterreichischen Musealvereins* 1999: 129-146.

Kilikoglou, V., Bassiakos, Y., Grimanis, A.P. and Souvatzis, K. 1996. Carpathian obsidian in Macedonia, Greece. *Journal of Archaeological Science* 23: 343-349.

Krajnović, D. and Janković, S. 1995. Copper Mineralization as Potential Raw Material Source of Ancient Copper Metallurgy in Serbia. Pp. 21-28 in *Ancient Mining and Metallurgy in Southeast Europe, International Symposium, Gornji Milanovac, May 20-25, 1990* (ed. B. Jovanović). Belgrade, Bor: Archaeological Institute, Museum of Mining and Metallurgy.

Kuna, M. 1981. Zur Neolithischen und Äneolithischen Kupferverarbeitung im Gebiet Jugoslawiens. Pp. 13-81 in *Godišnjak Akademije BiH 17. Centar za balkanološka ispitivanja, knjiga 19*. Sarajevo: Akademija Nauka i Umjetnosti Bosne i Hercegovine.

Kuzmanović- Cvetković, J. 1998. Prokuplje, grad Svetog Prokopija (*Prokuplje, St. Prokopius's City*, in Serbian). Prokuplje: Narodni muzej Toplice.

Lechtman, H. 1996. Arsenic Bronze: Dirty Copper or Chosen Alloy? A view from the Americas. *Journal of Field Archaeology* 23: 477-514.

Lemmonier, P. 1992. *Elements for Anthropology of Technology*. Michigan: University of Michigan.

Ljamić-Valović, H. and Valović, S. 1988. Amuleti i privesci iz Vinčanskog naselja u Ratini (Amulets and Pendants from Vinča Culture Settlement in Ratina, in Serbian). *Zbornik Narodnog muzeja (Čačak)* XIII-1: 21-27.

Maddin, R., Stech, T. and Muhly J.D. 1991. Çayönü Tepesi. The Earliest Archaeological Metal Artefacts. Pp 375- 386 in *Découverte du Métal* (eds. J.-P. Mohen and C. Éluère). Paris: Picard.

Makkay, J. 1991. The most ancient gold and silver in Central and South-East Europe. Pp 119-130 in *Découverte du Métal* (eds. J.-P. Mohen and C. Éluère). Paris: Picard.

Milojčić, V. 1949. *Die Chronologie der jüngeren Steinzeit Mittel- und Südosteuropas*. Berlin: Mann.

Muhly, J.D. 1988. The beginnings of metallurgy in the Old World. Pp 2-20 in *The Beginning of the Use of Metals and Alloy* : Papers from the Second International Conference on the Beginning of the Use of Metals and Alloys, Zhengzhou, China, 21-26 October, 1986 (ed. R. Maddin). Cambridge, Mass.: MIT Press.

Muhly, J.D. 1989. Çayönü Tepeşi and the Beginnings of Metallurgy in the Old World. Pp 1- 13 in *Old World Archaeometallurgy* (eds. A. Hauptmann, E. Pernicka and G. A. Wagner). Bochum: Deutsches Bergbau-Museum.

Müller, R., Rehren, Th. and Rovira, S. 2004. Almozaraque and the Early Copper Metallurgy of Southeast Spain: New Data. *Madrider Mitteilungen* 45: 33-56.

Neeumann, J. P., Zhong, T. and Chang, Y. A. 1984. Binary Alloy Phase Diagrams: Cu-O (Copper-Oxygen). *Bulletin of Alloy Phase Diagrams* 5(2): 942-944.

Neuninger, H., Pittioni, R. and Siegl, W. 1964. Frühkeramikzeitliche Kupfergewinnung in Anatolien. *Archaeologia Austriaca* 35: 98- 110.

Nikolova, L. 1999. *The Balkans in Later Prehistory*. Oxford: BAR International Series 791.

Nikolova, L. (ed.). 2003. *Early symbolic systems for communication in Southeast Europe*. Oxford: Archaeopress.

Odriozola, C.P. and Pérez, V.M.H. 2007. The Manufacturing Process of 3rd millennium BC bone based incrustrated pottery decoration from the Middle Guadiana River Basin (Badajoz, Spain). *Journal of Archaeological Science* 20: 1-10.

Ottaway, B. 1979. Analysis of the Earliest Metal Finds from Gomolava. *Rad Vojvođanskih Muzeja* (Novi Sad) 25: 53-59.

Ottaway, B.S. 2001. Innovation, Production and Specialization in Early Prehistoric Copper Metallurgy. *European Journal of Archaeology* 4(1): 87-112.

Özdoğan, M. 1993. Vinča and Anatolia: A new look at a very old problem (or redefining Vinča Culture from the perspective of Near Eastern tradition). *Anatolica* 19: 173- 193.

Özdoğan, M. and Özdoğan, A. 1999. Archaeological evidence on the early metallurgy at Çayönü Tepeşi. Pp 13-22 in *The Beginnings of Metallurgy*, Der Anschnitt, Beiheft 9 (eds. A. Hauptmann, E. Pernicka, Th. Rehren and Ü. Yalçın). Bochum: Deutsches Bergbau-Museum.

Pernicka, E. 1990. Gewinnung und Verbreitung der Metalle in prähistorischer Zeit. *Jahrbuch des Römisch- Germanischen Zentralmuseums Mainz* 37: 21-129.

Pernicka, E., Begemann, F. and Schmitt-Strecker, S. 1993. Eneolithic and Early Bronze Age copper artefacts from the Balkans and their relation to Serbian copper ores. *Prähistorische Zeitschrift* 68: 1-54.

Pernicka, E., Begemann, F., Schmitt-Strecker, S., Todorova, H. and Kuleff, I. 1997. Prehistoric copper in Bulgaria. Its composition and provenance. *Eurasia Antiqua* 3: 41-180.

Pigott, V.C. 1999. A heartland of metallurgy. Pp 107- 120 in *The Beginnings of Metallurgy*, Der Anschnitt, Beiheft 9 (eds. A. Hauptmann, E. Pernicka, Th. Rehren and Ü. Yalçın). Bochum: Deutsches Bergbau-Museum.

Radivojević, M. 1998. Planigrafija i rekognosciranje vinčanskog lokaliteta Kremen-Macina (*Planigraphy and Field Survey of the Vinča culture Site Kremen-Macina*, in Serbian). *Selected Students' Papers of Petnica Science Centre* (Petnica Science Centre, Valjevo) 48/98: 316-340.

Radivojević, M. 2007. Prilog tipologiji i distribuciji bakarnih sekira tip Pločnik (*Contribution to Typology and Distribution of Pločnik Hammer-Axes*, in Serbian). *Glasnik Srpskog Arheološkog Društva (Journal of Serbian Archaeological Society, Belgrade)* 21.

Renfrew, C. 1967. Cycladic Metallurgy and the Aegean Early Bronze Age. *The American Journal of Archaeology* 71: 1-26.

Renfrew, C. 1969. The Autonomy of the South-East European Copper Age. *Proceedings of the Prehistoric Society* 35: 12-47.

Renfrew, C. 1970. The three-ring calibration of radiocarbon: an archaeological evaluation. *Proceedings of the Prehistoric Society* 36: 280-311.

Renfrew, C. 1973. *Before Civilization*. London: Penguin Books.

Schubert, F. 1965. Zu den südosteuropäischen Kupferäxten. *Germania* 43/2: 274-295.

Scott, D.A. 1991. *Metallography and Microstructure of Ancient and Historic Metals*. Singapore: The J. Paul Getty Trust.

Shugar, A. N. 2000. *Archaeometallurgical investigation of the Chalcolithic Site of Abu Matar, Israel. A Reassessment of Technology and its Implications for the Ghassulian Culture*. University College London, Institute of Archaeology, Dissertation submitted in partial fulfilment of the requirements for the degree of Doctor of Philosophy of the University of London in 2000.

Simić, V. 1951. *Istorijski razvoj našeg rudarstva (The Historical Development of Our Mining, in Serbian)*. Belgrade.

Slag Atlas. 1995. 2nd edition (ed. Verein Deutscher Eisenhüttenleute). Düsseldorf: Verlag Stahleisen GmbH.

Srejović, D. 1969. *Lepenski Vir* (in Serbian). Belgrade: Srpska književna Zadruga.

Srejović, D. and Babović, Lj. 1981. *Lepenski Vir- Menschenbilder einer frühen europäischen Kultur*. Mainz: Von Zabern.

Stalio, B. 1960. Pločnik-Prokuplje-naselje (*Pločnik-Prokuplje-settlement, in Serbian*). *Arheološki pregled* (Belgrade) 2: 33-36.

Stalio, B. 1962. Pločnik, Prokuplje- naselje vinčanske grupe (*Pločnik, Prokuplje- the Vinča culture settlement*, in Serbian). *Arheološki pregled* (Belgrade) 4: 19-25.

Stech, T. 1990. Neolithic Copper Metallurgy in Southwest Asia. *Archeomaterials* 4: 55-61.

Stöllner, Th. 2003. Mining and Economy. A Discussion of Spatial Organisations and Structures of Early Raw Material Exploitation. Pp 415-446 in *Man and Mining*, Studies in honour of Gerd Weisgerber, Der Anschnitt, Beiheft 16 (eds. Th. Stöllner, G. Körlin, G. Steffens, J. Cierny). Bochum: Deutsches Bergbau-Museum.

Šljivar, D. 1996. The Eastern Settlement of the Vinča Culture at Pločnik: a Relationship of its Stratigraphy to the Hoards of Copper Objects. *Старинар* (Belgrade) 47: 85-97.

Šljivar, D. 1999. Плочник, насеље винчанске културе и проблем ране металургије бакра (*Pločnik, the settlement of Vinča culture and the problem of early copper metallurgy*, in Serbian). Стр. 31-44 у *Прокупље у праисторији, антици и средњем веку* (ур. Д. Маринковић). Београд и Прокупље: Археолошки институт и Народни музеј Топлице.

Šljivar, D. 2006. The Earliest Copper Metallurgy in the central Balkans. *Journal of Metallurgy* (Belgrade) 2-3: 93- 104.

Šljivar, D. and Jacanović, D. 1996. Veliko Laole, Belovode- Vinča culture settlement in Northeastern Serbia. *Préhistoire Européene* 8: 175-188.

Шљивар, Д. и Јацановић, Д. 1996. Велико Лаоле-Беловоде, насеље винчанске културе (Veliko Laole- Belovode, the Vinča culture settlement, in Serbian). *Гласник Српског Археолошког Друштва* (*Journal of Serbian Archaeological Society*, Belgrade) 12: 55-60.

Шљивар, Д. и Јацановић, Д. 1997. Велико Лаоле-Беловоде, насеље винчанске културе (Veliko Laole- Belovode, the Vinča culture settlement, in Serbian). *Гласник Српског Археолошког Друштва* (*Journal of Serbian Archaeological Society*, Belgrade) 13: 115-125.

Шљивар, Д. и Јацановић, Д. 1998. Велико Лаоле-Беловоде, истраживања у 1997 (Veliko Laole- Belovode, the research in 1997, in Serbian). *Гласник Српског*

Археолошког Друштва (Journal of Serbian Archaeological Society, Belgrade) 14: 73-78.

Шљивар, Д., и Кузмановић-Цветковић, Ј. 1998. Најстарија металургија бакра на Плочнику код Прокупља, насељу винчанске културе (*The Oldest copper metallurgy on Pločnik near Prokuplje, in Serbian*). *Археометалургија (Belgrade) 6: 1-8.*

Шљивар, Д. и Јацановић, Д. 2003. Прелиминарни извештај о археолошким истраживањима од 1998. до 2002. године, Велико Лаоле, Беловоде (Preliminary reports on archaeological research from 1998 to 2002, in Serbian). *Viminacium 13-14: 297-302.*

Šljivar, D., Jacanović, D. and Kuzmanović- Cvetković, J. 2006. Belovode- Plocnik, New Contributions Regarding the Copper Metallurgy in the Vinča Culture. 251-258 in *Homage to Milutin Garašanin* (eds. N. Tasić and C. Grozdanov). Belgrade: Serbian Academy of Sciences and Arts and Macedonian Academy of Sciences and Arts.

Taylor, J.W. and McGeehan, V. 1987. Yugoslavian Tin Deposits and the Early Bronze Age Industries of the Aegean Region. *Oxford Journal of Archaeology 6 (3): 287- 300.*

Todorova, H. 1978. *The Eneolithic Period in Bulgaria in the Fifth Millenium B.C.* Oxford: BAR International Series 49.

Todorova, H. 1981 Die kupferzeitlichen Äxte und Beile in Bulgarien. *Prähistorische Bronzefunde 9/14.* München: C.H. Beck'sche Verlagsbuchhandlung.

Todorova, H. 2002. Chronologie, horizontale Stratigraphie und Befunde. Pp 35-52 in *Durankulak- Die Prähistorischen Gräberfelder* (hrg. H. Todorova). Sofia: The Bulgarian Academy of Sciences.

Tringham, R., Brukner, B. and Voytek, B. 1985. The Opopo Project: a Study of Socioeconomic Change in the Balkan Neolithic. *Journal of Field Archaeology 12 (4): 459-465.*

Tringham, R. and Stevanović, M. 1990. Field Research. Pp 57- 156 in *Selevac, A Neolithic Village in Yugoslavia*, (eds. R. Tringham and D. Krstić). Los Angeles: University of California.

- Tylecote, R. F. 1962. *Metallurgy in Archaeology*. London: Edward Arnold.
- Valović, S. 1985. Rezultati istraživanja Vinčanskog naselja u Ratini (The excavation results from Vinča culture site Ratina, in Serbian). *Istraživanja* (Novi Sad) 2: 95- 98.
- Vasić, M. 1932. *Preistoriska Vinča I* (*The Prehistoric Vinča I*, in Serbian). Belgrade: Državna štamparija.
- Wertime, T. 1973. The beginnings of metallurgy: a new look. *Science* 182: 875- 887.
- Yalçın, Ü. 2000. Anfänge der Metallverwendung in Anatolien. Pp 17- 30 in *Anatolian Metal I*, Der Anschnitt, Beiheft 13 (ed. Ü. Yalçın). Bochum: Deutsches Bergbau-Museum.
- Yener, K.A. 2000. *The Domestication of Metals: The Rise of Complex Metal Industries in Anatolia (c.4500- 2000 BC)*. Leiden, Boston, Köln: Brill.
- Žeravica, Z. 1993. Äxte und Beile aus Dalmatien und anderen Teilen Kroatiens, Montenegro, Bosnia und Herzegowina. *Prähistorische Bronzefunde* IX/18. Stuttgart: Steiner.

